

VRIJE UNIVERSITEIT

Scale Dependence of Correlations on the Light-Front

ACADEMISCH PROEFSCHRIFT

ter verkrijging van de graad van doctor aan
de Vrije Universiteit Amsterdam,
op gezag van de rector magnificus
prof.dr. T. Sminia,
in het openbaar te verdedigen
ten overstaan van de promotiecommissie
van de faculteit der Exacte Wetenschappen
op woensdag 2 februari 2005 om 13.45 uur
in het auditorium van de universiteit,
De Boelelaan 1105

door

Alexander Adriaan Henneman

geboren te Santiago de Chile, Chili

promotor: prof.dr. P.J.G. Mulders

Publications

This thesis is partly based on the following publications.

1. A.A. Henneman, D. Boer and P.J. Mulders,
Evolution of transverse momentum dependent distribution and fragmentation functions
Nucl. Phys. **B** 620 (2002), p. 331.
2. A.A. Henneman,
Bounds on transverse momentum dependent distribution functions
Talk presented at International Workshop on Symmetries and Spin,
Prague, Czech Republic, 17-22 Jul 2000
Czech. Jour. Phys. Suppl. **A** 51 (2001) p. 129.
3. A. Bacchetta, M. Boglione, A.A. Henneman and P.J. Mulders,
Bounds on transverse momentum dependent distribution and fragmentation functions
Phys. Rev. Lett. 85 (2000), p. 712.

Sponsors

The publication of this thesis was supported by the following sponsors:

- www.klup.nl
- www.deamerica.net

CONTENTS

1	Introduction	1
1.1	Hadrons and quantum chromodynamics	1
1.2	Hard electro-weak processes and hadrons	3
1.3	QCD and hard processes	4
2	Factorization	9
2.1	Introduction	9
2.1.1	The naive parton model	10
2.2	Factorization in quantum chromodynamics	12
2.2.1	The operator product expansion	13
2.2.2	Diagrammatic approaches to factorization	15
2.3	Factorization theorems	20
2.4	Two-hadron processes	22
3	Distribution and fragmentation functions	29
3.1	Introduction	29
3.2	Relevant hadronic matrix elements	30
3.2.1	Light-like correlations	31
3.2.2	Collinear structure	34
3.3	Quark transverse momentum	36
3.3.1	Quark transverse momentum	36
3.3.2	Lorentz-invariance relations	40
3.3.3	Equation of motion relations	40
3.4	Fragmentation functions	41
4	Bounds	45
4.1	Partonic densities	45
4.2	Target spin structure	46
4.3	Quark spin structure	46
4.3.1	Quark-spin structure including transverse momentum	47
4.4	The bounds	48
4.5	Discussion	49

5	Scale dependence	51
5.1	Introduction	51
5.2	Calculation of scale dependence	51
5.2.1	The local approach	52
5.2.2	The non-local approach	53
5.3	A simple case	54
5.3.1	Real diagram	55
5.3.2	The virtual contributions	57
5.4	Non-collinear functions	58
5.4.1	Closed evolution system	59
5.5	Large number of colors	60
5.6	Calculation of the large- N_c contributions	61
5.6.1	Real contributions	62
5.6.2	Virtual contributions	62
5.6.3	Evolution of 3PI soft parts	62
5.A	Generalized Θ -functions	64
6	A local-operator approach	67
6.1	Introduction	67
6.2	Large number of colors	67
6.2.1	Twist-3 distribution functions	69
6.3	Connection to the light-front	69
6.3.1	Evolution equations	71
6.3.2	Fragmentation functions	72
6.3.3	Discussion and conclusions	76
7	Non-collinear evolution	79
7.1	Introduction	79
7.2	Unpolarized hadrons	79
7.2.1	Scale dependence of $e(x)$	80
7.2.2	Scale dependence of $h_1^{\perp(1)}(x)$	80
7.3	Longitudinally polarized hadrons	82
7.3.1	Scale dependence of $h_{1L}^{\perp(1)}(x)$	83
7.3.2	Scale dependence of $e_L(x)$	84
7.4	Transversally polarized hadrons	84
7.4.1	Scale dependence $g_{1T}^{(1)}(x)$	85
7.4.2	Scale dependence of the Sivers function	88
7.4.3	Diagonal evolution of the pure interaction part	88
7.5	Reducing redundancy	89
7.6	Discussion	90
8	Summary and discussion	93

Introduction

1.1 Hadrons and quantum chromodynamics

We perceive our surroundings because light from all around us, reaches our eyes. This light, consisting of particles called photons, the quanta of the electro-magnetic field, are emitted by atoms making transitions between states with different energies. These electrically neutral atoms are composed of electrons, carrying negative electric charge, and positively charged nuclei, both bound together by the electro-magnetic force that is mediated by these same photons.

Electrons are almost mass-less compared to the total mass of the atom, but are responsible for almost all of its volume, and therefore for almost all chemical properties of the atom. The nucleus of the atom, on the other side, composed of protons and neutrons, is of almost negligible size compared to the total size of the atom, but is responsible for almost all of its mass. Protons carry electric charge that is equal in magnitude to that of electrons, but is opposite in sign. Being packed, together with neutrons, which are electrically neutral, in the small space occupied by the nucleus, a force much stronger than the electro-magnetic force is necessary to overcome the electro-magnetic repulsion between protons. This force is known as the *strong* force. Besides their different roles in building up atoms, there is a more fundamental difference between electrons and nucleons, the collective name given to protons and neutrons. Electrons, are examples of particles known as *leptons*, which are, by definition, particles that are not sensitive to the strong force. Protons and neutrons are sensitive to this force and are therefore examples of particles called *hadrons*.

Our understanding of the leptons and hadrons is very different. The basic understanding of the behavior of subatomic particles is contained in what is called the *Standard Model*. It refers to a framework that unifies the principles of quantum mechanics and the theory of special relativity, in which fundamental spin-1/2 particles interact by means of exchange of integer-spin particles. All forces in nature, electro-magnetic-, weak- and strong force, except for one, are described in the Standard Model. The remaining force, gravity, has not been incorporated in the model, yet, but for the calculation purposes at subatomic scales that are addressed in this thesis gravity plays a negligible role.

Leptons are included in the Standard Model. There are three families of leptons,

that, to our knowledge, are fundamental. They have no inner structure. Moreover, due to weak coupling strengths, their interactions are weak and the behavior of leptons can be described to a very high degree of accuracy. This description is contained in the electro-weak sector of the Standard Model.

Hadrons, in contrast, do not appear in the Standard Model as fundamental particles. When enough energy is available, hadrons with different properties and with many spin values can be formed. Furthermore, experimentally they appear to have a finite size and an inner structure. Similarities among the many hadrons that can be formed, have led to the hypothesis that all hadrons are mere combinations of a handful of *quark* species, which are given the name *flavors* (up, down, strange, charm, bottom, top). The most stable hadrons encountered are either composed of three quarks or a quark and anti-quark pair, although more exotic combinations seem to be possible [Naka03, Barm03]. The role of fundamental particle is not played by hadrons but by the field-theoretical object corresponding to these quarks.

On one side, this "constituent" quark model brought order in a zoo of hadronic particles, but on the other side it brought a problem in relation with the *Pauli exclusion principle*. This principle inhibits more than one quark to be in a specific state, while this seemed necessary for some hadrons. In order to solve this problem, an additional degree of freedom had to be introduced for quarks; *color*. The resulting color currents became the natural sources for the forces among quarks that hold them together to form hadrons. Starting as a mnemonic for cataloging the large number of hadrons, quarks have evolved into the fermionic components of a very rich theory known as quantum chromodynamics (QCD), the theory of quarks and gluons in which hadrons are its bound states.

QCD is a quantum field theory based on a local $SU(N_c)$ gauge symmetry of quarks, with $N_c = 3$ being the number of colors. The gauge field of QCD, that mediates the interaction between charged quarks, is called the gluon field. As in most quantum field theories, calculations involve infinities which have to be removed. In order to use the theory, they have to be removed. This involves a subtraction of the infinities at a specific scale. In this process, most relevant objects of the theory acquire a energy scale dependence. One of these objects is $\alpha_s(Q)$, a measure of the strength of the interaction between quarks and gluons as a function of the scale Q . In the form that QCD takes care of the hadronic sector of the standard model, the theory appears to be *asymptotically free*. This means that the scale dependence of $\alpha_s(Q)$ is such that the interaction strength vanishes gradually as the energy scale is increased. This is of great value in what are called *perturbative calculations*. In this type of calculation quarks are assumed to be free particles and their mutual interaction by means of gluon exchange, is treated as a small correction to this free state. The order of α_s corresponds to the number of gluon exchanges taken into account. The smallness of $\alpha_s(Q)$ at sufficiently large scales, legitimates neglecting higher orders in $\alpha_s(Q)$. The property of asymptotic freedom is seen as a charm of the theory, as high-energy experiments seem to be well described by models based on the notion of free quarks.

In spite of the beauty of the theory and its ability to explain many hadronic phenomena, the main players of the theory themselves, quarks and gluons, have never been detected. This is accepted as a phenomenological aspect of the theory and carries the name of *confinement*. How confinement comes about exactly in the theory, is not understood yet. A complete understanding of this fact will probably encompass the description

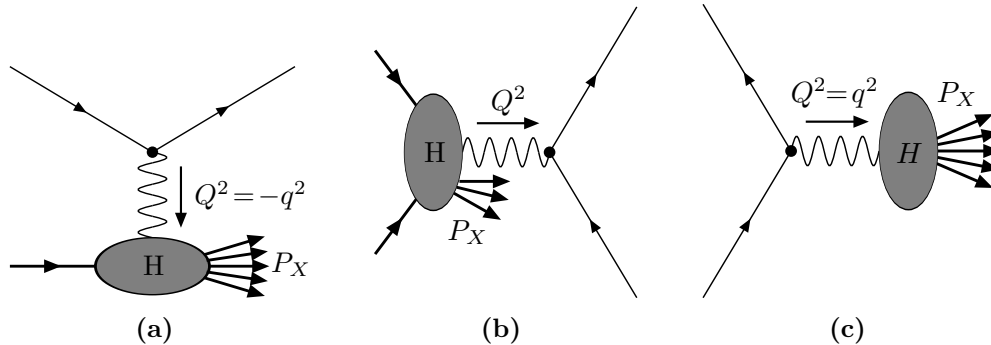


Figure 1.1: Examples of hard electro-weak processes. (a) An electron scatters off a nucleon. (b) A lepton anti-lepton pair is created in the collision of two hadrons. (c) A lepton and an anti-lepton annihilate into hadrons.

of hadrons as bound states of QCD. Until this happens, we will mainly rely on experiment to gain knowledge about the constitution of hadrons in terms of quarks and gluons. For this purpose, there is a class of processes that is very suitable which we will discuss in the next section.

1.2 Hard electro-weak processes and hadrons

In this thesis an *electro-weak* process will refer to a scattering process in which a leptonic system interacts with a hadronic system. Due to the nature of leptons, all their interactions have to be mediated by electro-weak bosons. The best-known examples of electro-weak bosons are photons, but they might as well be W^+ , W^- or Z^0 bosons. Electro-weak interactions are characterized by a small coupling constant, meaning that processes involving the smallest possible amount of boson exchanges gives the most important contributions. As we are interested in hard electro-weak processes, in which momentum transfer will be large, the description in terms of a *single* boson exchange will be a very good approximation.

Detecting the leptons, or extracting them from a beam with known energy, completely fixes the leptonic system and therefore the momentum, say a momentum q , carried by the electro-weak boson. This enables us to select only those events for which the relativistic invariant $Q^2 = \pm q^2$ is a large number compared to any of the masses of the hadrons under study. When this is the case, we will call the electro-weak process *hard*. This large scale compared to intrinsic hadronic scales, will be our theoretical handle for studying hadronic structure.

There are several ways for effectuating hard processes that can be of use to us. A very well-known example is the scattering of an electron off a proton and detecting the electron after delivering the hard momentum. The proton is usually obliterated and many new particles can be created. For this reason, this process is known as deep inelastic scattering (DIS) and it is shown schematically in figure 1.1(a). Another example of a hard electro-weak process is colliding two hadrons with a large center of mass energy and detecting a lepton anti-lepton pair that carries a large fraction of this center of mass energy. This type

of process is shown in figure 1.1(b) and is known as the Drell-Yan (DY) process. Similarly, one could collide an electron and an anti-electron, at large center of mass energy and detect hadrons emerging from the collision with a center of mass energy of the same order. This lepton anti-lepton annihilation process is shown in figure 1.1(c).

Studying figures 1.1(a)-(c) one sees some similarity among the three examples. In all cases a single (hard) boson connects the leptonic to the hadronic system. When writing down the cross-section this is reflected in the fact that it can be written as a product of a *leptonic* and a *hadronic* tensor. The leptonic tensor describes the emission or absorption of the electro-weak boson by the leptons and can be simply calculated. The hadronic tensor is the part that describes how the hadron deals with the hard boson. This object is much more difficult to calculate.

In specifying the hadronic tensor we can find some help in the fact that out of the quarks and gluons that make up hadrons, only quarks carry electro-weak charge and thus couple to the electro-weak boson. At the origin of lepton-hadron scattering one has lepton-quark scattering. Lepton-annihilation into hadrons has to be connected to lepton-annihilation into a quark anti-quark pair. Hard lepton-pair production in hadron-hadron scattering is connected to quark anti-quark annihilation. In fact, for each hard lepton-hadron process one can point out a lepton-quark analogue. As the quark-lepton sub-process is a hard process, we can apply *perturbative* QCD (pQCD) and calculate this sub-process with high precision. A problem remains in connecting the hard sub-process to our real-life hadron-lepton process.

An *ad hoc* connection is made in the surprisingly successful Parton Model [Bjor69, Feyn72] in which a probability for finding the quark in the hadron, or a hadron in a quark, is introduced. This probability is multiplied with the probability of the corresponding quark-lepton sub-process to obtain a cross-section for the process. This model has been very successful in explaining much of the phenomenology of hard scattering and played a very important role in the consolidation of the concept of quarks. The introduction of this two-step description of the scattering process can be motivated intuitively by assuming that at the scales that characterize the hard sub-process, a hadron is not capable to react. The reaction of the hadron to the hard sub-process is something happening at much slower time-scale. Only the availability of the parton within the hadron is of relevance to the cross-section.

This separation is known by the name of *factorization* and its realization in field theory is not straight-forward. Its goal is to write the hadronic tensor as a product of a hard part, which we can calculate accurately, and a soft part which summarizes the role played by the hadron in the hard process.

1.3 QCD and hard processes

An exact QCD description of interactions involving hadrons is at present beyond our capabilities. An infinite tower of equally important matrix elements of quarks and gluons evaluated between hadronic states have all to be considered when calculating the cross-section for the process. By looking at hard electro-weak processes substantial simplification can be attained.

In hard electro-weak processes the description simplifies in two important ways. First,

having a large scale available in the hard part, it makes sense to make an expansion of the process cross-section in inverse powers of this large scale, Q . Restricting the description up to a specific order in $1/Q$, results in a significant reduction in the number of contributions that have to be considered. Second, the fact that the hard scattering is dominated by a large scale enables us to profit from the asymptotic freedom of the theory and we can apply a perturbative approach in calculating the hard part. Limiting the accuracy to a specific power in $1/Q$ and using the smallness of $\alpha_s(Q)$, allows us to rearrange contributions in such a way that the cross-section can be written as a single product, or a sum of products, of hard and soft parts. The hard part is completely independent of all small-energy or large-distance scales, while the soft parts contain dependence only on those scales.

The value of this procedure becomes apparent when, after contraction of the factorized hadronic tensor with the leptonic tensor, a connection results between the experimentally measured cross-section and the soft object. For unpolarized inclusive DIS, the process for which the Parton Model was so successful, the emerging soft objects are the parton distribution functions. In the model this object is introduced *ad hoc*, while in a field theoretical framework, the object emerges in a much more intricate formulation in the operator product expansion.

For hadrons in the initial state the soft parts result in parton *distribution functions*. Depending on target polarization and nature of the hard process, all the ways in which the hadron can contribute to the hard process are encoded in a complete, rather small, set of functions. The functions depend on a particular momentum fraction, and are universal depending only on the type of parton and the parent hadron involved. For hadrons in the final state, a similar set of soft objects can be written down. In this case, they are called parton *fragmentation functions* and they form a set analogous to that formed by distribution functions. The appearance of these functions in the hard process referred to in section 1.2, is summarized in figures 1.2(a)-(c)

The dependence of these functions on a single variable, corresponding to *one* particular momentum fraction, reflects the relevance of a single direction in space-time for the hard process. The information contained in these functions is related to correlations between quark and gluon fields along this very specific direction. This direction corresponds to the mass-less approximation of the parent hadron momentum that can be constructed from the original hadron momentum and the hard boson momentum. Given the high virtuality of the exchanged boson, hadrons can be considered as mass-less particles. For this reason, the correlations encoded in the soft functions are often denoted as light-cone correlations. We will refer to the set of functions that only takes light-cone correlations into account, as the collinear set of functions.

In the same way as the hard boson momentum flowing through the hard part selects correlations along a specific direction, the same mechanism suppresses correlations along another direction. The two remaining dimensions of space-time are in fact unaffected and denoted as *transverse* directions. When more than a single hadron is involved in the hard process, it becomes possible to extract structural information in these directions.

A prerequisite for this is that the hadrons under study have momenta that are *hard* with respect to each other. This is the case when the two hadron momenta have an invariant product of the order of the hard scale. If this is the case, it is an indication that the two soft parts corresponding to each hadron, kinematically separated, are connected by a hard partonic sub-process. The factorized cross-section has the form of a prod-

uct of soft objects each involving one hadron but carrying some azimuthal dependence. Both hadrons, having negligible masses compared to the hard boson scale, can again be considered to be mass-less. The correlations encoded in their respective distribution or fragmentation functions correspond to correlations along different light-cone legs.

This configuration, in which the partonic correlations of two hadrons on *different* light-cone legs are connected by a hard sub-process, will give us a chance to extract more information than is possible with a single hadron. In general, the parton momentum will not be completely collinear with respect to the hadron momentum and will have components along the transverse direction, when being struck or when fragmenting into a hadron. This non-coplanarity that can be measured at the hadronic and hard boson level, can be used to extract additional correlations off the light-cone, which otherwise would average out. This additional information results in distribution and fragmentation functions that now not only depend on the longitudinal momentum fraction, but also on the parton momentum in the two transverse directions. The number of functions is larger than in the collinear case.

Experimentally, it is not possible to extract the full transverse momentum dependence of the new functions. By weighting the cross-section with a non-coplanar part of a hadron momentum it is possible to extract an asymmetry in which transverse-momentum weighted moments of these new functions can appear. The transverse moments also depend on a single longitudinal momentum fraction. Though these functions depend on the same variable as the old set they encode different information than the ones present in the collinear set. This additional information can only appear suppressed with an extra factor of $1/Q$ when azimuthal asymmetries are ignored.

The soft functions do not only depend on the single longitudinal momentum fraction and possibly transverse momentum. On top of this dependence there is a logarithmic dependence on the scale Q that is of perturbative origin. The dependence on the scale Q can accurately be calculated as an expansion in the coupling constant α_s . This dependence is of importance for relating the values of these functions in different experiments, which generally will involve measurements at different values of Q^2 .

In fact, some of the new non-collinear functions had been encountered in the past in studies [Bukh84b] of the Q^2 -dependence of the collinear functions that appear in the cross-section suppressed by factors of $1/Q$. In general, the structure of this Q^2 -dependence is complicated, due to many unknowns, and is of restricted applicability to experimental situations. An important simplification takes place in the limit of large number of colors. In this thesis we present, among other things, first results for the Q^2 -dependence of all new non-collinear functions that parametrize additional structure and that appear at leading order in $1/Q$ in the limit of large number of colors.

Outline

In chapter 2 we will discuss the separation of soft and hard parts in the cross-section for hard electro-weak processes in which one and two hadrons are detected. In chapter 3 we introduce the nomenclature and properties of the soft parts that we want to study in this thesis. In chapter 4 we derive inequalities that hold between leading order distribution functions at tree-level.

In chapter 5 we address the calculation of the scale dependence of distribution functions. In chapter 6 we study the scale dependence of non-collinear soft functions by

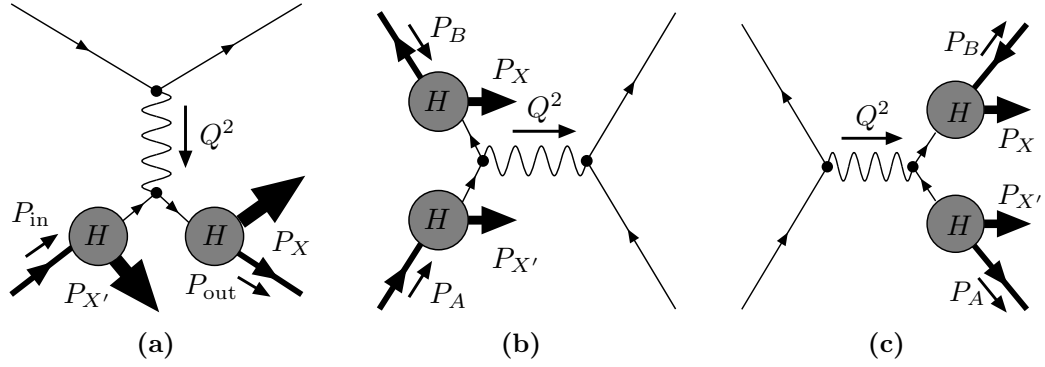


Figure 1.2: (a) Schematic representation of semi-inclusive deep inelastic scattering. (b) Schematic representation of lepton pair creation in hadron-hadron collision. (c) Schematic representation hadron fragmentation from lepton pair annihilation.

combining the scale dependence of $1/Q$ suppressed collinear functions in the large N_c limit, with relations following from the equations of motion and Lorentz-invariance. In chapter 7 the results of an independent calculation of scale dependence for all polarization states of the parent spin 1/2 hadron, are presented, taking into account quark transverse momentum. In chapter 8 we discuss these results and present an outlook beyond these investigations.

Factorization

2.1 Introduction

Factorization of the cross-section for a hard process in which hadrons are involved, refers to the separation of the cross-section into *hard* and *soft* parts. A cross-section is said to factorize to a specific order in $1/Q$, where Q is the large scale characterizing the hard process, when all contributions that are relevant up to this order, can be incorporated into products of hard and soft parts. The hard part describes a short time-scale, small-distance sub-process. It is characterized by the large momentum scale, Q , and is independent of any small invariants such as masses. The soft parts, on the other side, contain all the large-distance, long time-scale physics and summarize the role played by hadrons in the hard process. The soft parts contain the physics that connects the parent hadron to a specific parton, but is independent of the hard process.

The reason for pursuing a separation of hard and soft physics stems from the success achieved by the naive parton model. The model was originally developed to describe inclusive DIS and is based on incoherence between the hard scattering process and the soft physics that controls the dynamics of the hadronic bound state. In the naive parton model factorization is *postulated*. A hadron is regarded as a source of partons, whereas the partons participate independently in the hard scattering. This simple assumption led to results that explained experimental phenomena that were not understood at the time. It also led to predictions, concerning the nature of these partons, that were confirmed later. In a sense, experiment indicated that something like factorization was taking place when hadrons took part in hard scattering processes.

Considering the fact that hadrons are subject to the strong force and therefore its constituents as well, it is surprising that such incoherence is observed at all. One would expect this incoherence to be invalidated by mutual interaction of the constituents of hadrons. The property of asymptotic freedom of QCD provides a basis for sustaining a separation of hard and soft physics. In a QCD bound state, partons can participate in a hard sub-process being approximately insensitive to their hadronic surroundings, at least over the short time-scales or across the small-distances that are characteristic to the hard process.

The embedding of the ideas of the naive parton model in QCD, known by the name of

the "pQCD-improved parton model", was extended to other processes besides inclusive DIS, that had a partonic sub-process at their basis. Each detected hadron participating in the hard process is described by a corresponding soft function. The hadron itself is replaced by a parton in the hard process and the resulting cross-section is calculated using perturbation theory in the coupling constant. Due to the inclusion of interactions, the soft objects have to be redefined with respect to the soft objects in the naive parton model. Although the soft objects remain unspecified, and have to be extracted from experiment, they are defined consistently within a quantum field theoretic framework. They are universal objects that summarize the role played by hadrons in hard processes and can be extracted with systematically improvable accuracy.

A difficulty that was initially disregarded in the pQCD improved parton model is the effect of soft momentum gluons when more than a single hadron participates in the hard process. This type of contributions can lead to a break-down of factorization and is therefore important. Studies of these contributions have led to *factorization theorems* which enable one to write the cross-section in the desired factorized form under specific circumstances.

When more than one hadron is detected in a hard process, it is possible to obtain in the cross-section soft structure that has been disregarded in collinear treatments [Jaff91]. In chapter 3 we will define the nomenclature for this structure at tree level. In chapter 5, we will address the effect of including interactions in the hard part on these soft parts. Results of these studies will be presented in the chapters 6 and 7. In this chapter we will introduce the ideas of the naive parton model and discuss their extension to QCD.

2.1.1 The naive parton model

The naive parton model is best explained looking at the experiment it was introduced for, inclusive DIS. The experiment involves the scattering of an energetic lepton off a target proton and detecting the scattered lepton. As the lepton momentum is known both in the initial and final state, the momentum delivered to the target hadron can be reconstructed. This process, shown in figure 1.1(a), is determined by two momenta: The target hadron momentum P , and the momentum transferred by the lepton, q . The hadronic tensor, describing how a hadron deals with the momentum transfer by means of a single photon, has for an unpolarized hadron with momentum P , the form

$$W^{\mu\nu}(P, q) = \frac{1}{4\pi} \int d^4y e^{iq \cdot y} \langle P | [J^\mu(y), J^\nu(0)] | P \rangle. \quad (2.1)$$

It is symmetric in the current indices μ and ν , as the hadron is unpolarized, and due to electro-magnetic charge conservation the tensor should satisfy $W^{\mu\nu}q_\nu = 0$. As the energies involved increase, besides photons also weak vector-bosons can be exchanged between the leptons and the hadron. Restricting to photon exchanges the hadronic tensor can be parametrized in terms of two tensor structures multiplied by real functions that depend on the invariants that can be formed from P and q . Introducing the vector \tilde{P}^μ for a shorter notation

$$\tilde{P}^\mu \equiv P^\mu - \frac{P \cdot q}{q^2} q^\mu, \quad (2.2)$$

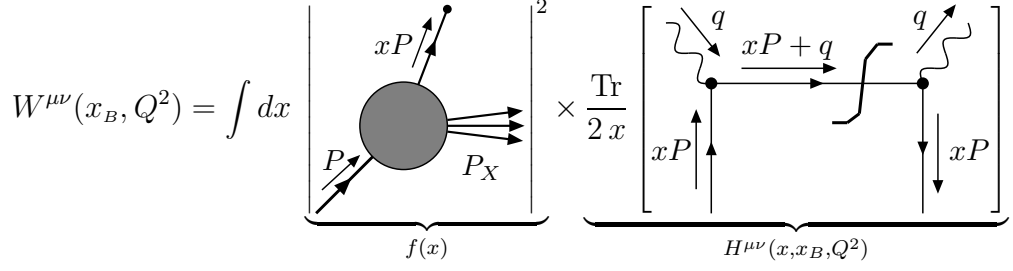


Figure 2.1: Schematic representation of the parton model description of unpolarized inclusive DIS. A probability density $f(x)$ is convoluted with the spin-averaged scattering of a spin-1/2 parton.

the hadronic tensor can be written as

$$W^{\mu\nu}(P, q) = \left(\frac{q^\mu q^\nu}{q^2} - g^{\mu\nu} \right) F_1(x_B, Q^2) + \frac{\tilde{P}^\mu \tilde{P}^\nu}{P \cdot q} F_2(x_B, Q^2) \quad (2.3)$$

As the hadron has a fixed mass $P^2 = M^2$, where M is the mass of the hadron, the functions can only depend on the invariants $P \cdot q$ and Q^2 . The former is traded in for the so-called Bjorken scaling variable

$$x_B = \frac{Q^2}{2P \cdot q}. \quad (2.4)$$

One of the physical phenomena that initially could not be explained [Bloo69] was the *scaling* of the structure functions. At large enough values of Q^2 the structure functions $F_1(x_B, Q^2)$ and $F_2(x_B, Q^2)$, ceased to show dependence on Q^2 , retaining only dependence on x_B . This was an unexpected result. For a quantity, assumed to arise from a local homogeneous distribution of matter, a decrease as $1/Q^2$ was expected.

This lack of dependence on Q^2 of the structure functions F_1 and F_2 could be reproduced in the parton model. The model introduces the notion of a parton that takes part in the hard scattering. In a sense, factorization was postulated by describing the process in two steps. There is the scattering of a parton that carries a momentum fraction $0 < x < 1$ of the parent hadron, and the hadron is described by a probability $dx f(x)$ of a parton with momentum fraction between x and $x+dx$ is found. This division is shown schematically in figure 2.1. The hard scattering part, chosen with hindsight, describes a spin-1/2 particle with charge e absorbing the hard photon and fragmenting into the final state, without interacting with the parent hadron. If the parent hadron mass is neglected, that is $P^2 = 0$, one finds for the hadronic tensor

$$\begin{aligned} W^{\mu\nu}(x_B, Q^2) &= e^2 \int dx f(x) \frac{1}{2} \text{Tr} [P \gamma^\mu (xP + \not{q}) \gamma^\nu] \theta(x - x_B) \delta((xP + q)^2) \\ &= \left(\frac{q^\mu q^\nu}{q^2} - g^{\mu\nu} \right) \underbrace{e^2 f(x_B)}_{F_1} + \frac{\tilde{P}^\mu \tilde{P}^\nu}{P \cdot q} \underbrace{2x_B e^2 f(x_B)}_{F_2}. \end{aligned} \quad (2.5)$$

Integrating over all parton momentum fractions x one finds that the structure functions

$$F_1(x_B, Q^2) = e^2 f(x_B) \quad (2.6)$$

$$F_2(x_B, Q^2) = 2x_B e^2 f(x_B), \quad (2.7)$$

reflect the parton distribution functions $f(x_B)$ in which x_B represents the parton momentum fraction. Besides the fact that the structure functions are independent of Q^2 , a relation between the two functions,

$$F_2(x_B) = 2x_B F_1(x_B), \quad (2.8)$$

known as the Callan-Gross relation [Call69], holds. This relation stems from the fact that the partons are spin-1/2 particles, and its experimental verification is considered as evidence for the reality of quarks.

Note that the structure functions F_1 and F_2 are only of relevance for unpolarized inclusive DIS and meaningless for other hard electro-weak processes. In contrast, the function $f(x)$, an example of a *distribution function*, is independent of the process and of broader applicability than inclusive DIS. It is a property of the hadron. It can appear in the cross-section in any process in which a hadron of the same type plays a similar role.

Asymptotic freedom in QCD opens the door for embedding the ideas of the parton model in a realistic theory of hadrons. The identification of the spin-1/2 partons of the naive parton model, with the quarks of QCD leads to significant modification of the concepts of the naive parton model.

2.2 Factorization in quantum chromodynamics

In a QCD framework, the probability density of the naive parton model, denoted by $f_1(x)$, has to arise from hadronic matrix elements containing quark and gluon fields. The longitudinal momentum dependence present in the object $f_1(x)$, indicates non-locality being involved in its definition in terms of field operators. While the physical picture of the parton model, promotes a non-local product of only quark fields as the source for $f_1(x)$, this cannot be the complete picture, as a non-local product of only quark fields is not color-gauge invariant, in general. The hadronic matrix element involving only quark fields has to be supplemented with other hadronic matrix elements involving an arbitrary amount of gluons, in order to construct a universal object like $f_1(x)$. It is only for particular choices of the gauge, that it is possible to trace back a distribution function to a matrix element involving only quark fields.

The inclusion of these interacting fields also has a profound impact on the notion of factorization. Interactions among quarks and gluons lead to a necessary redefinition of parton distribution functions which results in invalidation of exact scaling. Besides a dependence on a momentum fraction x , parton distribution functions acquire an additional dependence on a renormalization scale μ . Distribution and fragmentation functions are said to *evolve* with the scale μ .

For some observables in which no distinction is made between different flavors of quarks, flavor-singlet objects, it might be even inconsistent to consider a single scale-dependent distribution function. A well-known example is the mixing under evolution of the flavor-singlet unpolarized and longitudinally polarized quark and gluon distribution functions.

The massless nature of quarks and gluons complicates the feasibility of factorization of many interesting cross-sections. Divergences related to this massless nature of the fields invalidate factorization in several cases when high enough inverse powers of the hard

scale are considered. Failure of factorization beyond $1/Q^4$ for Drell-Yan has been shown [Dori80, Liet81, Basu84].

Although the degree of complexity rises by embedding the parton model in QCD, there are many gains from this effort. It leads to a redefinition of the soft objects in a way that they are consistent with field theory. The phenomenon of scaling violation, that is necessary when defining parton distribution functions in an interacting field theory, has been confirmed experimentally. This is often presented as strong evidence for the reality of QCD. Knowing the scale dependence of soft objects allows us to relate soft parts being measured in different events in the same experiment, or the same experiment under different conditions, even in the case of different processes.

Another gain of a full field-theoretic treatment is that such a description allows us to consider *power corrections*, contributions that are suppressed by powers of $1/Q$, within the same framework. By fully understanding these corrections, we can gain knowledge about how partons interact with their parent hadron, and learn more about how QCD bound states arise.

There are two approaches to factorization in QCD. The first is based on the operator product expansion (OPE), and expands the non-local matrix elements in terms of local ones. It has a firm base in perturbation theory but is assumed to work for non-local operators between hadronic states as well. The second approach is the diagrammatic one, and retains the non-locality of the matrix elements, though rearranges it into a complete set of objects of specific relevance. Both approaches are equivalent when both are applicable, but the second bears more similarity with the ideas of the parton model.

2.2.1 The operator product expansion

The traditional approach to factorization in QCD has been based on the OPE. The hadronic tensor in equation (2.1) can be related to the forward Compton amplitude

$$W^{\mu\nu} = \frac{1}{2\pi} \text{Im} \{T^{\mu\nu}\} = \frac{1}{2\pi} \text{Im} \left\{ i \int d^4x e^{iq \cdot x} \langle P | T J^\mu(x) J^\nu(0) | P \rangle \right\}, \quad (2.9)$$

by making use of the optical theorem. The time-ordered product appearing in $T^{\mu\nu}$ is subjected to a light-cone expansion around $x^2 = 0$, which takes the form, deleting the indices on the currents for clarity,

$$TJ(x)J(0) = \sum_{i,n} C_n^{(i)}(x^2) x^{\mu_1} \dots x^{\mu_n} \mathcal{O}_{\mu_1 \dots \mu_n}^{(i)}(0). \quad (2.10)$$

The time-ordered product has taken the form of a sum of terms, of which each is a product of a singular coefficient function $C_n^{(i)}(x^2)$, multiple factors of the expansion variable x^{μ_i} and a *local* operator $\mathcal{O}_{\mu_1 \dots \mu_n}^{(i)}(0)$. In order for the operators to be in an irreducible representation of the Lorentz group, they can be chosen symmetric in their (expansion) indices and traceless. In contrast to a regular Taylor expansion all operators with equivalent Lorentz structure and dimensionality have to be included. In the case of inclusive DIS there are two classes of operators contributing to leading order in $1/Q$. There are operators involving quark fields, and covariant derivatives $D^\mu = \partial_\mu - igA_\mu$,

$$\mathcal{O}_{\mu_1 \dots \mu_n}^q(0) = i^{n-1} \mathcal{S}_{\{\}} \bar{\psi} \gamma_{\{\mu_1} D_{\mu_2} \dots D_{\mu_n\}} \psi, \quad (2.11)$$

and operators involving gluon operators,

$$\mathcal{O}_{\mu_1 \dots \mu_n}^g(0) = i^{n-2} \mathcal{S}_{\{\}} F_{\lambda\{\mu_1} D_{\mu_2} \dots D_{\mu_{n-1}} F_{\mu_n\}}^\lambda, \quad (2.12)$$

where the symbol $\mathcal{S}_{\{\}}$ stands for symmetrization of all indices between curly brackets and $F_{\mu\nu} = i/g[D_\mu, D_\nu]$ is the field strength. After evaluating these operators between hadronic states, the operators take the form,

$$\langle P | \mathcal{O}_{\mu_1 \dots \mu_n}^{(i)}(0) | P \rangle = \Theta^{(i)} [P_{\mu_1} \dots P_{\mu_n} - \text{traces}]. \quad (2.13)$$

The terms denoted by traces correspond to terms that include the metric tensor $g_{\mu\nu}$ and contractions P^2 , and receive additional suppression by powers of $1/Q$. After Fourier transformation, the forward Compton scattering amplitude can be written as,

$$T = \sum_{i,n} \tilde{C}_n^{(i)}(Q^2, \mu^2) \Theta_n^{(i)}(M^2, \mu^2) \left[\left(\frac{1}{2x_B} \right)^n + \mathcal{O} \left(\frac{M^2}{Q^2} \right) \right], \quad (2.14)$$

where $\tilde{C}_n^{(i)}$ is the Fourier transform of the coefficient function $C_n^{(i)}$. The expression for the forward amplitude has taken a factorized form where \tilde{C} only depends on the hard scale Q^2 and the renormalization scale μ^2 . The operator matrix element only depends on a small scale M^2 and the renormalization scale μ^2 .

Dimensional arguments determine the dependence on Q^2 of the Fourier transform of the coefficient function,

$$\tilde{C}^{(i)}(Q^2, \mu^2) = c_n^{(i)}(\ln(Q^2/\mu^2)) (Q^2)^{2+n-d[\mathcal{O}_n^{(i)}]}, \quad (2.15)$$

where $c_n^{(i)}(\ln(Q^2/\mu^2))$ is a dimensionless function of its argument, n is the number of indices for a symmetric traceless operator, and $d[\mathcal{O}_n^{(i)}]$ stands for the canonical dimension of the operator in the expansion, $\mathcal{O}_n^{(i)}$. An important quantity here, is what is called the canonical *twist*, $t = d[\mathcal{O}_n^{(i)}] - n$, of an operator, as it determines the magnitude of its contribution in the cross-section for large values of Q^2 . The pQCD improved parton model corresponds to taking into account all operators with $t = 2$.

Related by renormalization group invariance, the scale dependence of the soft parts can be derived from the scale dependence of the coefficient functions \tilde{C} . In the limit of $\mu^2 \rightarrow \infty$, the function c_n contributes effectively as some power of Q^2 ,

$$c_n^{(i)}(\ln(Q^2/\mu^2)) \propto (Q^2)^{\gamma_n^{(i)}}. \quad (2.16)$$

The quantity $\gamma_n^{(i)}$ is known as the *anomalous dimension* corresponding to the operator $\mathcal{O}_n^{(i)}$, modifying the power behavior from the canonical expectation that has been made explicit in equation (2.15). In the asymptotic limit, for QCD, the anomalous dimensions $\gamma_n^{(i)}$ vanish. The behavior of the renormalized operators resembles what is expected based on the canonical dimensions of the operators, a phenomenon referred to as the approximate scaling in QCD. The first non-vanishing term of the anomalous dimension is of order α_s ,

$$\gamma_n^{(i)} = d_n^{(i)} \frac{g^2}{16\pi^2} + \mathcal{O}(g^4), \quad (2.17)$$

and leads to the slow logarithmic dependence of the coefficient functions in the large energy limit,

$$\tilde{C}^{(i)}(Q^2, \mu^2) = N_n^{(i)} (\ln(Q^2/\mu^2))^{\frac{-d_n^{(i)}}{2\beta_0}}. \quad (2.18)$$

which is typical of an asymptotically free theory.

The OPE cannot be applied in processes in which soft objects take part but no operator product is present. An example of such a case is inclusive e^+e^- -annihilation into a hadron. For this case, an extension can be devised in terms of cut vertices [Muel74].

Connection of OPE to the parton model

The results of the rather formal analysis above, can be put in a form more reminiscent of the naive parton model. Once the scale dependence of the coefficient functions has been calculated perturbatively, it is possible to rearrange all scale dependence into *kernels*. These kernels connect the values of a structure function, generically denoted F , at a scale equal to μ^2 with its values at a scale μ_0^2 ,

$$F(x, \mu^2) = \int_x^1 \frac{dy}{y} K\left(\frac{y}{x}, \mu^2, \mu_0^2\right) F(y, \mu_0^2). \quad (2.19)$$

The kernel function is given by the expression,

$$K(z, \mu^2, \mu_0^2) = \frac{1}{2\pi i} \int_{c-i\infty}^{c+i\infty} dn z^{n-1} \frac{\tilde{C}_n(\mu^2)}{\tilde{C}_n(\mu_0^2)}, \quad (2.20)$$

while the structure functions are related to the coefficient functions and matrix elements by means of inverse Mellin transforms,

$$F(x, \mu^2) = \frac{1}{2\pi i} \int_{c-i\infty}^{c+i\infty} dn x^{1-n} \tilde{C}_n(\mu^2) \Theta_n, \quad (2.21)$$

and operator mixing has been neglected for simplicity.

By means of a rather formal detour of the OPE, one arrives at a more realistic picture of parton distribution functions. Parton distribution functions acquire a scale dependence that can be calculated perturbatively through calculation of the coefficient functions $\tilde{C}_n^{(i)}(\mu^2)$. Although the Θ_n cannot be calculated and have to be extracted from experiment, precise knowledge of their corresponding coefficient functions, makes it possible to reconstruct parton distribution functions with data from different experimental conditions.

Furthermore, when flavor-singlet quantities are considered, operator mixing extends the naive parton model notion of a quark distribution, to a hybrid system of quark and gluon distributions that cannot be considered separately. The quark and gluon distributions mix under evolution and cannot be considered separately without an artificial factorization-scheme dependent distinction.

2.2.2 Diagrammatic approaches to factorization

An alternative to the expansion into local operators is found in the diagrammatic approaches. These methods stem from attempts to achieve a partonic treatment of soft

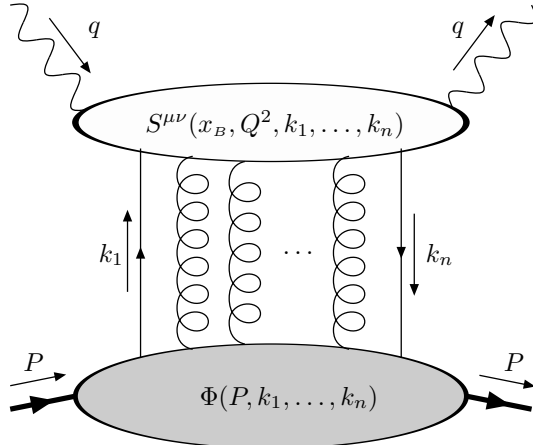


Figure 2.2: Generic diagram contributing to unpolarized inclusive DIS in which a hard part is connected to a soft part by some number of partons.

parts that are suppressed by a single power of $1/Q$ with respect to the leading order contribution. Seminal papers for this approach are those written by Ellis, Furmanski and Petronzio [Elli82, Elli83] in which unpolarized DIS is studied, and papers by Qiu and Sterman [Qiu91a, Qiu91b] in which order $1/Q$ contributions to polarized Drell-Yan are considered.

These diagrammatic methods are based on manipulations of diagrams, in which the relevant non-locality between the fields in hadronic matrix elements is retained, while less relevant non-locality is eliminated in favor of matrix elements involving more partons. Whether correlations are more or less relevant is determined by the suppression in powers of $1/Q$ that accompanies those structures in the cross-section.

A generic contribution to the hadronic tensor in unpolarized DIS has the form shown in figure 2.2, where an arbitrary number of quarks or gluons connect a hard and a soft part. The hard part $S^{\mu\nu}(k_1, \dots, k_n)$, describes how a number of partons with momenta k_1, \dots, k_n , take part in the hard interaction. It consists of the high energy limit of all diagrams that describe how the $n + 1$ partons take part in the hard process and can be calculated using perturbative techniques. The soft part, denoted by $\Phi(P, k_1, \dots, k_n)$, refers to a hadronic matrix element with quark and gluon fields carrying the momenta k_1, \dots, k_n . This is the part that determines the availability of these partons and it is assumed that all momenta connected to this soft part are soft. This means that all invariants that can be formed from the parent hadron momentum P and the parton momenta k_i are small compared to Q^2 .

From the hard boson and parent hadron momentum it is possible to construct a light-like approximation of the parent hadron momentum $P^2 = 0$. The softness of all partonic momenta implies that they are all approximately aligned along this direction. The parton momenta k_i^μ can be decomposed into a part collinear to this direction $x_i P^\mu$ and non-collinear part $(k_i - x_i P)^\mu$.

The most relevant correlations are obtained by expanding the hard part around a collinear alignment of all parton momenta,

$$S^{\mu\nu}(x_B, Q^2, k_1, \dots, k_n) = S_0^{\mu\nu}(x_B, Q^2, x_1 P, \dots, x_n P)$$

$$+ \sum_j \frac{\partial}{\partial (k_j - x_j P)^{\alpha_j}} S^{\mu\nu}(x_B, Q^2, k_1, \dots, k_n) \Big|_{\text{col}} (k_j - x_j P)^{\alpha_j} + \dots \quad (2.22)$$

For mass-less partons the only scale in the hard part is the hard scale Q^2 . From this, one concludes that the decreasing mass-dimensionality of the expansion coefficients through the differentiation, results in suppression by factors of $1/Q$. The first term in the expansion is therefore the leading one, and because of the collinear alignment of all the parton momenta in this first term, all non-collinearity in the soft part can be integrated over. After integration of all non-collinearity we are left with the object $\Phi(x_1, \dots, x_n)$ in which the reference to the parent hadron through P has been dropped. The leading part of this contribution to the hadronic tensor is given by,

$$w_n^{\mu\nu}(x_B, Q^2) = \int dx_1 \dots dx_n S^{\mu\nu}(x_B, Q^2, x_1, \dots, x_n) [\Phi(x_1, \dots, x_n) + \mathcal{O}(\frac{1}{Q})] \quad (2.23)$$

where the brackets $[[$ indicate that the parton spin components of hard and soft parts are still intertwined.

The parton spin structures of the hard and soft parts are disentangled by introducing a complete set of polarizers Γ_i such that $\Phi(x_1, \dots, x_i)$ is decomposed into a set of functions $f_j(x_1, \dots, x_i)$ of the collinear momentum fractions,

$$\Phi(x_1, \dots, x_i) = \sum_j \Gamma_j \Lambda^{D-D_j} f_j(x_1, \dots, x_i), \quad (2.24)$$

where D denotes the dimension of $\Phi(x_1, \dots, x_i)$ given by

$$D = \dim \Phi_n = \frac{3}{2}n_F + n_G - 2, \quad (2.25)$$

with n_F being the number of fermion fields in the matrix element and n_G the number of gluon fields. The quantity $\Lambda \ll Q$ denotes a scale of order of the hadronic mass. D_j is the dimension of the corresponding polarizer Γ_j . Projecting the hard part also on this basis of polarizers effectuates the separation of the parton polarization structures.

In order to give an example, we introduce two light-like, dimension-less vectors ζ^μ and η^μ such that

$$\zeta^2 = \eta^2 = 0, \quad (2.26)$$

$$\zeta \cdot \eta = 1. \quad (2.27)$$

The light-like nature of these vectors reflects the softness of the physics connected with hadrons, and we will identify the direction η^μ with the direction of the hadron momentum P^μ , such that

$$P^\mu = P \cdot \zeta \eta^\mu. \quad (2.28)$$

A soft parton momentum is then be represented by

$$k_i^\mu = x_i P \cdot \zeta \eta^\mu + \frac{(k^2 - k_T^2)}{2P \cdot \zeta x_i} \zeta^\mu + k_T, \quad (2.29)$$

where the transverse part of the momentum k is defined by

$$k_T^\mu = g_T^{\mu\nu} k_\nu \equiv (g^{\mu\nu} - \zeta^\mu \eta^\nu - \zeta^\nu \eta^\mu) k_\nu. \quad (2.30)$$

The invariants k^2 and k_T^2 are small compared to Q^2 , in order for the parton momentum to be soft. The properties (2.26) and (2.27) indicate that the vector ζ^μ can be used to project momentum components along the direction η . The longitudinal momentum fraction is defined in terms of this direction, absorbing a dimensional factor into the projector,

$$x_i = k_i^\alpha \left(\frac{1}{P \cdot \zeta} \zeta_\alpha \right) \equiv k_i^\alpha \tilde{\zeta}_\alpha. \quad (2.31)$$

Returning to our example, the contribution to the distribution function $f_1(x)$ from a matrix element $\Phi(k)$, containing only a quark field carrying momentum k , as shown in figure 2.3(a), can be written as

$$f_1(x) = \int d^4k \delta(k \cdot \tilde{\zeta} - x) \text{Tr} \left[\Phi(k) \frac{1}{2} \tilde{\zeta} \right]. \quad (2.32)$$

All parton momentum dependence in the hadronic matrix element $\Phi(k)$ is restricted by the delta function to the direction projected out by $\tilde{\zeta}$ and determined by the momentum fraction x . The polarizer Γ_i that extracts the function f_1 from $\Phi(k)$ is given by $\tilde{\zeta}/2$.

The light-like directions ζ and η , in inclusive DIS, are constructed from the hadron momentum, P , and the hard boson momentum, q . A soft parton with momentum along η absorbs the hard momentum q resulting in a quark with momentum along ζ going into the final state. In an arbitrary gauge, matrix elements with two quark fields and any number of gluon operators contribute at leading order in $1/Q$. In particular, matrix elements with any number of the operator $A \cdot \zeta$ contribute at leading order of $1/Q$. This infinity of matrix elements can be resummed into a gauge-link operator between the two quark fields, rendering a color-gauge invariant expression for the distribution function $f_1(x)$.

An important simplification can be achieved in the case of inclusive DIS by choosing a physical gauge in which the components present in the gauge-link operator, vanish. Choosing η as the hadronic correlation direction, the gauge condition

$$A \cdot \zeta = 0 \quad (2.33)$$

make the infinity of additional matrix elements vanish and the gauge-link operator reduce to unity. The only matrix element that then contributes to the distribution functions $f_1(x)$ is a matrix element containing two quark fields¹. In this case, one gets rid of the infinity of matrix elements with gluons polarized along η , and the gauge-link operator reduces to the identity. We will return to this subject in the next chapter.

With this choice of gauge, the suppression by a factor $(\Lambda/Q)^\tau$ in the cross-section of a specific soft part, is given by the formula

$$\tau = \frac{3}{2} n_F + n_G - 2 - \max \{ \mathcal{D}_i \}. \quad (2.34)$$

For unpolarized inclusive DIS, setting the quark mass equal to zero, this expression becomes [Furm81b, Elli82],

$$\tau = n_F + n_G - 2 + \frac{1}{2} [1 - (-1)^{n_G}], \quad (2.35)$$

¹Strictly speaking, this is only true when the contribution of a single quark flavor is considered.

ht

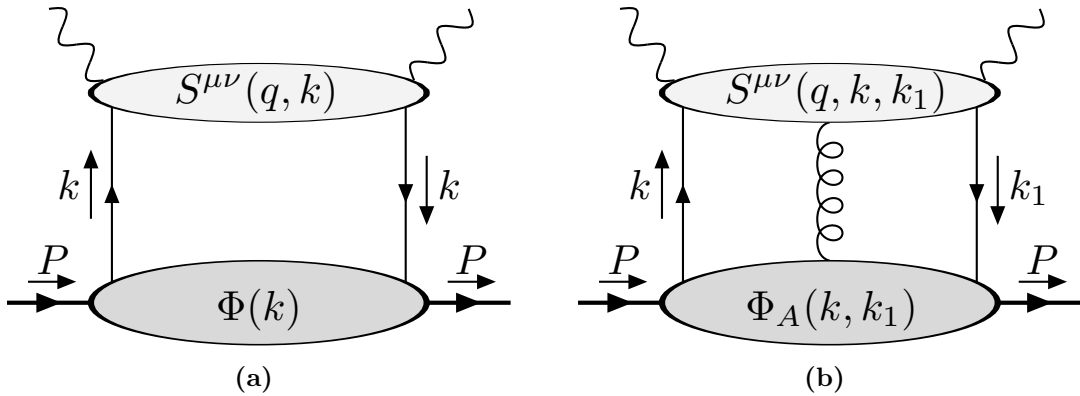


Figure 2.3: In a light-cone gauge all leading order in $1/Q$ contributions will come from diagram (a). Sub-leading contributions originate in diagram (a) and (b).

from which one can see that only even powers of τ appear. We will call this power τ corresponding to a specific non-local structure in a correlator, (non-local) *twist*. Although the term differs from the one with the same name in the OPE, this non-local twist determines the minimal suppression in powers of $1/Q$ that a soft part receives in the cross-section, based on the mass dimension of the soft part. For some soft functions, in particular collinear leading order functions, non-local twist-two can be made to correspond, by taking moments of the momentum fraction

$$\int dx x^n f(x), \quad (2.36)$$

to an infinite number of matrix elements containing only *local* twist two operators. For the non-collinear leading order functions, the relation is more complicated and is under investigation. Whenever we use in this thesis the term twist we will assume this 'working redefinition of twist' [Jaff95], and refer to the original term twist explicitly as *local* twist.

The consideration of *polarized* inclusive DIS, leads to Dirac and Lorentz structures in hadronic matrix elements that are not present in unpolarized scattering. Some of these structures are of such mass dimension, that they allow for contributions of order $1/Q$ in the cross-section, even in the case of vanishing quark mass. From such a diagrammatic analysis follows, that, in a suitable light-like gauge and only considering flavor non-singlet contributions, a calculation of the cross-section to order $1/Q$, only involves two diagrams. All leading order contributions arise from the diagram shown in figure 2.3(a). Sub-leading contributions, suppressed by a power of $1/Q$, arise in the diagram of figure 2.3(a) and in the diagram of figure 2.3(b) containing an additional gluon field. Due to the choice of gauge, it is the transverse components of the gluon field that have to be considered and are selected by the polarizer.

Perturbative corrections

In order to define the hard and soft parts in a way consistent with an interacting field theory, an analysis beyond tree level is necessary. The contribution shown in figure 2.4,

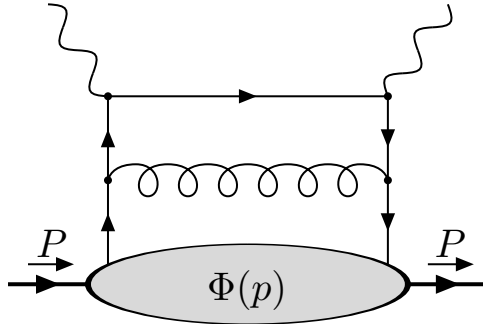


Figure 2.4: Example of a perturbative correction to inclusive DIS.

for instance, has to be taken into account as it contributes at leading order in $1/Q$. One could argue, due to asymptotic freedom and the fact that this diagram is order α_s , that its contribution is not very important. On the other side, due to the massless nature of quarks and gluons, divergences are generated in specific loop momentum integration regions leading to the appearance of large logarithmic contributions. Such a large logarithm that accompanies each occurrence of α_s can spoil an expansion in orders of α_s .

The solution of this problem is known as the *factorization of mass singularities* [Eli79a] and involves a redefinition of the soft parts. These corrections, containing logarithmic divergences connected to the massless nature of partons, not belonging in the hard part, are absorbed in the soft parts. A treatment to all orders in α_s for the case of unpolarized DIS is investigated in [Curc80b]. The redefinition of the soft parts leads to a logarithmic scale dependence,

$$\frac{d}{d \ln \mu^2} f(x, \mu^2) = \frac{\alpha_s(\mu^2)}{2\pi} \int_x^1 \frac{dy}{y} P\left(\frac{y}{x}, \alpha_s(\mu^2)\right) f(y, \mu^2), \quad (2.37)$$

in which the kernel, $P(y, \alpha_s(\mu^2))$, can be calculated order by order in α_s with increasing accuracy. We will return to the calculation of this dependence in chapter 5.

2.3 Factorization theorems

A consistent separation of hard and soft physics within an interacting field theory description, of the description of how hadrons participate in hard electro-weak processes, leads to a substantial modification of the concepts of the naive parton model, which formed the motivation for the separation. The soft parts are renormalized in order to absorb the mass divergences generated by perturbative corrections in the hard parts, and results in a perturbatively calculable scale dependence. Theorems exist that allow one to write the cross section for several processes in terms of these soft and hard parts.

The leading order in $1/Q$ contributions to the cross-section for inclusive unpolarized DIS can be written in the following form,

$$\frac{d\sigma}{dx_B dQ^2} = \int_{x_B}^1 \frac{dx}{x} \sum_a f_a(x, \mu^2) H_a\left(\frac{x_B}{x}, \frac{Q}{\mu}, \alpha_s(\mu^2)\right), \quad (2.38)$$

where a sum over parton types a is performed. The soft functions f_a denote parton distribution functions that depend on a longitudinal momentum fraction x and some scale μ^2 . The hard part H_a is characteristic for the type of parton a . Here, in order to concentrate on the physics of the hadronic tensor, the leptonic tensor has been contracted into the hard part and redundant leptonic degrees of freedom have been integrated over. The hard part depends on x_B , on the *factorization* scale Q , the renormalization scale μ and the coupling constant α_s . Note that the μ -dependence is artificial, introduced by renormalization, and the full derivative to μ of the left side vanishes. In practice, renormalization and factorization scales are set equal in order to obtain a more transparent description. Here we keep them different to reflect the different meaning of both scales. A factorization scale should be large enough compared to hadronic scales in order to be useful. The factorization scale is usually taken to be the scale characterizing a hard process.

Similarly, the leading order contribution to the cross-section for lepton anti-lepton annihilation into a single hadron, can be written in the form

$$\frac{d\sigma}{dz_h dQ^2} = \int_{z_h}^1 \frac{dz}{z} \sum_a H'_a\left(\frac{z_h}{z}, \frac{Q}{\mu}, \alpha_s(\mu^2)\right) D_a(z, \mu^2), \quad (2.39)$$

but where now the momentum fraction of the parton with respect to the fragmenting hadron is given by the expression

$$z_h = \frac{2P_h \cdot q}{Q^2}, \quad (2.40)$$

and the soft object $D_a(z, \mu^2)$ denotes a scale dependent fragmentation function.

The symbols $f_a(x)$ and $D_a(z)$ are often used to denote the distribution and fragmentation functions respectively, of *unpolarized* quarks in and into an *unpolarized* hadron. Experimental conditions can give a handle on parton and hadron polarization, allowing for the extraction of different soft parts than only the fully unpolarized functions mentioned above. The unpolarized functions are used here in a generic way in order to write down the factorization theorems. Identical theorems apply for polarized functions.

In principle, when only a single hadron is present, there are three distribution functions at *leading order* in $1/Q$ for a spin-1/2 hadron, that encode parton and hadron polarization. Two functions, $f_1(x, \mu^2)$ and $g_1(x, \mu^2)$, describe unpolarized quarks in an unpolarized hadron and the longitudinal polarization asymmetry of quarks in a longitudinally polarized hadron. A third function, $h_1(x, \mu^2)$, also describes the polarization asymmetry of quarks in a polarized hadron, but now along a direction *transverse* to the longitudinal direction determined by the hard process, while the hadron is also polarized in this direction. The last function $h_1(x, \mu^2)$ differs from the first two in being *chirally odd*. Any finite order diagram contributing to the hard part, disregarding quark masses, conserves chirality. As a consequence $h_1(x, \mu^2)$ can only appear with a suppression factor m/Q in the cross-section equation (2.38).

Analogously, sets of distribution and fragmentation functions can be defined for hadronic matrix elements involving only gluon fields. In general, both quark and gluon distribution and fragmentation functions have to be considered on the same footing. Simplification occurs when only flavor non-singlet quantities or chiral odd objects are considered. Disregarding quark masses, the hard parts cannot change quark chirality and furthermore they

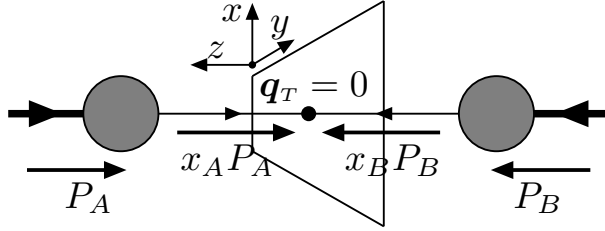


Figure 2.5: Schematic representation of the Drell-Yan process in a collinear approximation

preserve total quark flavor. As a consequence, pure gluonic contributions are of no relevance in these cases. In this thesis, we will only look at flavor non-singlet soft structure, allowing us to discard pure gluonic contributions and therefore simplify the description needed.

2.4 Two-hadron processes

The factorized form of the cross-sections in the last section can be extended to processes that depend on the soft physics of *two* hadrons. In order to separate soft and hard physics it is necessary that the hadrons are hard with respect to each other. Two hadrons are hard with respect to each other when the invariant product of the momenta of the two hadrons is of $\mathcal{O}(Q^2)$, where Q is the large scale characterizing the hard process. When this is this case, the contributions to the cross-section that are leading order in $1/Q$, arise from contributions in which a single parton emerges from each hadron and takes part in the hard process.

As in the single hadron case, a picture in which each hadron is replaced by a quark that takes part in the hard process, is complicated by the presence of soft gluons. The diagrams in which they appear contribute at the leading orders in $1/Q$ and thus cannot be disregarded. Careful analysis of all possible contributions of this type leads in several cases to either their cancellation or leads to a regrouping of these contributions, such that the cross-section can be written in the desired factorized form.

Considering the Drell-Yan process to be more specific, the large scale Q originates from the large center of mass energy with which two hadrons collide. A quark from one hadron annihilates with an anti-quark in the other hadron, while both partons carry a momentum fraction of $\mathcal{O}(1)$. The boson resulting from the annihilation decays into a lepton anti-lepton pair with a total momentum squared equal to Q^2 . In a frame in which $x_A \vec{P}_A + x_B \vec{P}_B = 0$, one could picture the lepton-pair to originate in the center of figure 2.5. In this figure the parton originating from hadron A has momentum $x_A P_A$ and the parton originating from hadron B has momentum $x_B P_B$. The partons are represented in the figure as if they were *collinear* to their parent hadrons. In general, this is not the case. The two hadron momenta and the hard boson momentum will not lie in the same plane. On the other side, if the cross-section is measured only in terms of the scaling variables x_A and x_B and Q^2 , in other words, all non-coplanarity is averaged over, the leading order contribution arises from this approximation. The cross-section can be put in the following

form,

$$\frac{d\sigma}{dx_A dx_B dQ^2} = \int_{x_A}^1 \frac{d\xi_A}{\xi_A} \int_{x_B}^1 \frac{d\xi_B}{\xi_B} \sum_{ab} H_{ab}''' \left(\frac{x_A}{\xi_A}, \frac{x_B}{\xi_B}, \frac{Q}{\mu}, \alpha_s(\mu) \right) f_a(\xi_A, \mu) f_b(\xi_B, \mu). \quad (2.41)$$

Although the analysis is more complex than the situation including only one hadron, the above expression looks like a straight-forward extension of equation (2.38). In the same manner, factorization theorems can be written down for other hard processes involving two hadrons. For one-particle inclusive DIS the cross-section can be written as,

$$\frac{d\sigma}{dx_B dz_h dQ^2} = \int_{x_B}^1 \frac{dx}{x} \int_{z_h}^1 \frac{dz}{z} \sum_{ab} H_{ab}'' \left(\frac{x_B}{x}, \frac{z_h}{z}, \frac{Q}{\mu}, \alpha_s(\mu^2) \right) f_a(x, \mu) D_b(z, \mu). \quad (2.42)$$

The cross-section for lepton anti-lepton annihilation into hadrons would be analogous to equation (2.42) but with a second fragmentation function in the place of the distribution function,

$$\frac{d\sigma}{dz_A dz_B dQ^2} = \int_{z_A}^1 \frac{dz}{z} \int_{z_B}^1 \frac{dz'}{z'} \sum_{ab} H_{ab}'' \left(\frac{z_A}{z}, \frac{z_B}{z'}, \frac{Q}{\mu}, \alpha_s(\mu^2) \right) D_a(z, \mu) D_b(z', \mu). \quad (2.43)$$

Although the proofs of factorization are complicated by the presence of a second detected hadron, the soft parts appearing in equations (2.42), (2.41) and (2.43) are, except that now chiral odd structures can appear unsuppressed, not different to those appearing in equations (2.38), and (2.39). In both the single hadron as the case involving two hadrons, the same correlations along light-like directions are relevant.

In general the two parent hadron momenta and the hard boson momentum will not be co-planar and in contrast to the single-hadron case, this additional direction protruding from the collinear plane can be used to define and extract additional soft parts at leading order in $1/Q$. This momentum components protruding from the collinear plane are called the transverse directions. Studies have shown the important role of transverse momentum of partons in hard processes involving more than one hadron [Rals79]. This will be illustrated in the next section considering the DY process at tree level.

Beyond collinearity

The presence of a second hadron enables us to go beyond the collinear approximation mentioned above. The two hadron momenta and the hard boson momentum will in general not be coplanar. In figure 2.6 the situation for Drell-Yan is depicted in a frame in which the two hadrons have no transverse momentum, but the boson has. This transverse momentum is transferred to the lepton pair and can be measured.

After definition of the momentum fractions x_A and x_B , the transverse part of the hard boson, q_T , in unambiguously specified

$$q^\mu \approx x_A P_A^\mu + x_B P_B^\mu + q_T^\mu. \quad (2.44)$$

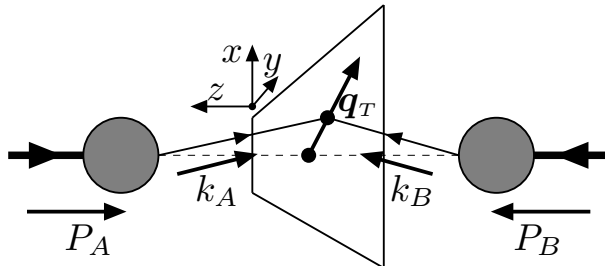


Figure 2.6: Schematic representation of the Drell-Yan process extended to include intrinsic momentum of quarks in the parent hadrons

The magnitude of this transverse part, $Q_T^2 = -q_T^2$, determines the type of factorization theorem that applies.

A first possibility is that the degree of non-coplanarity is comparable in magnitude to the hard scale, $Q_T^2 \approx Q^2$. In this case, the transverse components of the hard boson cannot originate from intrinsic transverse momentum in the parent hadrons, and has to be attributed to the emission of hard gluons. Inclusion of this type of corrections leads to a factorization theorem of the same form as the one shown in equation (2.41).

The degree of non-coplanarity of the three momenta can be much smaller than the hard scale, but still much larger than a typical hadronic scale, that is $\Lambda^2 \ll Q_T^2 \ll Q^2$. There is a theorem that applies in this case [Coll85b], and has been worked out for unpolarized hadrons. Although more complicated, the theorem can be extended to the polarized case.

The case that is most interesting to us, is the case in which the transverse component of the hard boson is soft, that is $Q_T^2 \approx \Lambda^2$. In this case the boson transverse momentum can be attributed to intrinsic transverse momentum of partons in hadrons and to soft gluon emission. For the case of measured soft transverse momentum a factorization theorem exists of the following form

$$\begin{aligned} \frac{d\sigma}{dQ^2 dx_1 dx_2 d^2\mathbf{q}_T} &= \sum_{a,b} \int_{x_1}^1 dx' \int_{x_2}^1 dx'' \int d^2\mathbf{k}_T d^2\mathbf{p}_T \int \frac{d^2\mathbf{b}}{(2\pi)^2} \\ &\times e^{-i\mathbf{b}\cdot(\mathbf{p}_T+\mathbf{k}_T-\mathbf{q}_T)} \Phi_a^A(x', \mathbf{k}_T) H^{ab}(x', x''; Q) e^{-S(\mathbf{b}, Q)} \Phi_b^B(x'', \mathbf{p}_T) \\ &+ Y(x_1, x_2, Q, Q_T), \end{aligned} \quad (2.45)$$

in which an additional factor $e^{-S(\mathbf{b})}$ appears, arising from soft gluon emission. This factor is called the Sudakov factor, which is of soft nature. It cannot be completely computed using perturbation theory, but partially has to be extracted from experiment. It is an important factor because it leads to suppression of the cross-section at larger values of \mathbf{q}_T as investigated in [Boer01]. The last term $Y(x_1, x_2, Q, Q_T)$ is negligible at small values of transverse momentum, $Q_T^2 \approx \Lambda^2$, but grows as Q_T^2 approaches Q^2 . This term makes the connection with the collinear form of equation (2.41) when integrating over all q_T .

Drell-Yan at tree-level

The factorized form of equation (2.45) suffices as a theoretical basis for the extraction of transverse momentum related structure from two colliding hadrons in Drell-Yan [Rals79].

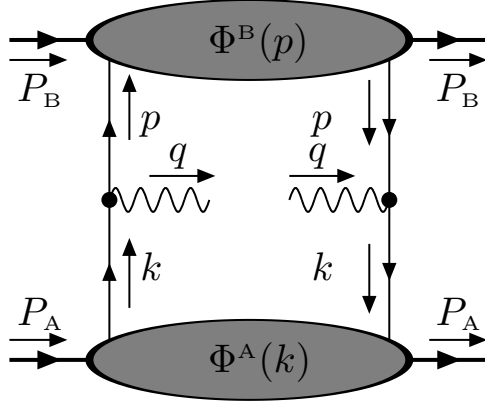


Figure 2.7: Diagrammatic representation of the leading order in $1/Q$ contribution to Drell-Yan.

The extraction of transverse momentum related additional structure, can be accomplished by weighting the cross-section with odd-powers of q_T and integrating over it.

The appearance of new soft parts in the cross-section can be illustrated looking at the tree level diagram shown in figure 2.7, and comparing the case in which the cross-section is multiplied by a single factor of q_T and the case in which it is not, before integration over q_T .

Hadron A , with momentum P_A collides with hadron B with momentum P_B and a lepton-pair with invariant mass Q^2 , that is created in the collision, is detected disregarding lepton polarization. In a frame in which the lepton-pair center of mass is at rest, the trajectories of the two colliding hadrons form the collision axis. The polarization of hadron A is longitudinal, approximately along the collision axis, and the polarization of hadron B is transverse, more or less transverse to the collision axis.

The contribution of figure 2.7 to the unweighted cross-section is given by the expression

$$w_0^{\mu\nu} = \int d^4k d^4p d^4q \delta^4(q + k - p) \text{Tr} [\Phi^A(k) \gamma^\mu \Phi^B(p) \gamma^\nu]. \quad (2.46)$$

Due to the soft nature of the quark momenta k and p it is possible to approximate the momentum conserving δ -function in the hadronic tensor in the following way

$$\begin{aligned} \delta^4(q + k - p) &\equiv \delta((q + k - p) \cdot \zeta) \delta((q + k - p) \cdot \eta) \delta^2(\mathbf{q}_T + \mathbf{k}_T - \mathbf{p}_T) \\ &= \delta(x_A - x) \delta(x_B - y) \delta^2(\mathbf{q}_T + \mathbf{k}_T - \mathbf{p}_T) + \mathcal{O}\left(\frac{1}{Q^2}\right). \end{aligned} \quad (2.47)$$

Here the vectors ζ^μ and η^μ are light-like vectors, that satisfy $\zeta^2 = \eta^2 = 0$ and $\zeta \cdot \eta = 1$. Each of these directions correspond to one of the parent hadrons. The hard photon momentum q is the only hard momentum, and therefore the only momentum with both ζ and η components large.

$$P_A^\mu = \frac{1}{x_B} \frac{Q}{\sqrt{2}} \eta^\mu \quad (2.48)$$

$$P_B^\mu = \frac{1}{x_A} \frac{Q}{\sqrt{2}} \zeta^\mu \quad (2.49)$$

$$q^\mu = \frac{x_A}{x_B} \frac{Q}{\sqrt{2}} \eta^\mu + \frac{x_B}{x_A} \frac{Q}{\sqrt{2}} \zeta^\mu \quad (2.50)$$

The parton momenta are soft themselves and predominantly a fraction of the parent hadron momentum, $k \approx xP_A$ and $p \approx yP_B$. Partons have additional momentum components with respect to their parent hadrons, but the magnitude of these components is small compared to Q .

Integration over all small and transverse momentum components, leads, with the polarizations chosen for the parent hadrons, to the following soft parts in the hadronic tensor,

$$\int d^4k d^4p \delta(x_A - x) \delta(x_B - y) \text{Tr} [\Phi^A(k) \gamma^\mu \Phi^B(p) \gamma^\nu] \propto l^{\mu\nu} \left(\frac{M_B}{Q} g_1(x_A) g_T(x_B) + \frac{M_A}{Q} h_L(x_A) h_1(x_B) \right), \quad (2.51)$$

where $l^{\mu\nu}$ denotes the structure to be contracted with the leptonic tensor, and the M_i denote the hadron masses. The relevant part in this expression is the soft part, the two products of distribution functions, $g_1(x_A) g_T(x_B)$ and $h_L(x_A) h_1(x_B)$. Although the exact meaning of these functions will not be clarified until the next chapter, it now matters that each function in a product, corresponds to each hadron involved, and that the type of function appearing indicates the role played by the hadron in the hard process. There are two terms because, with these specific hadron polarizations chosen, two different quark polarization configurations can contribute to the leading term of the cross-section. In this unweighted case, in which only collinear functions appear in the cross section, two functions g_1 and h_1 are leading order while the remaining two are sub-leading order. The presence of a leading order function in each product leads to an overall suppression factor of $1/Q$ in the cross-section.

If we weight the cross-section with an extra factor of q_T the contribution of the diagram in figure 2.7 to the hadronic tensor now is given by an expression of the form

$$\begin{aligned} a_0^{\mu\nu} &\equiv \int d^2\mathbf{q}_T (\mathbf{q} \cdot \mathbf{n}) w_0^{\mu\nu} \\ &= \int d^4k d^4p d^4q \mathbf{q}_T \cdot \mathbf{n} \delta^4(q + k - p) \text{Tr} [\Phi^A(k) \gamma^\mu \Phi^B(p) \gamma^\nu] \\ &= \int d^2\mathbf{k}_T d^2\mathbf{p}_T (\mathbf{p}_T - \mathbf{k}_T) \cdot \mathbf{n} \text{Tr} [\Phi^A(x_A, \mathbf{k}_T) \gamma^\mu \Phi^B(x_B, \mathbf{p}_T) \gamma^\nu] \\ &\propto l'^{\mu\nu} \left(g_1(x_A) g_{1T}^{\perp(1)}(x_B) + h_{1L}^{\perp(1)}(x_A) h_1(x_B) \right) \end{aligned} \quad (2.52)$$

where we see the appearance of *transverse moments* $f^{(1)}(x)$, defined as

$$f^{(1)}(x) \equiv \int d^2\mathbf{k}_T \frac{\mathbf{k}_T^2}{2M^2} f(x, \mathbf{k}_T^2) \quad (2.53)$$

of non-collinear functions from the soft parts, contributing to the cross-section. The object $l'^{\mu\nu}$ is just the tensor structure to be contracted with the leptonic tensor.

This example was aimed at clarifying two things. First, the weighting of the cross-section with an *odd* factor of \mathbf{q}_T allows the extraction of additional non-collinear soft

information from the participating hadrons. Second, by considering a q_T -weighted cross-section, no suppression factor of $1/Q$ accompanies the soft part. A detailed treatment of both collinear and non-collinear functions will follow in chapter 3.

In this section, the role of parton transverse momentum was illustrated using a rather restricted example. More elaborate treatments of the role of parton transverse momentum in Drell-Yan [Tang95], 1-particle inclusive deep-inelastic electro-production [Muld96], and e^+e^- -annihilation [Boer97a] exist. An extensive characterization of the soft structure in hadrons is necessary to treat the role played by hadrons when quark transverse momentum is taken into account. In the next chapter we will discuss the parametrization of non-collinear soft parts and its relation to the collinear set of distribution and fragmentation functions.

In the factorized forms of the cross-sections in equation (2.42) and equation (2.41), the same notation was used for a distribution function. The reappearance of the function in another factorized cross-section, reflects the fact that the hadron plays an identical role in the two processes. This identification of soft parts in different processes is an example of universality of distribution and fragmentation functions, and is known by the name of *strong* factorization [Coll83]. The least stringent extreme of factorization is known as *weak* factorization, only stating the feasibility of the separation into soft and hard parts. Strictly speaking, scale dependence of soft functions can be seen as a degradation of strong factorization to weak factorization as for each value of Q^2 the separation of hard and soft parts differs. However, perturbation theory provides us with a differential equation for connecting the factorized soft parts at different values of Q^2 . As a result, scale dependent soft parts regain their universal status in several processes. There is also the possibility of a restricted universality in which, for instance, factorized soft parts are universal only for a specific initial state and can be identified between processes involving different final states.

How strong factorization turns out in the case of \mathbf{k}_T -dependent functions is under study. The presence of the soft Sudakov factor in equation (2.45) indicate a more subtle situation when transverse momentum is included. The more complicated gauge-link operators when including transverse momentum, can generate additional factors, depending on the processes under consideration [Coll02, Metz02, Coll04, Bomh04] affecting the universality of non-collinear functions.

Distribution and fragmentation functions

3.1 Introduction

In this chapter we introduce the set of quark distribution and fragmentation functions that summarize the role played by hadrons in hard electro-weak processes. The distribution functions describe the hadron-to-quark transition, while the fragmentation functions describe the quark-to-hadron transition. They depend on the hadron and on specific components of the quark momentum.

In our case, the set takes into account intrinsic transverse momentum of quarks with respect to the parent hadron, or the hadron they fragment into, and leads therefore to a larger number of distribution and fragmentation functions than the usual collinear set, that neglects or averages out this transverse momentum. When more than one hadron takes part in a hard process and azimuthal asymmetries are considered, transverse momentum dependent functions are required to fully describe the cross-section, making the study of these functions relevant.

In this chapter we introduce the nomenclature of the functions and discuss their properties. We will restrict ourselves to the structure that can contribute to leading and sub-leading terms in an expansion of the cross-section in powers of $1/Q$, where Q is the large scale that characterizes the hard process. Furthermore, we will limit ourselves to spin-1/2 and spin-0 hadrons, although this approach can straightforwardly be extended to spin-1 hadrons [Bacc00].

In this chapter the functions will be considered at tree-level, assuming that the factorization program can be completed without problems and disregarding the scale dependence that results from that program. In chapter 5 we will address the calculation of the Q^2 -dependence that the functions necessarily develop in the process of factorization.

We will start by introducing the hadronic matrix elements that are relevant when considering structure that appears at leading and sub-leading order in $1/Q$. Next we will discuss the parametrization of all structure that is relevant for the study of non-collinear distribution and fragmentation functions. This parametrization results in a redundant base of functions. We will also discuss relations that reduce the set of functions into an independent set.

3.2 Relevant hadronic matrix elements

Which hadronic matrix elements are relevant in a hard process when only contributions up to a specific order in $1/Q$ are considered, is determined by dimensional arguments. In general, the answer counts an infinite number of matrix elements. Although including more fields in a matrix elements usually leads to more suppression by powers of $1/Q$, specific components of the gluon field contribute without giving rise to suppression. The resulting infinity of matrix elements can be resummed into gauge-invariant objects that can be put into their simplest form by a judicious choice of gauge.

If we restrict ourselves momentarily to target hadrons, the extension of the parton model ideas to QCD, leads to consideration of non-local matrix elements of quark fields evaluated between their parent hadron states. To consider in a gauge theory a non-local product of quark fields, disregarding gluons, clearly leads to trouble if we want to assign them the same degree of universality as that of the parton model's distribution functions. The correlations among quark fields that end up in the cross-section, the QCD analog of the parton distribution function, should be extracted from an object defined as

$$\Phi_{ij}(P, S; k) \equiv \Phi_{ij}(k) = \int \frac{d^4 y}{(2\pi)^4} e^{ik \cdot y} \langle P, S | \bar{\psi}_j(0) \mathcal{U}(0, y; \mathcal{X}) \psi_i(y) | P, S \rangle, \quad (3.1)$$

where P and S denote the parent hadrons momentum and polarization respectively, and specify its state, and k is the momentum carried by the quark. Besides quark fields, one also encounters in equation (3.1) a *gauge-link* operator

$$\mathcal{U}(0, y; \mathcal{X}) = \mathcal{P} \exp \left[-ig \int_0^1 d\tau A_\mu(\mathcal{X}) \frac{d\mathcal{X}^\mu(\tau)}{d\tau} \right], \quad (3.2)$$

which is necessary to make the non-local matrix element gauge-invariant in a gauge theory. The path \mathcal{X}^μ runs from $\mathcal{X}(0) = 0$ to $\mathcal{X}(1) = y$, and connects the two quark field operators, along some trajectory. The symbol \mathcal{P} denotes path-ordering of all the gluon color fields along the trajectory. The object in equation (3.1) is the fundamental soft object considered in this thesis and will be usually referred to by the shorthand $\Phi(k)$, in which all reference to the parent hadron state is dropped. A diagrammatic representation of this object is shown in figure 3.1(a).

Also of relevance in studying transverse momentum or sub-leading order distribution functions, is the matrix element that includes a gluon field operator at an additional space-time point and is defined as,

$$\begin{aligned} \Phi_{A_{ij}}^\mu(P, S; k, k_1) &= \int \frac{d^4 y}{(2\pi)^4} \frac{d^4 y_1}{(2\pi)^4} e^{i k_1 \cdot y + i (k - k_1) \cdot y_1} \\ &\times \langle P, S | \bar{\psi}_j(0) \mathcal{U}(0, y_1; \mathcal{X}) g A^\mu(y_1) \mathcal{U}(y_1, y; \mathcal{X}_1) \psi_i(y) | P, S \rangle. \end{aligned} \quad (3.3)$$

Note that the above matrix element is not gauge-invariant, in spite of two gauge-link operators running along the paths \mathcal{X} and \mathcal{X}_1 , compensating for gauge variance originating from the non-locality of the matrix element. A gauge invariant matrix element is easily constructed by replacing the gluon field operator by a covariant derivative, D_μ ,

$$\begin{aligned} \Phi_D^\alpha(k, k_1) &= \int \frac{d^4 y d^4 y_1}{(2\pi)^4} e^{i(k \cdot y + (k - k_1) \cdot y_1)} \\ &\times \langle P, S | \bar{\psi}(0) \mathcal{U}(0, y; \mathcal{X}) D^\alpha(y) \mathcal{U}(y, y_1; \mathcal{X}_1) \psi(y_1) | P, S \rangle. \end{aligned} \quad (3.4)$$

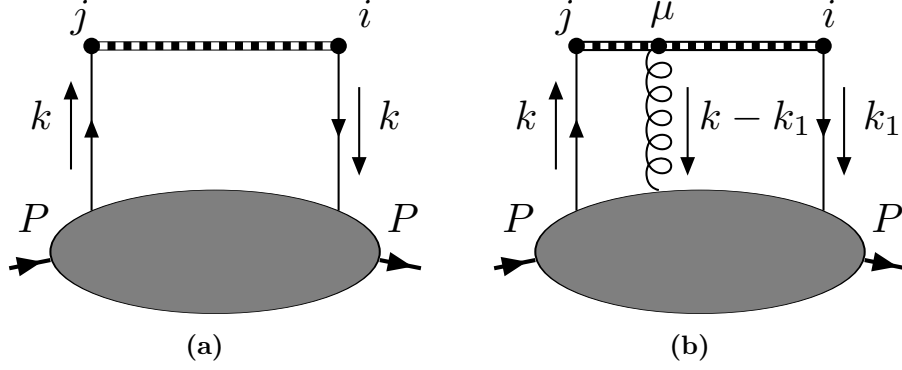


Figure 3.1: Diagrammatic representation of hadronic matrix elements in which non-local gauge variance is canceled by inclusion of gauge link operators. (a)) The matrix element $\Phi(k)$ involving only quark fields. (b)) A matrix element $\Phi_A^\mu(k, k_1)$ involving quark fields and an additional gluon.

Alternatively, a matrix element containing the field strength tensor $F_{\mu\nu}$,

$$\Phi_F^{\alpha\beta}(x, y) = \int \frac{d^4y d^4y_1}{(2\pi)^4} e^{i(k \cdot y + (k - k_1) \cdot y_1)} \times \langle P, S | \bar{\psi}_j(0) \mathcal{U}(0, y; \mathcal{X}) F^{\alpha\beta}(y) \mathcal{U}(y, y_1; \mathcal{X}_1) \psi(y_1) | P, S \rangle. \quad (3.5)$$

is gauge-invariant. As correlations between quark-spin and parent hadron spin are of interest to us, both $\Phi(k)_{ij}$ and $\Phi_A^\mu(k, k_1)_{ij}$ are 4×4 -matrices in Dirac space. The quark-gluon correlator carries an additional Lorentz-index from the gluon field.

Both objects $\Phi(k)$ and $\Phi_A^\mu(k, k_1)$ imply a summation over color components of the fields involved. In the case of $\Phi(k)$, this summation is of the form $\bar{\psi}_a \mathcal{U}_{ab} \psi_b$, in which \mathcal{U}_{ab} represents the effective color matrix resulting from the gauge link operator. In the case of the matrix element $\Phi_A^\mu(k, k_1)$, the summation can be written as $\bar{\psi}_a \mathcal{U}_{ab} A_{bc} \mathcal{U}'_{cd} \psi_d$, where besides summing over two gauge-link operator color structures, the color matrix of the gluon field, A_{bc} , is involved.

The expressions introduced in this section are the most important in considering intrinsic transverse momentum of quarks in their parent hadrons. It should be noted that these matrix elements are defined in terms of *renormalized* operators, and this fact will be manifest in the scale dependence of the distribution and fragmentation functions that will parametrize the relevant structures in hard processes. In this section we will restrict ourselves to tree level, in order to define these structures.

In hard process not all possible correlations over space-time are of equal importance. The most relevant correlations are most easily described in terms of light-cone vectors. In the next section we will introduce the use of these directions and their meaning in hard processes.

3.2.1 Light-like correlations

Correlations between different space-time points in the matrix element of equation (3.1) are not of equal importance in hard processes. This can be seen by looking at the handbag

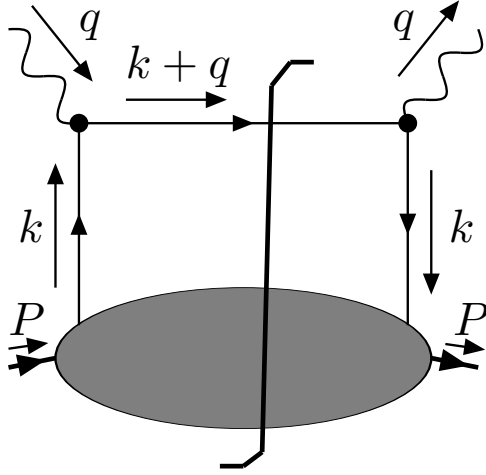


Figure 3.2: The most important contribution to the simplest of all hard processes: Inclusive DIS

diagram contribution to inclusive DIS. This contribution, shown in figure 3.2, is given by the expression

$$w_0^{\mu\nu} = 2\pi \int d^4k \delta((k+q)^2) \theta((k+q) \cdot \zeta) \text{Tr} [\Phi(k) \gamma^\mu (\not{k} + \not{q}) \gamma^\nu]. \quad (3.6)$$

In this analysis it is convenient to use light-cone vectors η and ζ with properties (2.26) and (2.27), to describe the parton momenta. Choosing again the parent hadron momentum and all related partonic momenta along η , the light-cone vectors can be chosen such that the parent hadron momentum P , quark-momentum k and hard boson momentum q are decomposed in the following way

$$P^\mu = P \cdot \zeta \eta^\mu + \frac{M^2}{2P \cdot \zeta} \zeta^\mu \quad (3.7)$$

$$q^\mu = -x_B P \cdot \zeta \eta^\mu + \frac{Q^2}{2x_B P \cdot \zeta} \zeta^\mu \quad (3.8)$$

$$k^\mu = x P \cdot \zeta \eta^\mu + \frac{(k^2 - k_T^2)}{2x P \cdot \zeta} \zeta^\mu + k_T^\mu, \quad (3.9)$$

where x_B is defined as in equation (2.4) and M denotes the parent hadrons mass. The decomposition of the quark momentum shows that after specifying ζ^μ and η^μ the transverse sub-space, in which k_T resides, is determined according to equation (2.30). The invariants M^2 , k^2 and k_T^2 are all of order of some hadronic scale Λ^2 , which is small compared to Q^2 . One obtains the collinear approximation of the parton model if the scales k^2 and k_T^2 are set to zero in the hard part, and these variables are integrated over in the soft part. In that case, both the parent hadron and quark momentum lie on a light-cone, $P^2 = k^2 = 0$, and are proportional to each other, $k = x P$, so that they lie on the same light-cone leg. The inclusion of quark transverse momentum is a small deviation from this collinear alignment of parent hadron and quark momenta.

A parton model result is obtained by taking the first term in the collinear expansion of the hard part as shown in equation (3.6). It is also possible to study the full expression for

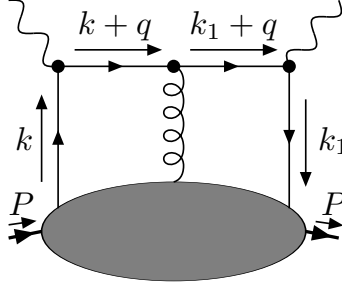


Figure 3.3: In a general gauge this diagram contains parts that contribute at leading order in $1/Q$. Leading parts from this diagram and analogous diagrams involving more gluons, can be summed into gauge-link operators.

$w_0^{\mu\nu}$ and track down the terms of $\mathcal{O}(1)$. Our starting point is the assumption that when any of the invariants k^2 or k_T^2 reaches a magnitude of order Q^2 , the soft matrix element $\Phi_{ij}(k)$ vanishes. Under this assumption the tree-level contribution to the hadronic tensor in inclusive DIS is given by

$$2\pi \int d^4k \delta((k+q)^2) \theta((k+q) \cdot \zeta) \text{Tr} [\Phi(k) \gamma^\mu (\not{k} + \not{q}) \gamma^\nu] = \int dx \delta(x - x_B) \int \frac{dk^2}{2x P \cdot \zeta} \int d^2k_T \text{Tr} [\Phi(k) \gamma^\mu \tilde{\zeta} \gamma^\nu] + \mathcal{O}\left(\frac{1}{Q^2}\right). \quad (3.10)$$

where the shorthand $\tilde{\zeta} = \not{\zeta} / P \cdot \zeta$ is used to indicate the absorption of a dimensionful quantity.

The important thing here is that the leading part in powers of $1/Q^2$ of the hard part is independent of k^2 and k_T . As a result of this, these variables can be integrated over, resulting in a soft part contributing at leading order in $1/Q$, that only depends on the longitudinal momentum fraction x ,

$$\Phi_{ij}(x) \equiv \int d^4k \delta(k \cdot \zeta - x P \cdot \zeta) \Phi_{ij}(k). \quad (3.11)$$

Inserting the definition of $\Phi(k)$ in equation (3.11) exposes the space-time correlations between the two quark fields that contribute at leading order in $1/Q$. The correlations have $y \cdot \zeta = 0$ and $y_T = 0$, and thus lie on a straight line along the light-cone.

Another relevant tree-level diagram is shown in figure 3.3, and is given by the following expression,

$$w_1^{\mu\nu} = \int d^4k d^4k_1 \frac{\text{Tr} [\Phi_A^\alpha(k, k_1) \gamma^\mu (\not{k}_1 + \not{q}) \gamma_\alpha (\not{k} + \not{q}) \gamma^\nu]}{((k+q)^2 + i\epsilon)((k_1+q)^2 + i\epsilon)} \quad (3.12)$$

The leading order contribution in this diagram is given by

$$\begin{aligned} w_1^{\mu\nu} &= \int d^4k d^4k_1 \frac{\text{Tr} [\Phi_A^\alpha(k, k_1) \gamma^\mu \tilde{\zeta} \gamma_\alpha \tilde{\zeta} \gamma^\nu]}{(x - x_B + i\epsilon)(x_1 - x_B + i\epsilon)} + \mathcal{O}(1/Q) \\ &= \int dx dx_1 \frac{\Phi_A^\zeta(x, x_1) \text{Tr} [\gamma^\mu \tilde{\zeta} \gamma^\nu]}{(x - x_B + i\epsilon)(x_1 - x_B + i\epsilon)} + \mathcal{O}(1/Q), \end{aligned} \quad (3.13)$$

where the last line follows from the identity $\not{\zeta}\not{k}\not{\zeta} = 2k \cdot \zeta \not{\zeta}$, and

$$\Phi_A^\zeta(x, x_1) \equiv \int d^4k d^4k_1 \delta(k \cdot \zeta - xP \cdot \zeta) \delta(k_1 \cdot \zeta - x_1P \cdot \zeta) \Phi_A^\alpha(k, k_1) \zeta_\alpha. \quad (3.14)$$

is the first term in the expansion of the gauge-link operator in a color-gauge invariant $\Phi(x)$.

As a consequence of all relevant correlations laying on a straight line along the light-cone, it is possible to choose a gauge satisfying $A \cdot \zeta = 0$, in which the component of the gauge field that is picked up by the hard interaction, vanishes. In this case the gauge link in equation (3.1) reduces to the unit matrix in color space. This is easily realized in the case of a single hadron, like the example of inclusive DIS discussed here. In that case all leading order in $1/Q$ contributions arise from a single matrix element, the light-cone correlation function [Sope77, Sope79, Jaff83, Mano90],

$$\Phi_{ij}(x) = \int \frac{d\lambda}{2\pi} e^{i\lambda x} \langle P, S | \bar{\psi}_j(0) \psi_i(\lambda \tilde{\zeta}) | P, S \rangle \quad (3.15)$$

When more than one hadron, that are hard with respect to each other, are taken into account, this cannot be done in general and gauge-link operators have to be considered.

3.2.2 Collinear structure

In the collinear approximation, the most general parametrization of the soft structure for a spin-1/2 hadron in leading order in $1/Q$, in accordance with the required symmetries (hermiticity, parity, time reversal), is given by three distribution functions,

$$\Phi^{\text{twist}-2}(x) = \frac{1}{2} \{ f_1(x) \not{\eta} + S_L g_1(x) \gamma_5 \not{\eta} + h_1(x) \gamma_5 \not{S}_T \not{\eta} \}. \quad (3.16)$$

The spin vector of the hadron has been decomposed into the following components,

$$S^\mu = \frac{S_L}{M} \frac{P \cdot \zeta}{M} \eta^\mu - \frac{S_L}{M} \frac{M^2}{2 P \cdot \zeta} \zeta^\mu + S_T^\mu. \quad (3.17)$$

Denoting these functions as twist-two makes sense because the local operators connected to the Mellin moments of these functions are related to the matrix elements of local twist-two operators, like $\bar{\psi} \not{\zeta} (D \cdot \zeta)^n \psi$.

Being in this thesis mainly interested in flavor singlet hadronic structure, all distribution and fragmentation functions should be considered to correspond to a specific quark flavor. In order to simplify the notation of the functions we will suppress the flavor specification ¹ and assume it to be understood.

A calculation of the hadronic tensor up to order $1/Q$, requires the introduction of additional soft structure that is accompanied by a factor of $M/P \cdot \zeta$. The quantity $P \cdot \zeta$ reflects our choice of frame, in particular boosts along the η^μ direction. When these soft parts are combined with their corresponding hard parts, the factors of $M/P \cdot \zeta$ are canceled by a factor of $P \cdot \zeta/Q$, giving rise to suppression in powers of $1/Q$ in the cross-section.

¹Common quark flavor q assignments are $f_1^q(x) = q(x)$, $g_1^q(x) = \Delta q(x)$ and $h_1^q(x) = \Delta_T q(x) = \delta q(x)$.

The parametrization of the sub-leading order structure in the quark-quark correlator, now requiring only the correct behavior under hermitian conjugation and parity reversal,

$$\begin{aligned}\Phi^{\text{twist-3}}(x) &= \frac{M}{2P \cdot \zeta} \left\{ e(x) + g_T(x) \gamma_5 \not{S}_T + S_L h_L(x) \gamma_5 \frac{[\not{\eta}, \not{\zeta}]}{2} \right\} \\ &+ \frac{M}{2P \cdot \zeta} \left\{ -i S_L e_L(x) \gamma_5 - f_T(x) \epsilon_T^{\rho\sigma} \gamma_\rho S_{T\sigma} + i h(x) \frac{[\not{\eta}, \not{\zeta}]}{2} \right\}. \quad (3.18)\end{aligned}$$

where the quantity $\epsilon_T^{\mu\nu}$ is the projection of the Levi-Civita tensor off the light-cone and will be defined in this thesis by,

$$\epsilon_T^{\mu\nu} = \epsilon^{\sigma\rho\mu\nu} \zeta_\sigma \eta_\rho. \quad (3.19)$$

We have not imposed time-reversal invariance in order to study also the time-reversal odd (T-odd) functions.

The functions e , g_T and h_L are time-reversal even (T-even), the functions e_L , f_T and h are time-reversal odd (T-odd). We will not concern ourselves with the formal problems related to T-odd distribution functions [Coll93, Boer98]. Our goal is to also study the scale dependence of non-collinear T-odd distribution functions, and in light of recent developments in making their existence plausible [Brod02a, Brod02b]), we will assume these functions are non-vanishing.

A treatment up to order $1/Q$ without considering quark-gluon correlations is not consistent, and leads for instance to violation of electro-magnetic gauge invariance of the hadronic tensor. This is evident from the equations of motion connecting quark matrix elements and quark-gluon matrix elements. In a $A \cdot \zeta = 0$ gauge quark-gluon matrix elements start contributing to the cross-section at order $1/Q$ through the transverse components of the gluon field. For a color-gauge invariant parametrization one considers the collinear remnant of the matrix element in equation (3.4),

$$\Phi_{Dij}^\alpha(x, y) \equiv \int d^4k d^4k_1 \delta(k \cdot \zeta - xP \cdot \zeta) \delta(k_1 \cdot \zeta - yP \cdot \zeta) \Phi_{Dij}^\alpha(k, k_1) \quad (3.20)$$

where $x = k \cdot \zeta / P \cdot \zeta$ and $y = k_1 \cdot \zeta / P \cdot \zeta$. This sub-leading collinear object is parameterized, requiring only the correct behavior under parity reversal, in terms of two-argument functions [Jaff92].

$$\begin{aligned}\Phi_D^\alpha(x, y) &= \frac{1}{2} \left\{ G_D(x, y) i \epsilon_T^{\alpha\beta} S_{T\beta} \not{\eta} + \tilde{G}_D(x, y) S_T^\alpha \gamma_5 \not{\eta} \right. \\ &\quad \left. + H_D(x, y) S_L \gamma_5 \gamma_T^\alpha \not{\eta} + E_D(x, y) \gamma_T^\alpha \not{\eta} \right\}. \quad (3.21)\end{aligned}$$

Hermiticity determines the symmetry under interchange of the arguments

$$G_D^*(x, y) = -G_D(y, x), \quad (3.22)$$

$$\tilde{G}_D^*(x, y) = \tilde{G}_D(y, x), \quad (3.23)$$

$$H_D^*(x, y) = H_D(y, x), \quad (3.24)$$

$$E_D^*(x, y) = -E_D(y, x). \quad (3.25)$$

Time reversal invariance requires these functions to be real.

3.3 Quark transverse momentum

In the example of inclusive DIS in the last section, the δ -function that originates from the Cutkovsky rule [Cutk60] for the handbag diagram, fixes the quark momentum in the final state to also be light-like (neglecting quark masses). The absorption of the hard momentum q has knocked a quark from one leg of a light-cone into the other leg. The hadronic correlations, soft by nature, only describe the physics close to the light-cone leg that corresponds to the parent hadron momentum. This picture of light-like hadrons and constituents, that can only flip to an opposite light-cone leg under influence of a hard interaction, applies to all hard processes we are interested in. This picture together with the perturbative calculation of the "light-cone leg flipping mechanism" is in fact the essence of factorization.

The collinear set of functions suffices for inclusive DIS, due to the form of the hard part in equation (3.6). This is different, if a hard hadron with respect to the target hadron is detected in the final state. The same simple light-cone leg flipping picture applies, but it is now possible to construct more complex cross-sections. In some of these cross-sections quark transverse momentum off the light-cone is relevant and leads to soft structure appearing at leading order in $1/Q$ in the cross-section, that is not contained in the collinear approximation. We will now review the determination of this additional structure and its nomenclature.

3.3.1 Quark transverse momentum

Our treatment of quark transverse momentum starts with the characterization of the most general Lorentz-invariant structure in $\Phi(k)$. From its definition in equation (3.1), one finds the behavior of the correlator under conjugation and space inversion,

$$\Phi^\dagger(P, S; k) = \gamma_0 \Phi(P, S; k) \gamma_0 \quad [\text{Hermiticity}] \quad (3.26)$$

$$\Phi(P, S; k) = \gamma_0 \Phi(\bar{P}, -\bar{S}; \bar{k}) \gamma_0 \quad [\text{Parity}], \quad (3.27)$$

where the notation $\bar{k} = (k^0, -\mathbf{k})$ is used for brevity.

Writing down all possible structures that are compatible with behavior (3.27) under parity, leads to the following decomposition into amplitudes depending on k^2 and $P \cdot k$ [Rals79, Muld96],

$$\begin{aligned} \Phi(k) = & A_1 M + A_2 \not{P} + A_3 \not{k} + (A_4/M) \sigma^{\mu\nu} P_\mu k_\nu + i A_5 (k \cdot S) \gamma_5 + M A_6 \not{S} \gamma_5 + \\ & (A_7/M) (k \cdot S) \not{P} \gamma_5 + (A_8/M) (k \cdot S) \not{k} \gamma_5 + i A_9 \sigma^{\mu\nu} \gamma_5 S_\mu P_\nu + \\ & i A_{10} \sigma^{\mu\nu} \gamma_5 S_\mu k_\nu + i (A_{11}/M^2) (k \cdot S) \sigma^{\mu\nu} \gamma_5 k_\mu P_\nu + \\ & (A_{12}/M) \epsilon_{\mu\nu\rho\sigma} \gamma^\mu P^\nu k^\rho S^\sigma. \end{aligned} \quad (3.28)$$

Condition equation (3.26) requires *all* amplitudes A_i in equation (3.28) to be *real*.

Special attention should be paid to the amplitudes A_4 , A_5 and A_{12} . In the case of a quark distribution in a target hadron that we are considering, the state $|P, S\rangle$ can be taken to be a plane wave. In that case, an additional symmetry restricts the number of amplitudes A_i . This restriction follows from time-reversal invariance and is given by the expression,

$$\Phi^*(P, S; k) = \gamma_5 C \Phi(\bar{P}, \bar{S}; \bar{k}) C^\dagger \gamma_5 \quad [\text{Time Reversal}]. \quad (3.29)$$

In the above C denotes the charge conjugation matrix with the properties,

$$C^T = C^\dagger = -C \quad (3.30)$$

and,

$$CC^\dagger = C^\dagger C = 1. \quad (3.31)$$

Imposing the restriction of equation (3.29) leads to the condition $A_i^* = A_i$ for the amplitudes A_4 , A_5 and A_{12} , hence they vanish.

Note that time-reversal invariance cannot be applied when states are present that cannot be described by plane waves, or when non-trivial gauge-links are present [Coll02]. One can still use relation (3.29), which in that case is sometimes referred as *naive* time-reversal, to distinguish time reversal even (T-even), $A_i^* = A_i$, and time-reversal odd (T-odd), $A_i^* = -A_i$, amplitudes. A hadron created by quark fragmentation cannot be described by a plane wave, so one cannot discard the amplitudes A_4 , A_5 and A_{12} ab initio.

All Dirac structures that accompany the amplitudes are decomposed into collinear and transverse components. The parent hadron and quark momentum according to equation (3.7) and the parent spin vector according to equation (3.17).

Next, one has to integrate over the $k \cdot \eta$ -component of the quark momentum. This is done by integrating over both k^2 and $P \cdot k$ and introducing quark transverse momentum through a δ -function.

$$\begin{aligned} \Phi(x, \mathbf{k}_T) &\equiv \int dk \cdot \eta \Phi(k) \\ &= \int dk^2 d(k \cdot P) \delta\left((xP - k)^2 - \mathbf{k}_T^2\right) \Phi(k) \\ &\equiv \int_{\sigma(x, \mathbf{k}_T)} \Phi(k) \end{aligned} \quad (3.32)$$

The result is the following parameterization of the quark-correlator including transverse quark momentum, that does not vanish if equation (3.29) is imposed,

$$\begin{aligned} \Phi(x, \mathbf{k}_T)|_{TE} &= \frac{1}{2} \left\{ \not{\eta} f_1(x, \mathbf{k}_T^2) + \gamma_5 \not{\eta} g_{1s}(x, \mathbf{k}_T) - i\gamma_5 [\not{\eta}, \not{\mathcal{S}}_T] h_{1T}(x, \mathbf{k}_T^2) \right. \\ &\quad \left. - i\gamma_5 [\not{\eta}, \frac{\not{k}_T}{M}] h_{1s}^\perp(x, \mathbf{k}_T) \right\} \\ &+ \frac{M}{P \cdot \zeta} \left\{ e(x, \mathbf{k}_T^2) + \frac{\not{k}_T}{M} f^\perp(x, \mathbf{k}_T^2) + \gamma_5 \not{\mathcal{S}}_T g'_T(x, \mathbf{k}_T^2) \right. \\ &\quad \left. + \gamma_5 \frac{\not{k}_T}{M} g_s^\perp(x, \mathbf{k}_T) - i\gamma_5 [\not{\mathcal{S}}_T, \frac{\not{k}_T}{M}] h_T^\perp(x, \mathbf{k}_T^2) - i\gamma_5 [\not{\eta}, \not{\zeta}] h_s(x, \mathbf{k}_T) \right\}, \end{aligned} \quad (3.33)$$

where

$$f_{\dots}(x, \mathbf{k}_T) = S_L f_{\dots L}(x, \mathbf{k}_T^2) + \frac{\mathbf{k}_T \cdot \mathbf{S}_T}{M} f_{\dots T}(x, \mathbf{k}_T^2) \quad (3.34)$$

is shorthand for a frequently occurring combination of functions. The time-reversal odd part, that vanishes if equation (3.29) can be used,

$$\Phi(x, \mathbf{k}_T)|_{TO} = \frac{1}{2} \left\{ f_{1T}^\perp(x, \mathbf{k}_T^2) \frac{\epsilon_T^{k_T S_T}}{M} \not{\eta} \right.$$

$$\begin{aligned}
& + f_T(x, \mathbf{k}_T^2) \epsilon_T^{\rho S_T} \gamma^\rho + S_L f_L^\perp(x, \mathbf{k}_T^2) \frac{\epsilon_T^{\rho k_T}}{M} \gamma^\rho \\
& - e_s(x, \mathbf{k}_T) i \gamma_5 + h_1^\perp(x, \mathbf{k}_T^2) \frac{\sigma_{\mu\nu} k_T^\mu \eta^\nu}{M} + h(x, \mathbf{k}_T^2) \sigma_{\mu\nu} \eta^\mu \zeta^\nu \}, \quad (3.35)
\end{aligned}$$

where we have used the following notation for the contracted form of the transverse Levi-Civita tensor,

$$\epsilon_T^{k_T \beta} = \epsilon_T^{k \beta} \equiv \epsilon_T^{\alpha \beta} k_\alpha. \quad (3.36)$$

The connection of these functions to the amplitudes A_i is, defining the shorthand,

$$\Sigma = \frac{k \cdot P - x M^2}{M^2}, \quad (3.37)$$

given by

$$f_1(x, \mathbf{k}_T^2) = \int_{\sigma(x, \mathbf{k}_T)} [A_2 + x A_3] \quad (3.38)$$

$$g_{1L}(x, \mathbf{k}_T^2) = \int_{\sigma(x, \mathbf{k}_T)} [-A_6 - \Sigma (A_7 + x A_8)] \quad (3.39)$$

$$g_{1T}(x, \mathbf{k}_T^2) = \int_{\sigma(x, \mathbf{k}_T)} [A_7 + x A_8] \quad (3.40)$$

$$h_{1T}(x, \mathbf{k}_T^2) = \int_{\sigma(x, \mathbf{k}_T)} [-(A_9 + x A_{10})] \quad (3.41)$$

$$h_{1L}^\perp(x, \mathbf{k}_T^2) = \int_{\sigma(x, \mathbf{k}_T)} [A_{10} - \Sigma A_{11}] \quad (3.42)$$

$$h_{1T}^\perp(x, \mathbf{k}_T^2) = \int_{\sigma(x, \mathbf{k}_T)} [A_{11}] \quad (3.43)$$

$$e(x, \mathbf{k}_T^2) = \int_{\sigma(x, \mathbf{k}_T)} [A_1] \quad (3.44)$$

$$f^\perp(x, \mathbf{k}_T^2) = \int_{\sigma(x, \mathbf{k}_T)} [A_3] \quad (3.45)$$

$$g'_T(x, \mathbf{k}_T^2) = \int_{\sigma(x, \mathbf{k}_T)} [-A_6] \quad (3.46)$$

$$g_L^\perp(x, \mathbf{k}_T^2) = \int_{\sigma(x, \mathbf{k}_T)} [-\Sigma A_8] \quad (3.47)$$

$$g_T^\perp(x, \mathbf{k}_T^2) = \int_{\sigma(x, \mathbf{k}_T)} [A_8] \quad (3.48)$$

$$h_T^\perp(x, \mathbf{k}_T^2) = \int_{\sigma(x, \mathbf{k}_T)} [-A_{10}] \quad (3.49)$$

$$h_L(x, \mathbf{k}_T^2) = \int_{\sigma(x, \mathbf{k}_T)} [-(A_9 + x A_{10}) - \Sigma A_{10} + \Sigma^2 A_{11}] \quad (3.50)$$

$$h_T(x, \mathbf{k}_T^2) = \int_{\sigma(x, \mathbf{k}_T)} [-\Sigma A_{11}] \quad (3.51)$$

$$(3.52)$$

and for the T-odd functions,

$$f_{1T}^\perp(x, \mathbf{k}_T^2) = \int_{\sigma(x, \mathbf{k}_T)} [A_{12}] \quad (3.53)$$

$$h_1^\perp(x, \mathbf{k}_T^2) = \int_{\sigma(x, \mathbf{k}_T)} [-A_4] \quad (3.54)$$

$$e_L(x, \mathbf{k}_T^2) = \int_{\sigma(x, \mathbf{k}_T)} [-\Sigma A_5] \quad (3.55)$$

$$e_T(x, \mathbf{k}_T^2) = \int_{\sigma(x, \mathbf{k}_T)} [A_5] \quad (3.56)$$

$$f_L^\perp(x, \mathbf{k}_T^2) = \int_{\sigma(x, \mathbf{k}_T)} [-A_{12}] \quad (3.57)$$

$$f_T(x, \mathbf{k}_T^2) = \int_{\sigma(x, \mathbf{k}_T)} [-\Sigma A_{12}] \quad (3.58)$$

$$h(x, \mathbf{k}_T^2) = \int_{\sigma(x, \mathbf{k}_T)} [\Sigma A_4]. \quad (3.59)$$

After integrating equation (3.33) over quark transverse momentum \mathbf{k}_T , one recovers the collinear parametrization in equation (3.16), for leading order functions, and the first line of equation (3.18) for sub-leading functions. Integrating over transverse momentum in the T-odd part, shown in equation (3.35), leads to the reduced structure to the last line in equation (3.18). It should be stressed that including transverse momentum leads to T-odd structure at leading order in $1/Q$ in the cross-section, while such structures are absent in the collinear case (at least, for spin 0 and spin 1/2).

The introduction of transverse momentum allows, on one side, more detailed study of the collinear structure, to which the more elaborate \mathbf{k}_T -dependent structure reduces after integration,

$$f_1(x) = \int d^2\mathbf{k}_T f_1(x, \mathbf{k}_T^2), \quad (3.60)$$

$$g_1(x) = \int d^2\mathbf{k}_T g_{1L}(x, \mathbf{k}_T^2), \quad (3.61)$$

$$h_1(x) = \int d^2\mathbf{k}_T \left[h_{1T}(x, \mathbf{k}_T^2) + \frac{\mathbf{k}_T^2}{2M^2} h_{1T}^\perp(x, \mathbf{k}_T^2) \right], \quad (3.62)$$

$$(3.63)$$

but, more importantly, also introduces additional functions which are called \mathbf{k}_T -odd functions because of the way they contribute to the hadronic tensor. One needs a specially constructed cross-section, as in several azimuthal asymmetries, in order to find these functions in the cross-section, instead of averaging them out as happens in the collinear approximation. We are interested in the leading order \mathbf{k}_T -odd functions in equations 3.33 and 3.35, which are present in the \mathbf{k}_T -weighted quark-quark matrix element, given by,

$$\begin{aligned} \Phi_\rho^\rho(x) &\equiv \int d^2k_T \frac{k_T^\rho}{M} \Phi(x, \mathbf{k}_T) \\ &= -\frac{M}{2} P \cdot \zeta \left[i f_{1T}^{\perp(1)}(x) i \epsilon_T^{\rho S_T} \not{\eta} - g_{1T}^{(1)}(x) S_T^\rho \gamma_5 \not{\eta} \right. \\ &\quad \left. + h_{1L}^{\perp(1)}(x) S_L \gamma_5 \gamma_T^\rho \not{\eta} + i h_1^{\perp(1)}(x) \gamma_T^\rho \not{\eta} \right] + \text{Higher twist}, \end{aligned} \quad (3.64)$$

in which one encounters the transverse moments, defined generally,

$$f^{(n)}(x) = \int d^2\mathbf{k}_T \left(\frac{\mathbf{k}_T^2}{2M^2} \right)^n f(x, \mathbf{k}_T^2). \quad (3.65)$$

3.3.2 Lorentz-invariance relations

At this point one can invoke Lorentz-invariance as a possibility to rewrite some functions. All functions in $\Phi(x)$ and $\Phi_\delta^\alpha(x)$ involve non-local matrix elements of two quark fields, although involving different gauge-links. Before constraining the matrix elements to the light-cone or light-front only a limited number of amplitudes can be written down [Mul96]. This leads to the following Lorentz-invariance relations [Bukh83a, Bukh83b, Bukh84a, Bukh84b, Mul96, Boer98]

$$g_T(x) = g_1(x) + \frac{d}{dx}g_{1T}^{(1)}(x) \quad (3.66)$$

$$g_L^\perp(x) = -\frac{d}{dx}g_T^{\perp(1)}(x) \quad (3.67)$$

$$h_L(x) = h_1(x) - \frac{d}{dx}h_{1L}^{\perp(1)}(x) \quad (3.68)$$

$$h_T(x) = -\frac{d}{dx}h_{1T}^{\perp(1)}(x) \quad (3.69)$$

$$h_{1L}^{\perp(1)}(x) = h_T^{(1)}(x) - h_T^{\perp(1)}(x) \quad (3.70)$$

Also for the T-odd sector there are too many functions originating from too few amplitudes leading to the following relations

$$f_T(x) = -\frac{d}{dx}f_{1T}^{\perp(1)}(x), \quad (3.71)$$

$$h(x) = -\frac{d}{dx}h_1^{\perp(1)}(x), \quad (3.72)$$

$$e_L(x) = -\frac{d}{dx}e_T^{(1)}(x), \quad (3.73)$$

$$f_{1T}^\perp(x) = -f_L^\perp(x). \quad (3.74)$$

From these relations, it is clear that the transverse moments of the k_T -dependent functions, appearing in $\Phi_\delta^\alpha(x)$, involve both local twist-two and local twist-three operators.

The relations in this section are currently under criticism [Goek03, Bacc04, Boer03]. Although no consensus has been reached yet on the validity of these relations, we will use these relations in chapter 6 in the derivation of evolution equations for leading order k_T -odd functions.

3.3.3 Equation of motion relations

A different source of relations among different functions is found in the equation of motion of the fields. The equation of motion allows one to split up order $1/Q$ functions found in the quark-quark correlator, into a Wandzura-Wilczek (WW) part that only involves leading order in $1/Q$ functions, and a pure interaction part that arises from a quark-gluon matrix element. For the T-even functions one finds the following decomposition,

$$e(x) = \frac{m}{M} \frac{1}{x} f_1(x) + \underbrace{\frac{2}{x} \int dy \operatorname{Re} \{E_A(x, y)\}}_{\tilde{e}(x)} \quad (3.75)$$

$$h_L(x) = \frac{m}{M} \frac{1}{x} g_1(x) - \frac{2}{x} h_{1L}^{\perp(1)}(x) + \underbrace{\frac{2}{x} \int dy \operatorname{Re} \{H_A(x, y)\}}_{\tilde{h}_L(x)} \quad (3.76)$$

$$g_T(x) = \frac{m}{M} \frac{1}{x} h_1(x) + \frac{1}{x} g_{1T}^{(1)}(x) + \underbrace{\frac{1}{x} \int dy \operatorname{Re} \{G_A(x, y) + \tilde{G}_A(x, y)\}}_{\tilde{g}_T(x)} \quad (3.77)$$

and for the T-odd functions one finds,

$$f_T(x) = -\frac{1}{x} f_{1T}^{\perp(1)}(x) + \underbrace{\frac{1}{x} \int dy \operatorname{Im} \{G_A(x, y) + \tilde{G}_A(x, y)\}}_{\tilde{f}_T(x)} \quad (3.78)$$

$$e_L(x) = -\frac{2}{x} \int dy \operatorname{Im} \{H_A(x, y)\} = \tilde{e}_L(x) \quad (3.79)$$

$$h(x) = -\frac{2}{x} h_1^{\perp(1)}(x) + \underbrace{\frac{1}{x} \int dy \operatorname{Im} \{E_A(x, y)\}}_{\tilde{h}(x)} \quad (3.80)$$

In the above expressions the pure-interaction parts involving two-argument functions and the integration of a momentum fraction are often indicated the corresponding single argument function name with a tilde.

3.4 Fragmentation functions

When considering the fragmentation of a quark into a hadron, the momentum fraction plays the inverse role compared to the case of distribution functions. Although the treatment is completely analogous, some differences result in the expressions that are given here for further reference in this thesis.

The relevant part of the quark-quark correlator in the case of fragmentation is given by [Coll82a]

$$\begin{aligned} \Delta_{ij}(z, \mathbf{k}_T) &= \sum_X \int \frac{dy \cdot \zeta d^2 \mathbf{y}_T}{(2\pi)^3} e^{ik \cdot y} \\ &\times \langle 0 | \mathcal{U}(\infty, y) \psi_i(y) | P_h, X \rangle \langle P_h, X | \bar{\psi}_j(0) \mathcal{U}(0, \infty) | 0 \rangle \Big|_{y \cdot \eta = 0}. \end{aligned} \quad (3.81)$$

Note that because of the use of fragmentation functions together with distribution functions, it is convenient to interchange the role of the vectors ζ^μ and η^μ for fragmentation functions with respect to distribution functions. For the production of unpolarized or spin-1/2 hadrons h in semi-inclusive hard scattering processes one needs to leading order in $1/Q$ the correlation function [Mul96]

$$\begin{aligned} \Delta(z, \mathbf{k}_T) &= \left\{ z D_1(z, \mathbf{k}_T^{\prime 2}) \not{\zeta} - z G_{1s}(z, \mathbf{k}_T^{\prime 2}) \not{\zeta} \gamma_5 \right. \\ &\quad \left. + z H_{1s}^\perp(z, \mathbf{k}_T^{\prime 2}) \frac{[k_T, \not{\zeta}] \gamma_5}{2M_h} + z H_{1T}(z, \mathbf{k}_T^{\prime 2}) \frac{[\not{\mathcal{S}}_{hT}, \not{\zeta}] \gamma_5}{2} \right\} \end{aligned}$$

$$\begin{aligned}
& + \left\{ -z D_{1T}^\perp(z, \mathbf{k}'_T) \frac{\epsilon_T^{k_T S_{hT}}}{M_h} + i z H_1^\perp(z, \mathbf{k}'_T) \frac{[\not{k}_T, \not{\zeta}]}{2M_h} \right\} \\
& \frac{M_h}{P_h \cdot \eta} \left\{ E(z, \mathbf{k}'_T) + D^\perp(z, \mathbf{k}'_T) \frac{\not{k}_T}{M_h} \right. \\
& \quad - G'_T(z, \mathbf{k}'_T) \not{\mathcal{S}}_T \gamma_5 - G_s^\perp(z, \mathbf{k}_T) \frac{\not{k}_T \gamma_5}{M_h} \\
& \quad \left. - H_T^\perp(z, \mathbf{k}'_T) \frac{i \sigma_{\mu\nu} \gamma_5 S_T^\mu k_T^\nu}{M_h} - H_s(z, \mathbf{k}'_T) i \sigma_{\mu\nu} \gamma_5 \zeta^\mu \eta^\nu \right\} \\
& + \frac{M_h}{P_h \cdot \eta} \left\{ -E_s(z, \mathbf{k}'_T) i \gamma_5 + H(z, \mathbf{k}'_T) \sigma_{\mu\nu} \zeta^\mu \eta^\nu - D_T(z, \mathbf{k}'_T) \epsilon_T^{\rho S_{hT}} \right\} \\
& + \mathcal{O} \left(\frac{M_h^2}{(P_h \cdot \eta)^2} \right). \tag{3.82}
\end{aligned}$$

We used the shorthand notation

$$G_{1s}(z, \mathbf{k}_T) \equiv S_{hL} G_{1L}(z, \mathbf{k}'_T) + \frac{(\mathbf{k}_T \cdot \mathbf{S}_{hT})}{M_h} G_{1T}(z, \mathbf{k}'_T), \tag{3.83}$$

etc. The arguments of the fragmentation functions are $z = P_h \cdot \eta / k \cdot \eta$ and $\mathbf{k}'_T = -z \mathbf{k}_T$. The first is the (light-cone) momentum fraction of the produced hadron, the second is the transverse momentum of the produced hadron with respect to the quark. The \mathbf{k}_T -integrated results are, using

$$F(z) \equiv \int d^2 k'_T F(z, \mathbf{k}'_T) \tag{3.84}$$

and

$$\begin{aligned}
F^{(n)}(z) & \equiv \int d^2 k'_T (\mathbf{k}_T^2 / 2M_h^2)^n F(z, \mathbf{k}'_T) \\
& = \int d^2 k'_T (\mathbf{k}'_T^2 / 2z^2 M_h^2)^n F(z, \mathbf{k}'_T), \tag{3.85}
\end{aligned}$$

separating contributions at different orders in $1/Q$,

$$\Delta^{\text{twist}-2}(z) = \frac{D_1(z)}{z} \not{\zeta} + S_{hL} \frac{G_1(z)}{z} \gamma_5 \not{\zeta} + \frac{H_1(z)}{z} \gamma_5 \not{\mathcal{S}}_{hT} \not{\zeta} \tag{3.86}$$

$$\begin{aligned}
\Delta^{\text{twist}-3}(x) & = \frac{M_h}{P_h \cdot \eta} \left\{ \frac{E(z)}{z} + \frac{G_T(z)}{z} \gamma_5 \not{\mathcal{S}}_{hT} + S_{hL} \frac{H_L(z)}{z} \gamma_5 \frac{[\not{\zeta}, \not{\eta}]}{2} \right\} \\
& + \frac{M_h}{P_h \cdot \eta} \left\{ -i S_{hL} \frac{E_L(z)}{z} \gamma_5 - \frac{D_T(z)}{z} \epsilon_T^{\rho\sigma} \gamma_\rho S_{hT\sigma} + i \frac{H(z)}{z} \frac{[\not{\zeta}, \not{\eta}]}{2} \right\}, \tag{3.87}
\end{aligned}$$

$$\begin{aligned}
\Delta_\partial^\alpha(z) & = -\frac{G_{1T}^{(1)}(z)}{z} S_{hT}^\alpha \not{\zeta} \gamma_5 - S_{hL} \frac{H_{1L}^{\perp(1)}(z)}{z} \frac{[\gamma^\alpha, \not{\zeta}] \gamma_5}{2} \\
& \quad - \frac{D_{1T}^{\perp(1)}(z)}{z} \epsilon_T^{\alpha S_T} \not{\eta} - i \frac{H_1^{\perp(1)}(z)}{z} \frac{[\gamma^\alpha, \not{\zeta}]}{2}. \tag{3.88}
\end{aligned}$$

An alternative notation [Jaff96] for the fragmentation functions is \hat{f} , \hat{g} , \hat{e} and \hat{h} instead of D , G , E and H .

In the sub-leading order functions one can again isolate the interaction-dependent parts as done for the distribution functions. They are now given by

$$\tilde{G}_T(z) = G_T(z) - z G_{1T}^{(1)}(z) - \frac{m}{M_h} z H_1(z), \quad (3.89)$$

$$\tilde{H}_L(z) = H_L(z) + 2z H_{1L}^{\perp(1)}(z) - \frac{m}{M_h} z G_1(z), \quad (3.90)$$

$$\tilde{E}(z) = E(z) - \frac{m}{M_h} z D_1(z), \quad (3.91)$$

$$\tilde{D}_T(z) = D_T(z) + z D_{1T}^{\perp(1)}(z), \quad (3.92)$$

$$\tilde{H}(z) = H(z) + 2z H_1^{\perp(1)}(z), \quad (3.93)$$

$$\tilde{E}_L(z) = E_L(z). \quad (3.94)$$

For the \mathbf{k}_T -integrated or the $\mathbf{k}_T^2/2M_h$ -weighted fragmentation functions all results are obtained from the distribution functions by replacing $x \rightarrow 1/z$ and $f_{\dots}(x) \rightarrow D_{\dots}(z)/z$, $g_{\dots}(x) \rightarrow G_{\dots}(z)/z$ and $h_{\dots}(x) \rightarrow H_{\dots}(z)/z$. The same applies to the relations from Lorentz-invariance [Mul96, Jako97]

$$G_T(z) = G_1(z) - z^3 \frac{d}{dz} \left[\frac{G_{1T}^{(1)}(z)}{z} \right], \quad (3.95)$$

$$H_L(z) = H_1(z) + z^3 \frac{d}{dz} \left[\frac{H_{1L}^{\perp(1)}(z)}{z} \right], \quad (3.96)$$

$$D_T(z) = z^3 \frac{d}{dz} \left[\frac{D_{1T}^{\perp(1)}(z)}{z} \right], \quad (3.97)$$

$$H(z) = z^3 \frac{d}{dz} \left[\frac{H_1^{\perp(1)}(z)}{z} \right]. \quad (3.98)$$

Bounds

4.1 Partonic densities

The notion of a positive definite object, as the probability density $f_1(x)$ in the parton model, can be maintained in a field theory. In a suitable light-cone gauge and restricting to the flavor singlet part, the probability density $f_1(x)$ stems from correlations between quark fields along a light-cone direction ζ^μ . Furthermore, only specific components of the quark field are relevant for the function $f_1(x)$. Defining the projections $\psi_\zeta(y)$ and $\psi_\eta(y)$, of the quark field ψ at space-time point y ,

$$\psi(y) = \psi_\zeta(y) + \psi_\eta(y) \quad (4.1)$$

$$\psi_\zeta(y) = P_\zeta \psi(y) = \frac{1}{2} \not{\eta} \not{\zeta} \psi(y) \quad (4.2)$$

$$\psi_\eta(y) = P_\eta \psi(y) = \frac{1}{2} \not{\zeta} \not{\eta} \psi(y) \quad (4.3)$$

$$(4.4)$$

called *good* and *bad* fields [Kogu70] respectively, the expression, can be written, after the insertion of a complete set of intermediate states,

$$\begin{aligned} f_1(x) &\equiv \int \frac{d\lambda}{2\pi} e^{i\lambda x} \langle P | \bar{\psi}(0) \not{\zeta} \psi(\lambda \zeta) | P \rangle \\ &= \sum_n \langle P | (\psi_\zeta^\dagger(0))_i | P_n \rangle \langle P_n | (\psi_\zeta(0))_i | P \rangle \delta(P_n \cdot \zeta - (1-x)P \cdot \zeta), \end{aligned} \quad (4.5)$$

as a manifestly positive definite quantity.

A generalization of the above expression to include the full spin structure of the parent hadron is given by,

$$\begin{aligned} (\Phi \not{\zeta})_{ij, s' s} &= \int \frac{d\lambda}{2\pi} e^{i\lambda x} \langle P, s' | (\psi_\zeta^\dagger(0))_j (\psi_\zeta(\lambda \zeta))_i | P, s \rangle \\ &= \sum_n \langle P_n | (\psi_\zeta(0))_j | P, s' \rangle^* \langle P_n | (\psi_\zeta(0))_i | P, s \rangle \delta(P_n \cdot \zeta - (1-x)P \cdot \zeta), \end{aligned} \quad (4.6)$$

where s' and s denote the (possibly *non-diagonal*) hadron spins. The above matrix, mapping from product space $i \times s$ space to the product space $j \times s'$, clearly has positive diagonal elements.

We will use a representation of the matrix in equation (4.6) in the hadron rest-frame and in a suitable basis for the quark field, to derive a set of inequalities among non-collinear leading order functions analogous to the Soffer-bound [Soff95] that applies to collinear leading order functions. First, we will illustrate the method re deriving the Soffer bound and we will proceed by showing the results when non-collinear functions are taken into account.

4.2 Target spin structure

In order to study the correlation function in a spin-1/2 target, one introduces a spin vector S^μ that parametrizes the spin density matrix $\rho(P, S)$. It satisfies $P \cdot S = 0$ and it is space-like, having a negative norm. Its norm, S^2 , ranges from -1 for a pure state, to zero for a mixed state. Using $S_L \equiv MS \cdot \zeta / P \cdot \zeta$ and the transverse spin vector S_T , the condition becomes $S_L^2 + \mathbf{S}_T^2 \leq 1$, as can be seen from the rest-frame expression $S = (0, \mathbf{S}_T, S_L)$. The precise equivalence of a 2×2 matrix $\tilde{M}_{ss'}$ in the target spin space and the S -dependent function $M(S)$ is

$$M(S) = \text{Tr} [\rho(S) \tilde{M}]. \quad (4.7)$$

Explicitly, the S -dependent function $M(S) = M_O + S_L M_L + S_T^1 M_T^1 + S_T^2 M_T^2$, corresponds to a matrix, which in the target rest-frame with as basis the spin 1/2 states with $S_L = +1$ and $S_L = -1$ becomes

$$\tilde{M}_{ss'} = \begin{pmatrix} M_O + M_L & M_T^1 - i M_T^2 \\ M_T^1 + i M_T^2 & M_O - M_L \end{pmatrix}. \quad (4.8)$$

The corresponding expression for the density matrix ρ is the rest-frame value of

$$\rho(S) = 1 + \sigma_3 S_L + \sigma_T \cdot \mathbf{S}_T \quad (4.9)$$

From equation (4.6) follows that after transposing in Dirac space, and subsequently extending the matrix $M(S) = (\Phi \zeta)^T$ to the target spin space gives a matrix in the combined Dirac \otimes target spin space which satisfies $v^\dagger M v \geq 0$ for any vector v in that combined space.

4.3 Quark spin structure

Taking only collinear structure into account, the quantity $\Phi \zeta$ for a spin-1/2 target in terms of the spin vector is

$$\Phi(x)\zeta = \left\{ f_1(x) + S_L g_1(x) \gamma_5 + h_1(x) \gamma_5 \mathcal{S}_T \right\} P_\zeta, \quad (4.10)$$

where the functions f_1 , g_1 and h_1 are the leading order quark distribution functions. By tracing over the Dirac indices one projects out f_1 , which is the quark momentum density (see equation (4.6)). By writing γ_5 as the difference of the chirality projectors $P_{R/L} = \frac{1}{2}(1 \pm \gamma_5)$ it follows that in a longitudinally polarized target ($S_L \neq 0$) g_1 is the difference of densities for right-handed and left-handed quarks. By writing $\gamma^i \gamma_5$ as the difference of the

transverse spin projectors $P_{\uparrow/\downarrow} = \frac{1}{2}(1 \pm \gamma^i \gamma_5)$, it follows that in a transversely polarized target ($S_T \neq 0$) h_1 is the difference of quarks with transverse spin along and opposite the target spin [Artr90, Cort92, Jaff92]. Since $f_1(x)$ is the sum of the densities it is positive and gives bounds $|g_1(x)| \leq f_1(x)$ and $|h_1(x)| \leq f_1(x)$.

By considering the combined Dirac \otimes target-spin space, stricter bounds can be found. As mentioned above, we need to consider the function $M(S) = (\Phi \not{\zeta})^T$ in Dirac space. For this we use a chiral representation. In that representation the good projector P_ζ only leaves two (independent) Dirac spinors, one right-handed (R), one left-handed (L). On this (2-dimensional) basis of good R and L spinors the matrix $M = (\Phi(x) \not{\zeta})^T$ obtained from equation (4.10) is given by

$$M_{ij} = \begin{pmatrix} f_1(x) + S_L g_1(x) & (S_T^1 + i S_T^2) h_1(x) \\ (S_T^1 - i S_T^2) h_1(x) & f_1(x) - S_L g_1(x) \end{pmatrix}. \quad (4.11)$$

Next, we make the spin-structure of the target explicit as outlined in equation (4.8), yielding on the basis $+R, -R, +L$ and $-L$

$$\tilde{M} = \begin{pmatrix} f_1 + g_1 & 0 & 0 & 2 h_1 \\ 0 & f_1 - g_1 & 0 & 0 \\ 0 & 0 & f_1 - g_1 & 0 \\ 2 h_1 & 0 & 0 & f_1 + g_1 \end{pmatrix}. \quad (4.12)$$

From the positivity of the diagonal elements one recovers the trivial bounds $f_1(x) \geq 0$ and $|g_1(x)| \leq f_1(x)$, but requiring the eigenvalues of the matrix to be positive gives the stricter Soffer bound [Soff95],

$$|h_1(x)| \leq \frac{1}{2} (f_1(x) + g_1(x)). \quad (4.13)$$

4.3.1 Quark-spin structure including transverse momentum

Separating the terms corresponding to unpolarized (O), longitudinally polarized (L) and transversely polarized targets (T), the most general parametrizations *with \mathbf{p}_T -dependence*, relevant at leading order in $1/Q$, are

$$\Phi_O(x, \mathbf{p}_T) \not{\zeta} = \left\{ f_1(x, \mathbf{p}_T^2) + i h_1^\perp(x, \mathbf{p}_T^2) \frac{\not{\mathbf{p}}_T}{M} \right\} P_\zeta \quad (4.14)$$

$$\Phi_L(x, \mathbf{p}_T) \not{\zeta} = \left\{ S_L g_{1L}(x, \mathbf{p}_T^2) \gamma_5 + S_L h_{1L}^\perp(x, \mathbf{p}_T^2) \gamma_5 \frac{\not{\mathbf{p}}_T}{M} \right\} P_\zeta \quad (4.15)$$

$$\begin{aligned} \Phi_T(x, \mathbf{p}_T) \not{\zeta} = & \left\{ f_{1T}^\perp(x, \mathbf{p}_T^2) \frac{\epsilon_{T\rho\sigma} p_T^\rho S_T^\sigma}{M} + g_{1T}(x, \mathbf{p}_T^2) \frac{\mathbf{p}_T \cdot \mathbf{S}_T}{M} \gamma_5 \right. \\ & \left. + h_{1T}(x, \mathbf{p}_T^2) \gamma_5 \not{\mathbf{S}}_T + h_{1T}^\perp(x, \mathbf{p}_T^2) \frac{\mathbf{p}_T \cdot \mathbf{S}_T}{M} \frac{\gamma_5 \not{\mathbf{p}}_T}{M} \right\} P_\zeta. \end{aligned} \quad (4.16)$$

To put bounds on the transverse momentum dependent functions, we again make the matrix structure explicit. One finds, defining for short hand the following azimuthal phase factors

$$c = \frac{|p_T|}{M} e^{i\phi} \quad (4.17)$$

and its complex conjugate c^* , for $M = (\Phi(x, p_T) \zeta)^T$ the full spin matrix \tilde{M} to be

$$\begin{pmatrix} f_1 + g_{1L} & c(g_{1T} + i f_{1T}^\perp) & c^*(h_{1L}^\perp + i h_1^\perp) & 2h_1 \\ c^*(g_{1T} - i f_{1T}^\perp) & f_1 - g_{1L} & (c^*)^2 h_{1T}^\perp & -c^*(h_{1L}^\perp - i h_1^\perp) \\ c(h_{1L}^\perp - i h_1^\perp) & c^2 h_{1T}^\perp & f_1 - g_{1L} & -c(g_{1T} - i f_{1T}^\perp) \\ 2h_1 & -c(h_{1L}^\perp + i h_1^\perp) & -c^*(g_{1T} + i f_{1T}^\perp) & f_1 + g_{1L} \end{pmatrix}, \quad (4.18)$$

where ϕ is the azimuthal angle of \mathbf{p}_T . First of all, this matrix is illustrative as it shows the full quark helicity structure accessible in a polarized nucleon [Bogl99], which is equivalent to the full helicity structure of the forward anti-quark-nucleon scattering amplitude.

Note that although distribution functions are used, a complete analogous treatment can be performed on fragmentation functions.

4.4 The bounds

Bounds to assure positivity of any matrix element can for instance be obtained by looking at the 1-dimensional subspaces, giving the trivial bounds $f_1 \geq 0$ and $|g_{1L}| \leq f_1$. From the 2-dimensional subspace one finds, omitting the (x, \mathbf{p}_T^2) dependences for the distribution functions, and using here the \mathbf{p}_T -moment notation in an unintegrated sense,

$$f^{(1)} \equiv \frac{\mathbf{p}_T^2}{2M} f(x, \mathbf{p}_T) \quad (4.19)$$

the following bounds,

$$|h_1| \leq \frac{1}{2} (f_1 + g_{1L}) \leq f_1, \quad (4.20)$$

$$|h_{1T}^{\perp(1)}| \leq \frac{1}{2} (f_1 - g_{1L}) \leq f_1, \quad (4.21)$$

$$(g_{1T}^{(1)})^2 + (f_{1T}^{\perp(1)})^2 \leq \frac{\mathbf{p}_T^2}{4M^2} (f_1 + g_{1L})(f_1 - g_{1L}) \leq \frac{\mathbf{p}_T^2}{4M^2} f_1^2, \quad (4.22)$$

$$(h_{1L}^{\perp(1)})^2 + (h_1^{\perp(1)})^2 \leq \frac{\mathbf{p}_T^2}{4M^2} (f_1 + g_{1L})(f_1 - g_{1L}) \leq \frac{\mathbf{p}_T^2}{4M^2} f_1^2. \quad (4.23)$$

Besides the Soffer bound, show in equation (4.20) but now holding for each value of \mathbf{p}_T , new bounds for the distribution functions are found. In particular, one sees that functions like $g_{1T}^{(1)}$ and $h_{1L}^{\perp(1)}$ appearing in azimuthal asymmetries in leptonproduction are proportional to $|\mathbf{p}_T|$ for small p_T . In the case of the T-odd fragmentation functions, the Collins function, $H_1^{\perp(1)}$, describing fragmentation of a transversely polarized quark into an unpolarized or spin-less hadron, for instance a pion, is bounded by $(|\mathbf{P}_{\pi\perp}|/2zM_\pi)D_1(z, \mathbf{P}_{\pi\perp}^2)$ while the other T-odd function $D_{1T}^{\perp(1)}$ describing fragmentation of an unpolarized quark into a polarized hadron such as a Λ , is given by $(|\mathbf{P}_{\Lambda\perp}|/2zM_\Lambda)D_1(z, \mathbf{P}_{\Lambda\perp}^2)$.

Before sharpening these bounds via eigenvalues, it is convenient to introduce two positive definite functions $F(x, \mathbf{p}_T^2)$ and $G(x, \mathbf{p}_T^2)$ such that $f_1 = F + G$ and $g_1 = F - G$ and define

$$h_1 = \alpha F, \quad (4.24)$$

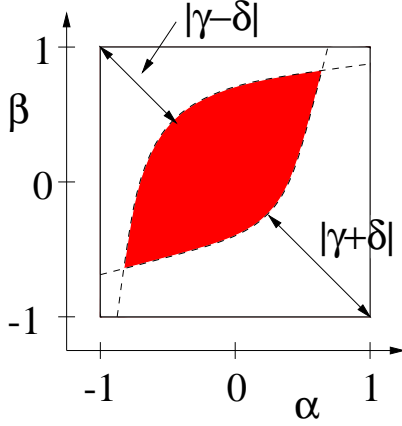


Figure 4.1: Allowed region (shaded) for α and β depending on γ and δ .

$$h_{1T}^{\perp(1)} = \beta G, \quad (4.25)$$

$$g_{1T}^{(1)} + i f_{1T}^{\perp(1)} = \gamma \frac{|p_T|}{M} \sqrt{FG}, \quad (4.26)$$

$$h_{1L}^{\perp(1)} + i h_1^{\perp(1)} = \delta \frac{|p_T|}{M} \sqrt{FG}, \quad (4.27)$$

where the x and \mathbf{p}_T^2 dependent functions α , β , γ and δ have absolute values in the interval $[-1, 1]$. Note that α and β are real-valued but γ and δ are complex-valued, the imaginary part determining the strength of the T-odd functions. Actually, one sees that the T-odd functions f_{1T}^{\perp} and h_1^{\perp} could be considered as imaginary parts of g_{1T} and h_{1L}^{\perp} , respectively.

Next we sharpen these bounds using the eigenvalues of the matrix, which are given by

$$e_{1,2} = (1 - \alpha)F + (1 + \beta)G \pm \sqrt{4FG|\gamma + \delta|^2 + ((1 - \alpha)F - (1 + \beta)G)^2}, \quad (4.28)$$

$$e_{3,4} = (1 + \alpha)F + (1 - \beta)G \pm \sqrt{4FG|\gamma - \delta|^2 + ((1 + \alpha)F - (1 - \beta)G)^2}. \quad (4.29)$$

Requiring them to be positive can be converted into the conditions

$$F + G \geq 0. \quad (4.30)$$

$$|\alpha F - \beta G| \leq F + G, \quad \text{i.e. } |h_{1T}| \leq f_1 \quad (4.31)$$

$$|\gamma + \delta|^2 \leq (1 - \alpha)(1 + \beta), \quad (4.32)$$

$$|\gamma - \delta|^2 \leq (1 + \alpha)(1 - \beta). \quad (4.33)$$

4.5 Discussion

It is interesting for the phenomenology of deep inelastic processes that a bound for the transverse spin distribution h_1 is provided not only by the inclusively measured functions f_1 and g_1 , but also by the functions g_{1T} and h_{1L}^{\perp} , responsible for specific azimuthal asymmetries [Mul96, Boer98]. This is illustrated in Fig. 4.1. The same goes for fragmentation functions, where for instance the magnitude of H_1^{\perp} constrains the magnitude of H_1 .

The bounds presented in this chapter involve only a treatment at tree level. The question arises about the effect of including interactions to these bounds. For guidance,

at leading order (LO) in α_s , the collinear Soffer bound was found to be stable [Baro97, Bour98] for evolution towards larger values of Q . Beyond LO, scheme dependence allows one to invalidate this inequality [Gold95], but for \overline{MS} and Drell-Yan factorization schemes, the inequality seems to be preserved even at next-to-leading order (NLO). One would, at best, expect a similar situation for the bounds derived here for non-collinear distribution functions.

Performing an analysis similar to those mentioned in this section, on the bounds presented, is complicated. The number of functions entering the equations and the functional form in which they enter, combined with the non-autonomous evolution of the functions involved, as we will discuss in later chapters, has prevented us from resolving the question of stability under evolution.

Although a thorough investigation of the effect of scale dependence on the bounds presented here still should be performed, the elementary bounds presented in this chapter can serve as important guidance to estimate the magnitudes of asymmetries expected in the various processes.

Scale dependence

5.1 Introduction

The main achievement of factorization is that the cross-section for a hard process involving hadrons is written as the product of a part of which we can systematically improve its accuracy, and an interesting soft part that bears the details of hadronic bound states. The part that we can calculate, corresponds to the high energy limit of a partonic hard scattering sub-process. Due to the hard nature of the partonic sub-process, the property of asymptotic freedom can be exploited, and we can systematically improve the determination of the hard part using an expansion in powers of the coupling constant. Improving the accuracy with which we determine the hard part directly improves the accuracy with which we can extract knowledge of the soft parts from experiment.

Straightforward application of perturbation theory to calculations of hard partonic sub-processes leads to divergences. Specific loop momentum integration regions lead to these divergences due to the massless nature of quarks and gluons. These divergences manifest themselves in the presence of large logarithms that accompany each order of α_s , and prevent taking advantage of the smallness of the coupling constant.

The solution of this problem is known as the *factorization of mass singularities* [Eli79a] and involves the absorption of the divergences into the soft parts. The result of this procedure is that the soft parts acquire a scale dependence. This scale dependence of the soft parts, often denoted by the name of scale-evolution of the soft parts, can be calculated using perturbative techniques.

5.2 Calculation of scale dependence

There are several methods for determining the scale dependence of distribution and fragmentation functions. A successful factorization program requires, an order by order in α_s , cancellation of mass-divergences, arising in the hard part, and ultra-violet (UV) divergences, which have their origin in the soft part. As a result the scale dependence of distribution and fragmentation functions can be either extracted from the study of perturbative corrections to the hard parts or to the soft parts.

Calculations of scale dependence can also differ depending on whether matrix elements of local or non-local operators are considered. Traditionally, calculations involved the study of hard partonic sub-processes, and involved taking longitudinal momentum moments of the objects involved. These are the approaches based on the OPE and they result in the perturbative determination of the anomalous dimensions of corresponding local matrix elements and, therefore, of their scale dependence. This approach to the calculation of scale dependence involves a nomenclature of its own, which we want to summarize in the coming section as it will be used further in this thesis in chapter 6.

A completely different, but equivalent, approach is in terms of non-local process-independent objects. This method is used in [Bukh83a] to calculate the scale dependence of sub-leading order in $1/Q$ functions. Working with non-local objects remains closer to a partonic interpretation of the soft parts. By introducing a projection operation on a hadronic matrix element, that summarizes how the hard process picks up a contribution from the soft part, we avoid making reference to the process in question.

In this thesis we want to study the effect of perturbative corrections to the distribution and fragmentation functions that are introduced by taking quark transverse momentum into account. To extend the analysis beyond tree level we start by looking at corrections of order α_s . To this order in α_s the leading logarithmic approximation (LLA) suffices to obtain the scale dependence of soft objects, and is the approximation we will use. The LLA amounts to collecting all contributions that involve the product of α_s and a single large logarithm, so that the scale dependence generated by all terms with a factor $(\alpha_s \ln(Q^2/\mu^2))^n$, that have been absorbed into the soft part are obtained.

5.2.1 The local approach

The first calculations of scale dependence of soft object involved structure functions instead of distribution and fragmentation functions and were performed using this method. The method starts by studying the partonic equivalent of a specific process in which the hadrons are replaced by on-shell partons. Depending on the order in α_s up to which the calculation is performed, all possible perturbative corrections are taken into account. The moments in the longitudinal momentum fraction are taken in order to obtain a sum of products of moments of coefficient functions as given in equation (2.15), and hadronic matrix elements involving only local operators. It boils down to the calculation of the anomalous dimensions of the moments of coefficient functions up to a specific order in α_s .

Considering all possible perturbative corrections up to a specific order of α_s , and taking moments, one obtains an expression for the coefficient function up to this order in α_s . Concentrating on the perturbatively generated part c_n and in particular in its Q^2 dependence, the anomalous dimension γ_n gives the behavior for large Q^2 of the perturbatively acquired logarithmic scale dependence. To leading order in α_s this behavior is given by

$$c_n(Q^2) = N_n \left(\ln \frac{Q^2}{\mu^2} \right)^{-\frac{\gamma_n}{2\beta_0}}, \quad (5.1)$$

where N_n is independent of Q and,

$$\beta_0 = \frac{1}{(4\pi)^2} \frac{11C_A - 4C_F T_R}{3}. \quad (5.2)$$

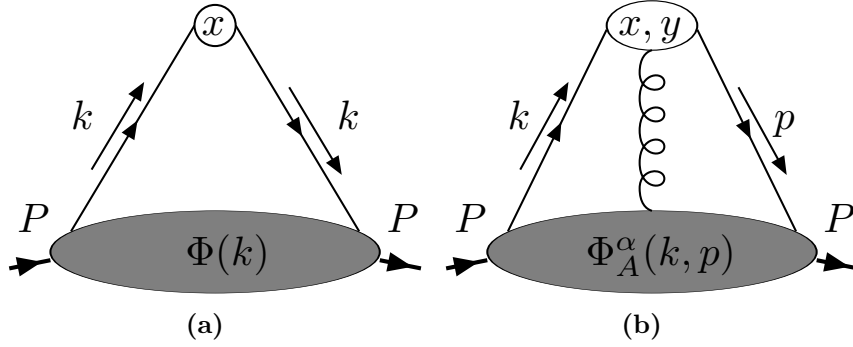


Figure 5.1: Diagrammatic representation of the projection of functions out of soft matrix elements. (a) Shows the projection of a single-argument distribution function as defined in equation (5.3). (b) Shows the projection of two-argument distribution functions as formulated in equation (5.4)

is the first order in α_s derivative of the coupling constant to the scale, a valid approximation in the asymptotic regime.

5.2.2 The non-local approach

We will follow an approach that was already used in [Bukh84a] in the context of obtaining the evolution equations for a polarized target in QED in a light-cone gauge. In spite of issues as gauge invariance and over-completeness of the set of soft functions appearing in the calculations, this approach is preferred due to its resemblance to the parton model.

To obtain all scale dependence in a soft part up to some order in α_s , one operates in the following way. As all perturbative corrections that give large logarithms have been absorbed into the soft parts, one can regard all this type of contributions to be included in the soft part.

Suppose we want to study the evolution of a function $f(x)$ that is defined in terms of a projection operation on a quark-correlator as follows

$$f(x) = \int d^4k \delta(k \cdot \zeta - x P \cdot \zeta) \text{Tr} [\Phi(k) \Gamma_f] \quad (5.3)$$

where the object Γ_f is a Dirac structure multiplied by a tensor such that it projects out of a soft part exactly that function. This operation can be depicted as shown in figures 5.1(a) and (b)

The study of the evolution of non-collinear leading order functions involves sub-leading order functions. The structure parametrized by these functions involves correlations in matrix elements including an additional gluon. In a similar manner, we will define a specific function in terms of a projection operation. In this case two longitudinal momentum fractions are involved as shown in figure 5.1(b), which is the diagrammatic representation of

$$F(x, y) = \int d^4k d^4p \delta(k \cdot \zeta - x P \cdot \zeta) \delta(p \cdot \zeta - y P \cdot \zeta) \text{Tr} [\Phi_A^\alpha(k, p) (\Gamma_F)_\alpha]. \quad (5.4)$$

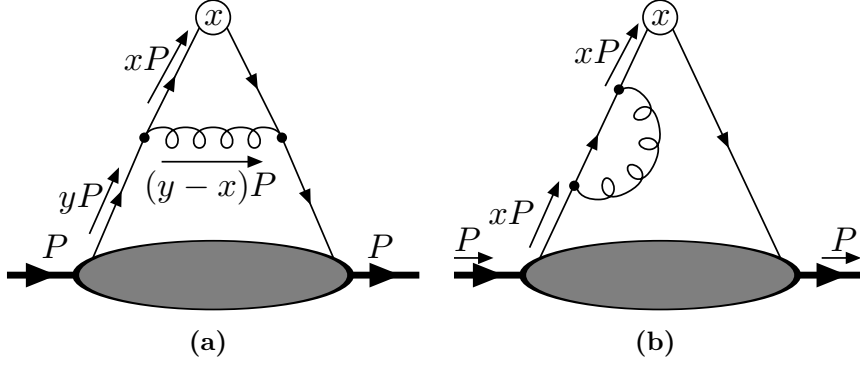


Figure 5.2: Examples of perturbative corrections to first order in α_s to functions defined in terms of quark-quark correlators. (a) Example of a real correction that changes longitudinal momentum fraction. (b) Example of a virtual correction that only contributes at an end-point in the kernel longitudinal momentum fraction integration.

Aiming for an accuracy of one order in α_s , and for the case that a function is defined in terms of a quark-quark correlator, one starts writing down all diagrams of order α_s . These contributions constitute what is called the evolution *kernel* to order α_s .

We will be interested in first order kernels, that is kernels that only contain a single power of α_s . This is the simplest case that can be considered. Still in this simplest case this first order analysis involves several diagrams. There are two types of diagrams.

The first type of diagrams are called *real* diagrams and correspond to real gluon emission, that is additional jet formation. These are diagrams in which the initial momentum fraction of the parton changes. An example of this type of diagram is shown in figure 5.2(a) The second type of diagrams are the virtual diagrams. This type of diagram does not change initial momentum fraction of the quark. An example of this type of diagram is shown in figure 5.2(b)

5.3 A simple case

In this section we will show the steps in the calculation of the flavor non-singlet evolution of the unpolarized quark momentum distribution in an unpolarized hadron, the function $f_1(x, \mu^2)$.

The evolution of the function $f_1(x, \mu^2)$ to this accuracy is certainly not new, but because of its simplicity we would like to use it to introduce a calculational method that will be extended to non-collinear functions, and also to introduce notations used elsewhere in this thesis.

To obtain the function $f_1(x, \mu^2)$ we need the projector $\not{\zeta}/2$, in the sense that the function can be defined, in a light-cone gauge $A \cdot \zeta = 0$, in the following way

$$f_1(x, \mu^2) = \int d^4k \delta(k \cdot \zeta - x P \cdot \zeta) \text{Tr} \left[\Phi(k; \ln \mu^2) \frac{1}{2} \not{\zeta} \right]. \quad (5.5)$$

In order to find the scale dependence of the function $f_1(x, \mu^2)$ to first order in α_s one differentiates the expression in equation (5.5) with respect to $\tau = \ln \mu^2$, exposing the

interactions included in $\Phi(k; \tau)$ up to this order.

$$\frac{\partial}{\partial \tau} \left\{ \text{triangle diagram with gluon loop} \right\} = \frac{\partial}{\partial \tau} \left\{ \text{triangle diagram with gluon loop} + \frac{1}{2} \left[\text{triangle diagram with gluon loop} + \text{triangle diagram with gluon loop} \right] \right\} + \mathcal{O}(\alpha_s^2) \quad (5.6)$$

The factor 1/2 accompanying the self-energy contributions arises from the fact that these interactions reside in a factor of $Z_q^{1/2}$ that is included in each renormalized quark field that appears in the definition of $\Phi(k; \tau)$ in equation (3.1).

Written explicitly, the contributions up to first order in α_s and considering only the flavor non-singlet sector, come from a single real diagram

$$\begin{aligned} \text{triangle diagram with gluon loop} &= \frac{-ig^2}{(2\pi)^4} \int d^4k \delta(k \cdot \zeta - x P \cdot \zeta) \\ &\times \int d^4p \frac{\text{Tr} \left[\Phi(p; \tau) \gamma^\mu \not{k} \frac{1}{2} \not{\zeta} \not{k} \gamma^\nu \right] d_{\mu\nu}(p-k)}{(k^2 + i\epsilon)^2 ((p-k)^2 + i\epsilon)}, \end{aligned} \quad (5.7)$$

also known as the gluon-rung diagram. Additional scale dependence arises in the self-energy diagrams for the quark field, and contribute according to the following expression

$$\begin{aligned} \frac{1}{2} \left[\text{triangle diagram with gluon loop} + \text{triangle diagram with gluon loop} \right] &= \frac{1}{2} \int d^4k \delta(k \cdot \zeta - x P \cdot \zeta) \\ &\times \text{Tr} \left[\Phi(k; \tau) \left\{ \frac{1}{2} \not{\zeta} \frac{i\not{k}}{(k^2 + i\epsilon)} \Sigma(k) + \Sigma(k) \frac{i\not{k}}{(k^2 + i\epsilon)} \frac{1}{2} \not{\zeta} \right\} \right], \end{aligned} \quad (5.8)$$

where the quark self-interaction part $\Sigma(k)$ is a Dirac matrix and given by

$$\Sigma(k) = -\frac{g^2}{(2\pi)^4} \int d^4l \frac{\gamma^\mu (\not{k} - \not{l}) \gamma^\nu d_{\mu\nu}(l)}{(l^2 + i\epsilon)((k-l)^2 + i\epsilon)}. \quad (5.9)$$

The calculations are performed in the gauge $A \cdot \zeta = 0$, in which the gluon polarization sum, $d_{\mu\nu}$, in the gluon propagator has the form

$$d_{\mu\nu}(l) = \left(g_{\mu\nu} - \frac{(l_\mu \zeta_\nu + l_\nu \zeta_\mu)}{l \cdot \zeta} \right). \quad (5.10)$$

5.3.1 Real diagram

The object that is traced with $\Phi(k; \tau)$ in equation (5.7) only contains three different Dirac structures

$$\begin{aligned} \frac{1}{2} \gamma^\mu \not{k} \not{\zeta} \not{k} \gamma^\nu d_{\mu\nu}(p-k) &= \\ &\not{\zeta} \left[\frac{\overbrace{4k \cdot \eta (k \cdot \zeta)^2 + k_T^2 (k \cdot \zeta + p \cdot \zeta)}^{\text{LL}} - 2k \cdot \zeta p_T \cdot k_T}{(p-k) \cdot \zeta} \right] \end{aligned} \quad (5.11)$$

$$-2\not{\eta} (k \cdot \zeta)^2 - 2\gamma_{T\alpha} \left[\frac{(k \cdot \zeta)^2}{(p-k) \cdot \zeta} (p_T^\alpha - k_T^\alpha) \right], \quad (5.12)$$

where all momenta and indices have been split up into collinear and transverse parts, as e.g.

$$k^\mu = k \cdot \zeta \eta^\mu + k \cdot \eta \zeta^\mu + k_T^\mu. \quad (5.13)$$

In order to obtain the LLA contribution we will make the following variable transformation

$$k \cdot \eta \rightarrow \frac{\alpha |\mathbf{k}_T|^2}{2P \cdot \zeta} \quad (5.14)$$

where $|\mathbf{k}_T|^2 = -k_T^2$ and $P \cdot \zeta$ is the large component of the parent hadron momentum. Now up to $\mathcal{O}(1/|\mathbf{k}_T|^2)$ we can write the denominators in equation (5.7) as

$$\frac{1}{((p-k)^2 + i\varepsilon)(k^2 + i\varepsilon)^2} = \frac{1}{|\mathbf{k}_T|^6} \frac{1}{(\alpha(x-y) - 1 + i\varepsilon)(\alpha x - 1 + i\varepsilon)^2} \quad (5.15)$$

The logarithmic divergence arises in the $|\mathbf{k}_T|$ integration and considering the Jacobian due to equation (5.14) and the denominator above, one sees that only the over-braced terms in equation (5.11) can lead to large logarithms. Keeping these terms, the α -integration can be performed introducing generalized θ -functions defined in the following way,

$$\Theta_{i_1 \dots i_k}^n(x_1, \dots, x_k) \equiv -i \int \frac{d\alpha}{2\pi} \frac{\alpha^n}{(\alpha x_1 - 1 + i\varepsilon)^{i_1} \dots (\alpha x_k - 1 + i\varepsilon)^{i_k}}. \quad (5.16)$$

Taking into account only the leading terms the real contribution, is

$$\begin{aligned} \text{Diagram} &= \frac{\alpha_s}{2\pi} \tau \int dy \left[\frac{x+y}{x-y} \Theta_{21}^0(x, x-y) + \frac{2x^2}{y-x} \Theta_{21}^1(x, x-y) \right] f_1(y, \mu^2) \\ &= \frac{\alpha_s}{2\pi} \tau \int dy \frac{x^2 + y^2}{y(y-x)} \Theta_{11}^0(x, x-y) f_1(y, \mu^2), \end{aligned} \quad (5.17)$$

where in the last line the reduction relations (5.49) and (5.51), contained in an appendix at the end of this chapter, are used to obtain an expression involving only regular θ -functions,

$$\Theta_{11}^0(x, y) = \frac{\theta(x)\theta(-y) - \theta(-x)\theta(y)}{x-y}. \quad (5.18)$$

The real contribution, due to the support properties of distribution and fragmentation functions, is given by the expression

$$\text{Diagram} = \frac{\alpha_s}{2\pi} \tau \int_x^1 dy \frac{x^2 + y^2}{y^2(y-x)} f_1(y, \mu^2). \quad (5.19)$$

Note that this contribution contains an integration end-point divergence corresponding to the emission of gluons with zero longitudinal momentum by the initial quark.

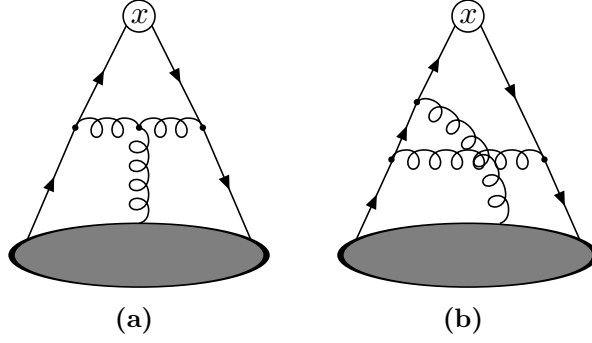


Figure 5.3: Examples of diagrams that introduce sub-leading functions into the scale dependence of non-collinear leading order in $1/Q$ distribution functions. (a) This diagram survives the limit of large number of colors. (b) This is an example of a non-planar diagram that vanishes in the limit of large number of colors.

5.4 Non-collinear functions

The evolution of non-collinear functions is more involved than that of $f_1(x, \mu^2)$. In this section we would like to sketch the calculation of the scale dependence of the function $g_{1T}^{(1)}$.

An operational definition of this function can be given by the following expression

$$g_{1T}^{(1)}(x, \mu^2) = \int d^4k \delta(k \cdot \zeta - x P \cdot \zeta) \text{Tr} \left[\Phi(k; \ln \mu^2) \frac{1}{2} \not{\zeta} \gamma_5 \frac{k_T \cdot S_T}{S_T^2} \right]. \quad (5.25)$$

The calculation of the contributions to $g_{1T}^{(1)}(x, \mu^2)$ from 2 particle irreducible (2PI) soft parts, as we will denote the soft part that gives rise to single argument functions, is similar to that described in the preceding section for the case of $f_1(x, \mu^2)$, although more care is necessary in obtaining *all* leading logarithms. The results are very different. Calculating the gluon-rung diagram with the projector corresponding to the function $g_{1T}^{(1)}(x, \mu^2)$ leads to the perturbative generation of the following scale dependence

$$\frac{\partial}{\partial \tau} g_{1T}^{(1)}(x, \tau) = \frac{\alpha_s}{2\pi} c_F \int_x^1 \frac{dy}{y} \left[\frac{x(2x^2 - xy + y^2)}{y^2(y-x)} g_{1T}^{(1)}(x, \tau) + \frac{x^2}{y} g_T(y, \tau) \right] \quad (5.26)$$

which indicates possible mixing of the function $g_{1T}^{(1)}(x)$ with sub-leading order functions in contrast to the f_1 case. Also different to the f_1 case is the contribution of non-partonic functions in its evolution. If one considers the contribution of the diagram shown in figure 5.3(a), denoting the contribution by the subscript UR, and performing the calculation in the gauge $A \cdot \zeta = 0$, one finds no additional contributions to f_1 , but the function $g_{1T}^{(1)}$ does receive contributions from the sub-leading order functions G_A and \tilde{G}_A ,

$$g_{1T}^{(1)}(x) \Big|_{\text{UR}} = \frac{\alpha_s}{2\pi} \ln \mu^2 \int_0^1 dy \int_0^1 dy_1 \left\{ \begin{aligned} & \Theta_{11}^0(x, x-y) \left[G_A(y, y_1) A(x, y, y_1) + \tilde{G}_A(y, y_1) B(x, y, y_1) \right] \\ & + \Theta_{11}^0(x, x-y_1) \left[-G_A(y, y_1) A(x, y_1, y) + \tilde{G}_A(y, y_1) B(x, y_1, y) \right] \end{aligned} \right\}, \quad (5.27)$$

where the kernel functions are given by the expressions,

$$A(x, y, y_1) = \frac{-(-x^2 - 2xy + y^2 + xy_1 + yy_1)}{2y(x - y_1)} \quad (5.28)$$

$$B(x, y, y_1) = \frac{-2x^3 + x^2y + y^3 + x^2y_1 - 3xyy_1 + xy_1^2 + yy_1^2}{2y(x - y_1)(y - y_1)}, \quad (5.29)$$

where the two-argument functions G_A and \tilde{G}_A are defined as in equation (3.21), parametrizing a matrix element involving an additional soft gluon. Note that these function can have imaginary parts, while $g_{1T}^{(1)}$ is a *real* function. The kernels that results from calculation, shown in equation (5.27) possess exactly the symmetry necessary, with respect to the symmetries of these functions, shown in equations (3.22) and (3.23) to only couple the *real* parts of these functions to $g_{1T}^{(1)}$.

This mixing of the distribution functions $g_{1T}^{(1)}$, g_T , the real part of G_A and \tilde{G}_A forces one to study the evolution of these functions as well. This is not necessary, as these four functions are not independent due to a relation following from equations of motion and Lorentz-invariance. On the other side, the relations are not always of great use, or complicate the calculation. It was to us preferable to calculate the mixing without use of these relations and apply the relations afterward as a check.

The calculation of the evolution of the functions G_A and \tilde{G}_A demands the calculation of virtual diagrams involving the gluon self-energy. The gluon self-energy contributions lead to the following form for the gluon propagator

$$G_{\mu\nu}(k) = (1 + \Pi^0(k))U_{\mu\rho}(k)\frac{d_{\rho\sigma}}{k^2 + i\varepsilon}U_{\sigma\nu}(k) \quad (5.30)$$

where

$$U_{\mu\nu}(k) = g_{\mu\nu} - \frac{1}{2}\Pi^1(k)\frac{k_\mu\zeta_\nu + k_\nu\zeta_\mu}{k \cdot \zeta} \quad (5.31)$$

and the quantities

$$\Pi^0(k) = \frac{\alpha_s}{2\pi}\tau \left[c_A \int dz \frac{(z^2 - zx + x^2)^2}{z(z-x)x^2} \Theta_{11}^0(z, z-x) - \frac{N_f}{3} \right] \quad (5.32)$$

$$\Pi^1(k) = \frac{\alpha_s}{4\pi}\tau c_A \int dz \frac{(5z^2(z-x) + 6z^2(z-x)^2 + 2x^4)}{z(z-x)x^2} \Theta_{11}^0(z, z-x) \quad (5.33)$$

5.4.1 Closed evolution system

The evolution of non-collinear leading order in $1/Q$ distribution and fragmentation functions cannot be seen separately from the evolution systems of sub-leading order collinear functions. The calculation of the evolution of leading order non-collinear functions is performed in a redundant basis of non-local objects. Of each of these functions is determined how it mixes with other functions under evolution. The result is that the evolution equations can be put in a matrix structure, in which a set of functions at one scale, mix with each other by means of the found evolution system, to form the same set of functions at a different scale. This system takes its simplest form in a light-cone gauge.

Performing the calculations in the gauge $A \cdot \zeta = 0$, where ζ^μ also denotes the hard direction probing the hadron, the coupled set of evolution equations have a four by four matrix structure. The mixing under evolution can be shown diagrammatically as follows

$$\frac{\partial}{\partial \ln \mu^2} \begin{pmatrix} \text{Diagram 1} \\ \text{Diagram 2} \end{pmatrix} = \begin{bmatrix} \text{2PI} & \text{2PI} \\ \text{3PI} & \text{3PI} \end{bmatrix} \begin{pmatrix} \text{Diagram 1} \\ \text{Diagram 2} \end{pmatrix} \quad (5.34)$$

where the boxes labeled 2PI and 3PI denote two-particle and three-particle irreducible kernels respectively, and the lower lines on the kernels have been truncated. In this diagram is implicit that the gauge $A \cdot \zeta = 0$ has been chosen. In this case the polarizations of the gluon that have to be considered are only the transverse ones.

Inclusion of a quark mass in the calculation of scale dependence increases the number of functions that mix under evolution. The presence of a quark mass operator introduce mixing from chiral-odd and chiral even sector of functions. Interactions in mass-less QCD cannot connect these sectors. The mixing of single argument functions into the evolution of two-argument functions is in identical proportions to those in which the single argument functions enter in the equations of motion relations (3.75), (3.76) and (3.77). Their presence can be eliminated through the use of these relations. This cross-talk between chiral-even and chiral-odd sectors of functions is trivial and we will discard it in our calculations by setting the quark mass to zero.

Although of limited applicability, we concentrate on the scale dependence of the flavor non-singlet distribution and fragmentation functions. For this case the structure of the mixing fits into the diagram in equation (5.34). When flavor singlet combinations of the functions are considered a more general kernel in which quark legs are replaced by gluons, has to be considered together with the mixing of gluon distribution functions under evolution.

5.5 Large number of colors

As the evolution of sub-leading order in $1/Q$ functions is rather complicated and seems to become more transparent when considering the limit of large number of colors, we will perform the calculation neglecting corrections of order $1/N_c$. In this limit all non-planar diagrams vanish as these diagrams are accompanied by a factor

$$c_F - \frac{1}{2}c_A \rightarrow 0 \quad (5.35)$$

as the color constants c_F and c_A obtain their limiting values

$$c_F \rightarrow \frac{1}{2}N_c \quad (5.36)$$

$$c_A \rightarrow N_c \quad (5.37)$$

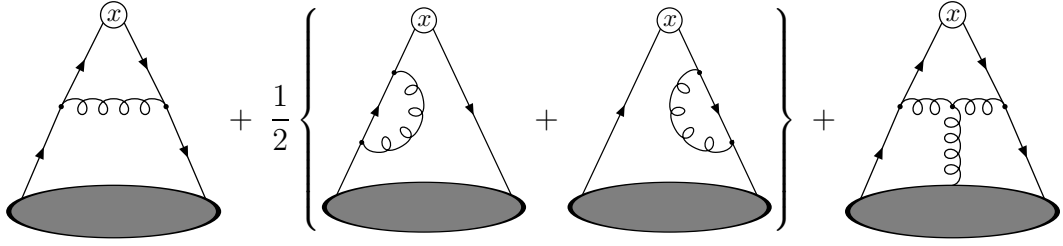


Figure 5.4: Contributions that have to be taken into account in first order in α_s to calculate the Q^2 -dependence of a single longitudinal momentum distribution function in a light-cone gauge in the large N_c limit.

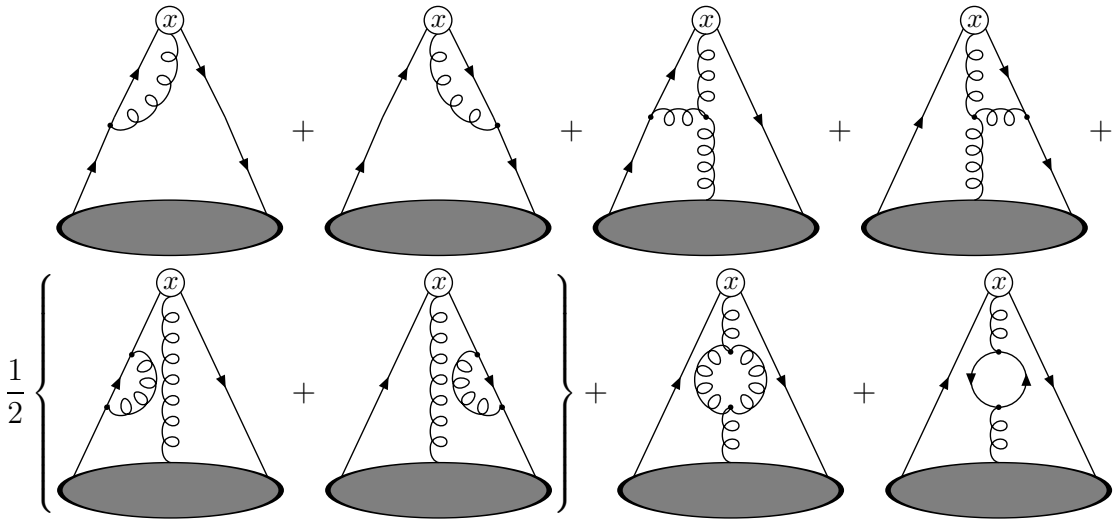


Figure 5.5: These are the first order in α_s contributions to two-argument functions in a light-cone gauge in the large N_c limit.

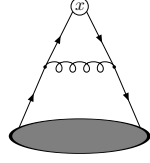
The diagrams that have to be considered in order to calculate the Q dependence of single argument distribution functions are shown in figure 5.4. Even in this limit the evolution systems will not be simple as also two-argument functions have to be considered. The diagrams that have to be taken into account to calculate the corrections to these functions are shown in figure 5.5.

5.6 Calculation of the large- N_c contributions

In this section we define for further reference all contributions that are relevant for the calculation of the evolution equations of transverse momentum dependent distribution functions at first order in α_s . In all expressions color factors have been taken into account and the large N_c limit has been taken. The projectors Γ and Γ^α are kept general in order to use these definitions to more evolution sectors than only that of $g_{1T}^{(1)}(x)$.

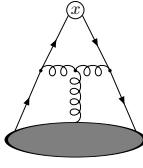
5.6.1 Real contributions

The ladder diagram contribution will be defined by



$$= -i g^2 N_c \int \frac{d^4 k d^4 p}{(2\pi)^4} \delta(k \cdot \zeta - x P \cdot \zeta) \times \frac{\text{Tr} [\Phi(p) \gamma^\alpha \not{k} \Gamma \not{k} \gamma^\beta]}{(k^2 + i\epsilon)((p-k)^2 + i\epsilon)} d_{\alpha\beta}(p-k) \quad (5.38)$$

where the gluon polarizer in the light-cone gauge has the form of equation (5.10). An additional contribution to 2PI soft parts is defined as



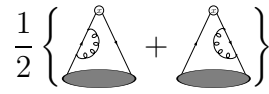
$$= -i g^2 N_c \int \frac{d^4 k d^4 p}{(2\pi)^4} \delta(k \cdot \zeta - x P \cdot \zeta) \times \frac{\text{Tr} [\Phi_A^\rho(p, p_1) \gamma^\alpha \not{k} \Gamma \not{k} \gamma^\beta]}{(k^2 + i\epsilon)^2} \times \frac{d_{\alpha\sigma}(p-k) d_{\lambda\beta}(p_1-k) V^{\sigma\lambda\rho}(k-p, p_1-k, p-p_1)}{((p-k)^2 + i\epsilon)((p_1-k)^2 + i\epsilon)}, \quad (5.39)$$

where now also the 3-gluon vertex enters the equations,

$$V^{\alpha\beta\gamma}(k, l, p) = i g (g^{\alpha\beta}(k-l)^\gamma + g^{\beta\gamma}(l-p)^\alpha + g^{\gamma\alpha}(p-k)^\beta) \quad (5.40)$$

5.6.2 Virtual contributions

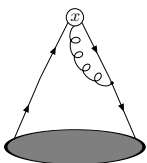
There are virtual diagrams contributing to the evolution of 2PI soft parts. The only diagrams that contribute are the quark self-energy diagrams and will always appear in the following combination, defined as



$$\frac{1}{2} \left\{ \text{triangle} + \text{triangle} \right\} = \int \frac{d^4 k}{(2\pi)^4} \delta(k \cdot \zeta - x P \cdot \zeta) \times \delta^4(p-k) \frac{1}{2} \frac{\text{Tr} [\Phi(k) \Sigma(k) \not{k} \Gamma + \Phi(k) \Gamma \not{k} \Sigma(k)]}{(k^2 + i\epsilon)} \quad (5.41)$$

5.6.3 Evolution of 3PI soft parts

For the projection of 3PI structure in the form of 2-argument functions, the following two diagrams have to be taken into account. One diagram emitting a gluon from the right quark leg,



$$= -i g^2 N_c \int \frac{d^4 k d^4 k_1 d^4 p}{(2\pi)^4} \delta(k \cdot \zeta - x P \cdot \zeta) \delta(k_1 \cdot \zeta - x_1 P \cdot \zeta)$$

$$\times \delta^4(k-p) \frac{\text{Tr} [\Phi(p) \gamma^\alpha \not{k}_1 \Gamma_\tau]}{(k_1^2 + i\epsilon)((p-k_1)^2 + i\epsilon)} d_{\alpha\tau}(p-k) \quad (5.42)$$

and a diagram in which the gluon is emitted from the left leg

$$= -i g^2 N_c \int \frac{d^4 k d^4 k_1 d^4 p}{(2\pi)^4} \delta(k \cdot \zeta - xP \cdot \zeta) \delta(k_1 \cdot \zeta - x_1 P \cdot \zeta) \\ \times \delta^4(k_1 - p) \frac{\text{Tr} [\Phi(p) \gamma^\alpha \not{k}_1 \Gamma_\tau]}{(k_1^2 + i\epsilon)((p-k_1)^2 + i\epsilon)} d_{\alpha\tau}(p-k) \quad (5.43)$$

There are two real diagrams that determine the contribution from two-argument functions to the evolution of two-argument functions. The first of these diagrams is

$$= -i g^2 N_c \int \frac{d^4 k d^4 k_1 d^4 p d^4 p_1}{(2\pi)^4} \delta(k \cdot \zeta - xP \cdot \zeta) \delta(k_1 \cdot \zeta - x_1 P \cdot \zeta) \\ \times \delta^4(p-k) \frac{\text{Tr} [\Phi_A^\rho(p, p_1) \gamma^\alpha \not{k} \Gamma^\beta]}{(k^2 + i\epsilon)} \\ \frac{d_{\alpha\sigma}(p_1 - k - 1) d_{\lambda\beta}(k_1 - k) V^{\sigma\rho\lambda}(p_1 - k, p - p_1, k_1 - k)}{((p_1 - k_1)^2 + i\epsilon)((k_1 - k)^2 + i\epsilon)}, \quad (5.44)$$

and the second

$$= -i g^2 N_c \int \frac{d^4 k d^4 k_1 d^4 p d^4 p_1}{(2\pi)^4} \delta(k \cdot \zeta - xP \cdot \zeta) \delta(k_1 \cdot \zeta - x_1 P \cdot \zeta) \\ \times \delta^4(p_1 - k) \frac{\text{Tr} [\Phi_A^\rho(p, p_1) \Gamma_\tau \not{k} \gamma^\alpha]}{(k^2 + i\epsilon)} \\ \frac{d_{\alpha\sigma}(k-p) d_{\lambda\beta}(k_1 - k) V^{\sigma\lambda\rho}(k-p, k_1 - k, p - p_1)}{((k-p)^2 + i\epsilon)((k_1 - k)^2 + i\epsilon)}. \quad (5.45)$$

The quark and gluon self-energy contributions to 3PI-function were not included in this section.

This chapter shows the necessary steps for the calculation of the evolution equations of leading order non-collinear functions and shows that this is much more involved than that of their collinear counterparts. We show the diagrams that have to be taken into account for a first order in α_s calculation in the large- N_c limit. The calculation resembles the calculation of evolution equations of sub-leading order functions [Bukh83a], except that in those calculations equations of motion relations and Lorentz-invariance relations are used to reduce the number of functions and eliminate the non-collinear functions. The fact that the latter relations are under discussion in the recent years, makes us be careful in applying them in the case of \mathbf{k}_T -odd functions.

In the next chapter we will use these relations to reconstruct the evolution of \mathbf{k}_T -odd functions from collinear evolution in the large N_c limit. In chapter 7 we will show the results from explicit calculation to the same accuracy *without* using these relations.

5.A Generalized Θ -functions

When performing a calculation of the evolution equations of \mathbf{k}_T -odd distribution and fragmentation functions in the large N_c limit, the following set of relations among generalized Θ -functions, defined as in equation (5.16), suffices, in order to reduce all results in terms of regular θ -functions and δ -functions.

By explicit evaluation of the integrals for these specific cases one finds,

$$\Theta_1^0(x) = 0, \quad (5.46)$$

$$\Theta_2^0(y) = \delta(x), \quad (5.47)$$

$$\Theta_{11}^0(x, y) = \frac{1}{x-y} (\theta(x)\theta(-y) - \theta(-x)\theta(y)). \quad (5.48)$$

All other Θ -functions encountered in a first order in α_s calculation of *real* diagrams can be reduced with the help of the following relations,

$$\Theta_{21}^0(x, y) = \frac{y}{x-y} \Theta_{11}^0(x, y) - \frac{x}{(x-y)} \Theta_2^0(x), \quad (5.49)$$

$$\Theta_{22}^0(x, y) = -\frac{2xy}{(x-y)^2} \Theta_{11}^0(x, y) + \frac{y^2}{(y-x)^2} \Theta_2^0(y) + \frac{x^2}{(y-x)^2} \Theta_2^0(x), \quad (5.50)$$

$$\Theta_{21}^1(x, y) = \frac{1}{x-y} \Theta_{11}^0(x, y) - \frac{1}{x-y} \Theta_2^0(x), \quad (5.51)$$

$$\Theta_{22}^1(x, y) = -\frac{(x+y)}{(x-y)^2} \Theta_{11}^0(x, y) + \frac{y}{(y-x)^2} \Theta_2^0(y) + \frac{x}{(y-x)^2} \Theta_2^0(x), \quad (5.52)$$

$$\Theta_{111}^0(x, y, z) = \frac{y}{z-y} \Theta_{11}^0(x, y) + \frac{z}{y-z} \Theta_{11}^0(x, z), \quad (5.53)$$

$$\Theta_{111}^1(x, y, z) = \frac{1}{z-y} \Theta_{11}^0(x, y) + \frac{1}{y-z} \Theta_{11}^0(x, z), \quad (5.54)$$

$$\begin{aligned} \Theta_{211}^0(x, y, z) &= \frac{y^2}{(z-y)(x-y)} \Theta_{11}^0(x, y) + \frac{z^2}{(y-z)(x-z)} \Theta_{11}^0(x, z) \\ &+ \frac{x^2}{(z-x)(y-x)} \Theta_2^0(x), \end{aligned} \quad (5.55)$$

$$\begin{aligned} \Theta_{221}^0(x, y, z) &= -\frac{xz^2}{(y-z)(x-z)(x-y)} \Theta_{11}^0(x, z) + \frac{yz^2}{(x-y)(x-z)(y-z)} \Theta_{11}^0(y, z) \\ &+ \frac{2y^2x^2 - xyz(x+y)}{(z-x)(z-y)(x-y)^2} \Theta_{11}^0(x, y), \end{aligned} \quad (5.56)$$

$$\begin{aligned} \Theta_{211}^1(x, y, z) &= \frac{y}{(z-y)(x-y)} \Theta_{11}^0(x, y) + \frac{z}{(y-z)(x-z)} \Theta_{11}^0(x, z) \\ &+ \frac{x}{(z-x)(y-x)} \Theta_2^0(x), \end{aligned} \quad (5.57)$$

$$\begin{aligned} \Theta_{221}^1(x, y, z) &= \frac{z^2}{(x-y)(x-z)(y-z)} \Theta_{11}^0(y, z) - \frac{z^2}{(x-y)(y-z)(x-z)} \Theta_{11}^0(x, z) \\ &+ \frac{xy(x+y) - z(x^2+y^2)}{(z-x)(z-y)(x-y)^2} \Theta_{11}^0(x, y), \end{aligned} \quad (5.58)$$

$$\Theta_{211}^2(x, y, z) = \frac{1}{(z-y)(x-y)} \Theta_{11}^0(x, y) + \frac{1}{(y-z)(x-z)} \Theta_{11}^0(x, z)$$

$$+ \frac{1}{(z-x)(y-x)} \Theta_2^0(x), \quad (5.59)$$

$$\Theta_{221}^2(x, y, z) = \frac{z}{(x-y)(x-z)(y-z)} \Theta_{11}^0(y, z) - \frac{z}{(y-z)(x-y)(x-z)} \Theta_{11}^0(x, z) - \frac{z(x+y) - 2xy}{(z-x)(z-y)(x-y)^2} \Theta_{11}^0(x, y) \quad (5.60)$$

A local-operator approach

6.1 Introduction

The logarithmic scale dependence acquired by distribution and fragmentation due to perturbative corrections is of considerable importance in extracting these functions from experimental data. In the past, studies have led to the determination of the scale dependence of the functions that compose the collinear set of distribution and fragmentation functions. The precision in order of α_s to which this scale dependence is known varies from next-to-next-to leading order (NNLO) (of order α_s^3) for $f_1(x, \mu^2)$ [Vogt04], to only leading order (LO) (order α_s) [Ali91, Bali96, Ji99] for sub-leading order functions. An important reason for this difference in accuracy, besides the additional suppression in powers $1/Q$ in the cross-section and therefore diminished relevance, is the complicated evolution structure. Sub-leading order functions mix under evolution, introducing much uncertainty for practical applications.

Very significant simplification in the evolution of sub-leading order functions, is obtained in the limit of a large number of colors. In this limit, the evolution of pure interaction parts, as can be obtained from equation of motion relations, becomes diagonal.

In contrast to the study presented in this thesis, the attention has always been directed towards a restricted set of distribution and fragmentation functions that describe partons with collinear momenta to their parent hadrons. Functions involving quark transverse momentum are usually eliminated by the use of equation of motion relations and relations following from Lorentz-invariance.

In this chapter we want to use the large N_c results together with the equations of motion and Lorentz-invariance relations, in order to construct Q^2 -evolution equations for leading order \mathbf{k}_T -odd functions.

6.2 Large number of colors

We will use the evolution equations for the collinear set of functions in the large N_c limit. Starting with the leading order functions of the collinear set, repeating the well known results of [Alta77, Bald81, Artr90] adapted to the limit of large number of colors

$c_F \rightarrow N_c/2$. Denoting by a dot the logarithmic scale derivative of a function

$$\dot{f}(\mu^2) \equiv \frac{1}{\mu^2} \frac{d}{d\mu^2} f(\mu^2), \quad (6.1)$$

the evolution equations for the leading order sector are given by,

$$\dot{f}_1(x, \mu^2) = \frac{\alpha_s}{4\pi} N_c \int_x^1 \frac{dy}{y} \left[\frac{1 + (\frac{x}{y})^2}{(1 - \frac{x}{y})_+} + \frac{3}{2} \delta(1 - \frac{x}{y}) \right] f_1(y, \mu^2), \quad (6.2)$$

$$g_1(x, \mu^2) = \frac{\alpha_s}{4\pi} N_c \int_x^1 \frac{dy}{y} \left[\frac{1 + (\frac{x}{y})^2}{(1 - \frac{x}{y})_+} + \frac{3}{2} \delta(1 - \frac{x}{y}) \right] g_1(y, \mu^2), \quad (6.3)$$

$$\dot{h}_1(x, \mu^2) = \frac{\alpha_s}{4\pi} N_c \int_x^1 \frac{dy}{y} \left[\frac{2(\frac{x}{y})}{(1 - \frac{x}{y})_+} + \frac{3}{2} \delta(1 - \frac{x}{y}) \right] h_1(y, \mu^2). \quad (6.4)$$

The +-prescription used above stands for the regularized form of the end-point divergence as defined in equation (5.22).

The connection to the evolution of non-collinear functions will be made in terms of moments, defined by

$$[f]_n \equiv \int dx x^{n-1} f(x). \quad (6.5)$$

The autonomous evolution equations shown in expressions (6.2)-(6.4) are of the form

$$\frac{d}{d\tau} f(x, \tau) = \frac{\alpha_s(\tau)}{2\pi} \int_x^1 \frac{dy}{y} P^{[f]} \left(\frac{x}{y} \right) f(y, \tau), \quad (6.6)$$

where f is any of the leading order functions, $\tau = \ln \mu^2$ and $P^{[f]}$ are the splitting functions. Using moments $A_n^{[f]}$ of these splitting functions, equal to the anomalous dimensions of the moments of the corresponding distribution function, this is

$$\frac{d}{d\tau} [f]_n(\tau) = \frac{\alpha_s(\tau)}{2\pi} A_n^{[f]} [f]_n(\tau). \quad (6.7)$$

The relation between the moments of the splitting function and the anomalous dimension can be seen by rewriting equation (6.7) as,

$$\frac{[f]_n(\tau_1)}{[f]_n(\tau_2)} = \left[\frac{\alpha_s(\tau_1)}{\alpha_s(\tau_2)} \right]^{\frac{-2 A_n^{[f]}}{\beta_0}}. \quad (6.8)$$

where τ_1 and τ_0 denote scale integration limits, and comparing this expression with the scale dependence following from a renormalization group analysis

$$A_n^{[f]} = -\frac{1}{4} d_n \quad (6.9)$$

where d_n is proportional to the leading coefficient in an expansion in the coupling constant of the anomalous dimension (2.17).

Applying this to the splitting functions in equations (6.2), (6.2) and (6.2), this results in the following anomalous dimensions for the leading order functions

$$A_n^{[f_1]} = A_n^{[g_1]} = \frac{N_c}{2} \left[\frac{3}{2} + \frac{1}{n(n+1)} - 2 \sum_{j=1}^n \frac{1}{j} \right], \quad (6.10)$$

$$A_n^{[h_1]} = \frac{N_c}{2} \left[\frac{3}{2} - 2 \sum_{j=1}^n \frac{1}{j} \right], \quad (6.11)$$

6.2.1 Twist-3 distribution functions

In the large N_c limit the evolution of the pure interactions parts of the collinear sub-leading order functions takes an autonomous form. To first order in α_s , the evolution equations for the collinear sub-leading order functions is known [Ali91, Bali96, Ji99]. The evolution equations in the large N_c limit for the pure interaction parts, as defined in equations (3.75)-(3.77), can be summarized by [Brau00]

$$\dot{\tilde{g}}_T(x, Q^2) = \frac{\alpha_s}{2\pi} N_c \int_x^1 \frac{dy}{y} \left[\frac{1}{2} \delta(1 - \frac{x}{y}) + \frac{2}{(1 - \frac{x}{y})_+} - 1 \right] \tilde{g}_T(y, Q^2), \quad (6.12)$$

$$\dot{\tilde{h}}_L(x, Q^2) = \frac{\alpha_s}{2\pi} N_c \int_x^1 \frac{dy}{y} \left[\frac{1}{2} \delta(1 - \frac{x}{y}) + \frac{2}{(1 - \frac{x}{y})_+} - 3 \right] \tilde{h}_L(y, Q^2), \quad (6.13)$$

$$\dot{\tilde{e}}(x, Q^2) = \frac{\alpha_s}{2\pi} N_c \int_x^1 \frac{dy}{y} \left[\frac{1}{2} \delta(1 - \frac{x}{y}) + \frac{2}{(1 - \frac{x}{y})_+} + 1 \right] \tilde{e}(y, Q^2), \quad (6.14)$$

where the autonomous evolution attributed to the pure interaction part of the function $g_2 = g_1 + g_T$, has been replaced by the interaction part of the function $g_T(x)$. Translating the above to moments gives,

$$A_n^{[\tilde{g}_T]} = \frac{N_c}{2} \left[\frac{1}{2} + \frac{1}{n} - 2 \sum_{j=1}^n \frac{1}{j} \right], \quad (6.15)$$

$$A_n^{[\tilde{h}_L]} = \frac{N_c}{2} \left[\frac{1}{2} - \frac{1}{n} - 2 \sum_{j=1}^n \frac{1}{j} \right], \quad (6.16)$$

$$A_n^{[\tilde{e}]} = \frac{N_c}{2} \left[\frac{1}{2} + \frac{3}{n} - 2 \sum_{j=1}^n \frac{1}{j} \right]. \quad (6.17)$$

6.3 Connection to the light-front

Using the equations of motion relations in equations (3.75) - (3.80) and the relations based on Lorentz-invariance in equations (3.66) - (3.74), it is straightforward to relate the various sub-leading order functions and the transverse moments of \mathbf{k}_T -dependent functions. The results, grouping relevant combinations, are

$$g_T(x) = \int_x^1 dy \frac{g_1(y)}{y} + \frac{m}{M} \left[\frac{h_1(x)}{x} - \int_x^1 dy \frac{h_1(y)}{y^2} \right]$$

$$+ \left[\tilde{g}_T(x) - \int_x^1 dy \frac{\tilde{g}_T(y)}{y} \right], \quad (6.18)$$

$$\frac{g_{1T}^{(1)}(x)}{x} = \int_x^1 dy \frac{g_1(y)}{y} - \frac{m}{M} \int_x^1 dy \frac{h_1(y)}{y^2} - \int_x^1 dy \frac{\tilde{g}_T(y)}{y}, \quad (6.19)$$

$$h_L(x) = 2x \int_x^1 dy \frac{h_1(y)}{y^2} + \frac{m}{M} \left[\frac{g_1(x)}{x} - 2x \int_x^1 dy \frac{g_1(y)}{y^3} \right] + \left[\tilde{h}_L(x) - 2x \int_x^1 dy \frac{\tilde{h}_L(y)}{y^2} \right], \quad (6.20)$$

$$\frac{h_{1L}^{\perp(1)}(x)}{x^2} = - \int_x^1 dy \frac{h_1(y)}{y^2} + \frac{m}{M} \int_x^1 dy \frac{g_1(y)}{y^3} + \int_x^1 dy \frac{\tilde{h}_L(y)}{y^2}, \quad (6.21)$$

$$e(x) = \tilde{e}(x) + \frac{m}{M} \frac{f_1(x)}{x}, \quad (6.22)$$

$$f_T(x) = \left[\tilde{f}_T(x) - \int_x^1 dy \frac{\tilde{f}_T(y)}{y} \right], \quad (6.23)$$

$$\frac{f_{1T}^{\perp(1)}(x)}{x} = \int_x^1 dy \frac{\tilde{f}_T(y)}{y}, \quad (6.24)$$

$$h(x) = \left[\tilde{h}(x) - 2x \int_x^1 dy \frac{\tilde{h}(y)}{y^2} \right], \quad (6.25)$$

$$\frac{h_1^{\perp(1)}(x)}{x^2} = \int_x^1 dy \frac{\tilde{h}(y)}{y^2}, \quad (6.26)$$

$$e_L(x) = \tilde{e}_L(x). \quad (6.27)$$

Note that often the combinations of tilde functions between brackets are denoted by a single ‘interaction-dependent’ function.

In order to study the evolution of these functions, we consider the moments, giving

$$[g_T]_n = \frac{1}{n} [g_1]_n + \frac{n-1}{n} [\tilde{g}_T]_n + \frac{m}{M} \frac{n-1}{n} [h_1]_{n-1}, \quad (6.28)$$

$$[g_{1T}^{(1)}]_n = \frac{1}{n+1} \left([g_1]_{n+1} - [\tilde{g}_T]_{n+1} - \frac{m}{M} [h_1]_n \right), \quad (6.29)$$

$$[h_L]_n = \frac{2}{n+1} [h_1]_n + \frac{n-1}{n+1} [\tilde{h}_L]_n + \frac{m}{M} \frac{n-1}{n+1} [g_1]_{n-1}, \quad (6.30)$$

$$[h_{1L}^{\perp(1)}]_n = -\frac{1}{n+2} \left([h_1]_{n+1} - [\tilde{h}_L]_{n+1} - \frac{m}{M} [g_1]_n \right), \quad (6.31)$$

$$[e]_n = [\tilde{e}]_n + \frac{m}{M} [f_1]_{n-1}, \quad (6.32)$$

$$[f_T]_n = \frac{n-1}{n} [\tilde{f}_T]_n, \quad (6.33)$$

$$[f_{1T}^{\perp(1)}]_n = \frac{1}{n+1} [\tilde{f}_T]_{n+1}, \quad (6.34)$$

$$[h]_n = \frac{n-1}{n+1} [\tilde{h}]_n, \quad (6.35)$$

$$[h_1^{\perp(1)}]_n = \frac{1}{n+2} [\tilde{h}]_{n+1}, \quad (6.36)$$

$$[e_L]_n = [\tilde{e}_L]_n. \quad (6.37)$$

Actually, we need not consider the five T-odd functions separately. They can be simply considered as imaginary parts of other functions, when we allow complex functions. In particular, one can expand the correlation functions into matrices in Dirac space [Bacc00b] to show that the relevant combinations are $(g_{1T} - i f_{1T}^{\perp})$ which we can treat together as one complex function g_{1T} . Similarly, we can absorb the imaginary parts into new functions

$$(h_{1L}^{\perp} + i h_1^{\perp}) \rightarrow h_{1L}^{\perp}, \quad (6.38)$$

$$(g_T + i f_T) \rightarrow g_T, \quad (6.39)$$

$$(h_L + i h) \rightarrow h_L, \quad (6.40)$$

$$(e + i e_L) \rightarrow e. \quad (6.41)$$

6.3.1 Evolution equations

Using the moment analysis of the previous section one can arrive at a set of evolution equations for \mathbf{k}_T -odd distribution functions [Henn02]. The evolution of $g_{1T}^{(1)}$ is driven not only by this function itself but also by a higher moment of g_1 and a similar situation for $h_{1L}^{\perp(1)}$. In the large N_c limit ($C_F \rightarrow N_c/2$) one obtains (omitting mass terms)

$$\begin{aligned} \frac{d}{d\tau} [g_{1T}^{(1)}]_n &= \frac{\alpha_s(\tau)}{4\pi} N_c \left\{ \left[\frac{1}{2} - \frac{1}{n+1} - 2 \sum_{j=1}^n \frac{1}{j} \right] [g_{1T}^{(1)}]_n \right. \\ &\quad \left. + \frac{1}{n+2} [g_1]_{n+1} \right\}, \end{aligned} \quad (6.42)$$

$$\begin{aligned} \frac{d}{d\tau} [h_{1L}^{\perp(1)}]_n &= \frac{\alpha_s(\tau)}{4\pi} N_c \left\{ \left[\frac{1}{2} - \frac{3}{n+1} - 2 \sum_{j=1}^n \frac{1}{j} \right] [h_{1L}^{\perp(1)}]_n \right. \\ &\quad \left. - \frac{1}{n+1} [h_1]_{n+1} \right\}, \end{aligned} \quad (6.43)$$

or in terms of the functions of light-cone momentum fractions

$$\begin{aligned} \frac{d}{d\tau} g_{1T}^{(1)}(x, \tau) &= \frac{\alpha_s(\tau)}{4\pi} N_c \int_x^1 dy \left\{ \left[\frac{1}{2} \delta(y-x) + \frac{x^2 + xy}{y^2(y-x)_+} \right] g_{1T}^{(1)}(y, \tau) \right. \\ &\quad \left. + \frac{x^2}{y^2} g_1(y, \tau) \right\}, \end{aligned} \quad (6.44)$$

$$\frac{d}{d\tau} h_{1L}^{\perp(1)}(x, \tau) = \frac{\alpha_s(\tau)}{4\pi} N_c \int_x^1 dy \left\{ \left[\frac{1}{2} \delta(y-x) + \frac{3x^2 - xy}{y^2(y-x)_+} \right] h_{1L}^{\perp(1)}(y, \tau) - \frac{x}{y} h_1(y, \tau) \right\}. \quad (6.45)$$

Next we note that apart from a γ_5 matrix the operator structures of the T-odd functions $f_{1T}^{\perp(1)}$ and $h_1^{\perp(1)}$ are in fact the same as those of $g_{1T}^{(1)}$ and $h_{1L}^{\perp(1)}$ (they can be considered as the imaginary part of these functions [Bacc00b]). This implies that for the non-singlet functions, one immediately can obtain the evolution of the T-odd functions,

$$\frac{d}{d\tau} [f_{1T}^{\perp(1)}]_n = \frac{\alpha_s(\tau)}{4\pi} N_c \left[\frac{1}{2} - \frac{1}{n+1} - 2 \sum_{j=1}^n \frac{1}{j} \right] [f_{1T}^{\perp(1)}]_n, \quad (6.46)$$

$$\frac{d}{d\tau} [h_1^{\perp(1)}]_n = \frac{\alpha_s(\tau)}{4\pi} N_c \left[\frac{1}{2} - \frac{3}{n+1} - 2 \sum_{j=1}^n \frac{1}{j} \right] [h_1^{\perp(1)}]_n. \quad (6.47)$$

Furthermore, for the chiral-odd functions, which do not mix with a gluon distribution, there is no difference between the non-singlet and the singlet evolution.

In the large N_c limit, the evolution equations for the non-singlet T-odd functions are of simple diagonal form with splitting functions

$$P^{[f_{1T}^{\perp(1)}]}(\beta) = \frac{N_c}{2} \left[\frac{1}{2} \delta(1-\beta) + \frac{\beta + \beta^2}{(1-\beta)_+} \right], \quad (6.48)$$

$$P^{[h_1^{\perp(1)}]}(\beta) = \frac{N_c}{2} \left[\frac{1}{2} \delta(1-\beta) + \frac{3\beta^2 - \beta}{(1-\beta)_+} \right]. \quad (6.49)$$

Actually, we also obtain the anomalous dimensions (and splitting functions) of the T-odd sub-leading order functions using $A^{[f_T]} = A^{[\tilde{f}_T]} = A^{[\tilde{g}_T]}$, $A^{[h]} = A^{[\tilde{h}]} = A^{[\tilde{h}_L]}$ and $A^{[e_L]} = A^{[\tilde{e}_L]} = A^{[e]} = A^{[\tilde{e}]}$.

6.3.2 Fragmentation functions

Combining relations following from Lorentz-invariance and equations of motion, one can construct the following relations,

$$\begin{aligned} \frac{G_T(z)}{z} &= - \int_z^1 dy \frac{G_1(y)}{y^2} + \frac{m}{M_h} \left[H_1(z) + \int_z^1 dy \frac{H_1(y)}{y} \right] \\ &\quad + \left[\frac{\tilde{G}_T(z)}{z} + \int_z^1 dy \frac{\tilde{G}_T(y)}{y^2} \right], \end{aligned} \quad (6.50)$$

$$G_{1T}^{(1)}(z) = - \int_z^1 dy \frac{G_1(y)}{y^2} + \frac{m}{M_h} \int_z^1 dy \frac{H_1(y)}{y} + \int_z^1 dy \frac{\tilde{G}_T(y)}{y^2}, \quad (6.51)$$

$$\begin{aligned} H_L(z) &= -2 \int_z^1 dy \frac{H_1(y)}{y} + \frac{m}{M_h} \left[z G_1(z) + 2 \int_z^1 dy G_1(y) \right] \\ &\quad + \left[\tilde{H}_L(z) + 2 \int_z^1 dy \frac{\tilde{H}_L(y)}{y} \right], \end{aligned} \quad (6.52)$$

$$z H_{1L}^{\perp(1)}(z) = \int_z^1 dy \frac{H_1(y)}{y} - \frac{m}{M_h} \int_z^1 dy G_1(y) - \int_z^1 dy \frac{\tilde{H}_L(y)}{y}, \quad (6.53)$$

$$E(z) = \tilde{E}(z) + \frac{m}{M_h} z D_1(z), \quad (6.54)$$

$$\frac{D_T(z)}{z} = \left[\frac{\tilde{D}_T(z)}{z} + \int_z^1 dy \frac{\tilde{D}_T(y)}{y^2} \right], \quad (6.55)$$

$$D_{1T}^{\perp(1)}(z) = - \int_z^1 dy \frac{\tilde{D}_T(y)}{y^2}, \quad (6.56)$$

$$H(z) = \left[\tilde{H}(z) + 2 \int_z^1 dy \frac{\tilde{H}(y)}{y} \right], \quad (6.57)$$

$$z H_1^{\perp(1)}(z) = - \int_z^1 dy \frac{\tilde{H}(y)}{y}, \quad (6.58)$$

$$E_L(z) = \tilde{E}_L(z). \quad (6.59)$$

The relations for the moments of fragmentation functions can be obtained from the above equations or from the results of the distribution functions via the replacement

$$n \rightarrow -n \quad (6.60)$$

in all expressions, followed by the replacement of the function moments by

$$[f]_{-n} \rightarrow [D/z]_n = [D]_{n-1}, \quad (6.61)$$

where the moments of fragmentation functions are defined as in equation (6.5) but involve the momentum fraction z . This yields

$$[G_T]_n = - \frac{1}{n+1} [G_1]_n + \frac{n+2}{n+1} [\tilde{G}_T]_n + \frac{m}{M_h} \frac{n+2}{n+1} [H_1]_{n+1}, \quad (6.62)$$

$$[G_{1T}^{(1)}]_{n+1} = - \frac{1}{n+1} \left([G_1]_n - [\tilde{G}_T]_n - \frac{m}{M_h} [H_1]_{n+1} \right), \quad (6.63)$$

$$[H_L]_n = - \frac{2}{n} [H_1]_n + \frac{n+2}{n} [\tilde{H}_L]_n + \frac{m}{M_h} \frac{n+2}{n} [G_1]_{n+1}, \quad (6.64)$$

$$[H_{1L}^{\perp(1)}]_{n+1} = \frac{1}{n} \left([H_1]_n - [\tilde{H}_L]_n - \frac{m}{M_h} [G_1]_{n+1} \right), \quad (6.65)$$

$$[E]_n = [\tilde{E}]_n + \frac{m}{M_h} [D_1]_{n+1}, \quad (6.66)$$

$$[D_T]_n = \frac{n+2}{n+1} [\tilde{D}_T]_n, \quad (6.67)$$

$$[D_{1T}^{\perp(1)}]_{n+1} = - \frac{1}{n+1} [\tilde{D}_T]_n, \quad (6.68)$$

$$[H]_n = \frac{n+2}{n} [\tilde{H}]_n, \quad (6.69)$$

$$[H_1^{\perp(1)}]_{n+1} = -\frac{1}{n} [\tilde{H}]_n, \quad (6.70)$$

$$[E_L]_n = [\tilde{E}_L]_n. \quad (6.71)$$

The autonomous evolution equations are again of the form

$$\frac{d}{d\tau} D(z, \tau) = \frac{\alpha_s(\tau)}{2\pi} \int_z^1 \frac{dy}{y} P^{[D]} \left(\frac{z}{y} \right) D(y, \tau), \quad (6.72)$$

or via the (usual) moments $A_n^{[D]} = \int_0^1 dz z^{n-1} P^{[D]}(z)$ of the splitting functions,

$$\frac{d}{d\tau} [D]_n(\tau) = \frac{\alpha_s(\tau)}{2\pi} A_n^{[D]} [D]_n(\tau). \quad (6.73)$$

For the leading order contributions the analytic structure of the corrections for fragmentation functions is similar as for distribution functions. We note a (generalized) Gribov-Lipatov reciprocity, summarized by the following procedure. The splitting functions for distribution functions $f(x, \tau)$ and corresponding fragmentation functions $zD(z, \tau)$ are related by

$$P^{[f]}(\beta) = \frac{\mathcal{N}(\beta)}{(1-\beta)_+}, \quad (6.74)$$

$$P^{[zD]}(\beta) = \frac{\beta^2 \mathcal{N}(1/\beta)}{(1-\beta)_+}. \quad (6.75)$$

This relation works for the leading order fragmentation functions *and* the interaction-dependent functions [Beli97b], for $\mathcal{N}(\beta)$ being (at most a quadratic) polynomial in β . In the case of the leading order functions the functional form of the splitting functions is the same for distribution and fragmentation functions. This is no longer true for the interaction-dependent functions. For the anomalous dimensions of distribution and fragmentation functions the relation becomes

$$A_n^{[f]} = \mathcal{A}(n) - 2 \sum_{j=1}^n \frac{1}{j} = \mathcal{A}(n) - 2\gamma_E - 2\psi(n+1), \quad (6.76)$$

$$A_{n+1}^{[D]} = \mathcal{A}(-(n+1)) - 2\gamma_E - 2\psi(n+1) = \mathcal{A}(-(n+1)) - 2 \sum_{j=1}^n \frac{1}{j}, \quad (6.77)$$

where $\mathcal{A}(n)$ is a rational function. We have not yet investigated the wider applicability of the above relations. We find for the leading order fragmentation functions the familiar results, which obey the original Gribov-Lipatov reciprocity relation $A_n^{[f]} = A_{n+1}^{[D]}$ between the leading order distribution functions $f = f_1, g_1, h_1$ and fragmentation functions $D = D_1, G_1, H_1$,

$$A_{n+1}^{[D_1]} = A_{n+1}^{[G_1]} = C_F \left[\frac{3}{2} + \frac{1}{n(n+1)} - 2 \sum_{j=1}^n \frac{1}{j} \right], \quad (6.78)$$

$$A_{n+1}^{[H_1]} = C_F \left[\frac{3}{2} - 2 \sum_{j=1}^n \frac{1}{j} \right]. \quad (6.79)$$

In the large N_c limit, our generalized reciprocity relations in equations (6.76) and (6.77) applied to equations (6.15) - (6.17) give the results for the interaction-dependent functions [Beli97b, Beli97]

$$A_{n+1}^{[\tilde{G}_T]} = \frac{N_c}{2} \left[\frac{1}{2} - \frac{1}{n+1} - 2 \sum_{j=1}^n \frac{1}{j} \right], \quad (6.80)$$

$$A_{n+1}^{[\tilde{H}_L]} = \frac{N_c}{2} \left[\frac{1}{2} + \frac{1}{n+1} - 2 \sum_{j=1}^n \frac{1}{j} \right], \quad (6.81)$$

$$A_{n+1}^{[\tilde{E}]} = \frac{N_c}{2} \left[\frac{1}{2} - \frac{3}{n+1} - 2 \sum_{j=1}^n \frac{1}{j} \right]. \quad (6.82)$$

Again one then also knows $A^{[D_T]} = A^{[\tilde{D}_T]} = A^{[\tilde{G}_T]}$, $A^{[H]} = A^{[\tilde{H}]} = A^{[\tilde{H}_L]}$ and $A^{[E_L]} = A^{[\tilde{E}_L]} = A^{[E]} = A^{[\tilde{E}]}$.

Using the moment analysis (the reciprocity relations cannot be used straightforwardly) one obtains, omitting the mass terms,

$$\begin{aligned} \frac{d}{d\tau} [G_{1T}^{(1)}]_{n+1} &= \frac{\alpha_s(\tau)}{4\pi} N_c \left\{ \left[\frac{1}{2} + \frac{1}{n} - 2 \sum_{j=1}^n \frac{1}{j} \right] [G_{1T}^{(1)}]_{n+1} \right. \\ &\quad \left. - \frac{n}{(n-1)(n+1)} [G_1]_n \right\}, \end{aligned} \quad (6.83)$$

$$\begin{aligned} \frac{d}{d\tau} [H_{1L}^{\perp(1)}]_{n+1} &= \frac{\alpha_s(\tau)}{4\pi} N_c \left\{ \left[\frac{1}{2} + \frac{3}{n} - 2 \sum_{j=1}^n \frac{1}{j} \right] [H_{1L}^{\perp(1)}]_{n+1} \right. \\ &\quad \left. + \frac{n-1}{n^2} [H_1]_n \right\}, \end{aligned} \quad (6.84)$$

with in this case mixing with a lower moment of the leading order functions. In terms of the functions of light-cone momentum fractions one finds

$$\begin{aligned} \frac{d}{d\tau} z G_{1T}^{(1)}(z, \tau) &= \frac{\alpha_s(\tau)}{4\pi} N_c \int_z^1 dy \left\{ \left[\frac{1}{2} \delta(y-z) + \frac{y+z}{y(y-z)_+} \right] y G_{1T}^{(1)}(y, \tau) \right. \\ &\quad \left. - \frac{y^2+z^2}{2y^2z} G_1(y, \tau) \right\}, \end{aligned} \quad (6.85)$$

$$\begin{aligned} \frac{d}{d\tau} z H_{1L}^{\perp(1)}(z, \tau) &= \frac{\alpha_s(\tau)}{4\pi} N_c \int_z^1 dy \left\{ \left[\frac{1}{2} \delta(y-z) + \frac{3y-z}{y(y-z)_+} \right] y H_{1L}^{\perp(1)}(y, \tau) \right. \\ &\quad \left. + \frac{1+\ln(z/y)}{y} H_1(y, \tau) \right\}. \end{aligned} \quad (6.86)$$

Given the fact that, apart from an additional γ_5 , the operator structure for the T-odd Sivers fragmentation analog and Collins fragmentation function, $D_{1T}^{\perp(1)}$ and $H_1^{\perp(1)}$, are the same as those of $G_{1T}^{(1)}$ and $H_{1L}^{\perp(1)}$ but without mixing with G_1 or H_1 , one finds in the large N_c limit an autonomous evolution for the T-odd functions, with anomalous dimensions

$$A_{n+1}^{[D_{1T}^{\perp(1)}]} = \frac{N_c}{2} \left[\frac{1}{2} + \frac{1}{n} - 2 \sum_{j=1}^n \frac{1}{j} \right], \quad (6.87)$$

function	C	a_1	a_2	a_3	validity
f_1	—	0	-7/6	-25/12	
g_1	+	0	-7/6	-25/12	
h_1	—	-1/2	-3/2	-13/6	
\tilde{g}_T and \tilde{f}_T	+	-1/2	-2	-17/6	large N_c
\tilde{h}_L and \tilde{h}	—	-5/2	-3	-7/2	large N_c
\tilde{e}	+	+3/2	-1	-13/6	large N_c
$g_{1T}^{(1)}$ and $f_{1T}^{\perp(1)}$	—	-2	-17/6	-41/12	large N_c
$h_{1L}^{\perp(1)}$ and $h_1^{\perp(1)}$	+	-3	-7/2	-47/12	large N_c
zD_1	—	0	-7/6	-25/12	
zG_1	+	0	-7/6	-25/12	
zH_1	—	-1/2	-3/2	-13/6	
$z\tilde{G}_T$ and $z\tilde{D}_T$	+	-2	-17/6	-41/12	large N_c
$z\tilde{H}_L$ and $z\tilde{H}$	—	-1	-13/6	-35/12	large N_c
$z\tilde{E}$	+	-3	-7/2	-47/12	large N_c
$zG_{1T}^{(1)}$ and $zD_{1T}^{\perp(1)}$	—	-1/2	-2	-17/6	large N_c
$zH_{1L}^{\perp(1)}$ and $zH_1^{\perp(1)}$	+	+3/2	-1	-13/6	large N_c

Table 6.1: The anomalous dimensions from which the large Q^2 behavior of the moments, proportional to $[\alpha_s(Q^2)]^{d_n}$, is obtained. Defining the moments a_n taking out the factor C_F or $N_c/2$ from the anomalous dimensions A_n , one has for the leading order functions $d_n = -2a_n C_F/\beta_0$ with $\beta_0 = (11N_c - 2N_f)/3$, while for the large N_c results one has $d_n = -3a_n/11$. Also indicated is the charge conjugation behavior of the functions, $\tilde{f}(x) = \pm f(-x)$.

$$A_{n+1}^{[H_1^{\perp(1)}]} = \frac{N_c}{2} \left[\frac{1}{2} + \frac{3}{n} - 2 \sum_{j=1}^n \frac{1}{j} \right]. \quad (6.88)$$

corresponding to splitting functions

$$P^{[zD_{1T}^{\perp(1)}]}(\beta) = \frac{N_c}{2} \left[\frac{1}{2} \delta(1-\beta) + \frac{1+\beta}{(1-\beta)_+} \right], \quad (6.89)$$

$$P^{[zH_1^{\perp(1)}]}(\beta) = \frac{N_c}{2} \left[\frac{1}{2} \delta(1-\beta) + \frac{3-\beta}{(1-\beta)_+} \right]. \quad (6.90)$$

The results in equations (6.88) and (6.90) are relevant for studies of the Collins effect and equations (6.87) and (6.89) for studies of transversely polarized Λ production [Anse01], provided that the relations following from Lorentz-invariance can be reconciled with the use of non-collinear structure in cross-sections.

6.3.3 Discussion and conclusions

Our goal was to obtain the evolution equations of the functions that appear in azimuthal spin asymmetries. These \mathbf{k}_T -dependent functions appear in asymmetries that are not suppressed by explicit powers of the hard momentum. But as functions of transverse momentum they are not of definite (local) twist, which implies that in order to obtain the

evolution equations one has to calculate corrections to higher twist operators as well. For the first $\mathbf{p}_T^2/2M^2$ moment (transverse moment) of these p_T -dependent functions, such as for the Collins fragmentation function,

$$H_1^{\perp(1)} = \int d^2k'_T \mathbf{k}'_T{}^2 / 2z^2 M_h^2 H_1^{\perp}(z, \mathbf{k}'_T{}^2), \quad (6.91)$$

we obtain DGLAP-like evolution equations. Such moments appear in cross sections weighted with the momentum q_T^α , where only the directional (azimuthal) dependence remains. For explicit examples we refer to the literature [Boer97a, Boer97b, Boer98]. In case one does not weight the transverse momentum integration of the differential cross section, one is only sensitive to the leading order functions f_1, g_1 and h_1 (and their fragmentation counterparts), but in case one weights with one or more powers of the observed transverse momentum, one becomes sensitive to the functions $g_{1T}^{(1)}, h_{1L}^{\perp(1)}, f_{1T}^{\perp(1)}, h_1^{\perp(1)}$ (and their fragmentation counterparts), which are functions of the light-cone momentum fraction x (or z) only.

In the large- N_c limit, the non-singlet evolution of these functions involves, under the assumption of validity of the Lorentz invariance relations, only the functions themselves and (in the T-even case) only well-known leading order functions. For the chiral-odd functions the equations also apply to the singlet case, since there is no mixing with gluon distribution functions. The large- N_c evolution equations are expected to be good approximations to the full evolution equations which are not of this simple form gathered in [Brau00], because of the appearance of two-argument sub-leading order functions as in equation (3.21). It is not excluded that the first $1/N_c$ correction to the result obtained here may still lead to autonomous evolution equations, but we will not address this issue here. Especially the (large N_c) evolution equation we have obtained for $H_1^{\perp(1)}$,

$$\frac{d}{d\tau} z H_1^{\perp(1)}(z, \tau) = \frac{\alpha_s}{4\pi} N_c \int_z^1 dy \left[\frac{1}{2} \delta(y-z) + \frac{3y-z}{y(y-z)_+} \right] y H_1^{\perp(1)}(y, \tau), \quad (6.92)$$

should prove useful for the comparison of data on Collins function asymmetries from different experiments, performed at different energies.

It is worth investigating the large Q behavior of the solutions to the various evolution equations. For this purpose we have given the first 3 anomalous dimensions for the different functions in table 6.1. First we note that all (diagonal) anomalous dimensions of $g_{1T}^{(1)}, h_{1L}^{\perp(1)}, f_{1T}^{\perp(1)}$ and $h_1^{\perp(1)}$ are negative, implying that these functions will vanish asymptotically ($Q^2 \rightarrow \infty$), except that for the T-even functions there is mixing with g_1 and h_1 , but this does not alter the conclusion.

For the fragmentation counterparts the conclusion is similar, except for the fact that the lowest anomalous dimensions of $z H_{1L}^{\perp(1)}$ and $z H_1^{\perp(1)}$ are positive, potentially leading to divergent behavior of the functions as $Q^2 \rightarrow \infty$. This divergent behavior is readily cured if the first moment of these function vanishes, a condition that would lead to the Schäfer-Teryaev sum rule [Scha00, Tery00],

$$\sum_h \int dz z \left[H_1^{\perp(1)}(z) \right]_h = 0, \quad (6.93)$$

in which a summation over hadrons h is implied, being automatically satisfied. Similar sum rules hold for the other first transverse moments of fragmentation functions [Scha00,

Tery00, Anse01]. All higher moments will vanish asymptotically. The behavior of the sum rule for the first moment of the function e is discussed in reference [Jaff92].

In conclusion, using the so-called Lorentz-invariance relations and the QCD equations of motion, the operator structure of the transverse moments of \mathbf{k}_T -dependent quark distribution and fragmentation functions can be found in terms of twist-two and twist-three operators. Knowing their, for large N_c simple, evolution one also knows the evolution of azimuthal asymmetries in semi-inclusive hard scattering processes.

The Lorentz-invariance relations used here, might be incompatible with the notion of transverse momentum dependent functions. The relations, also known by the name of n -invariance due to the freedom in the precise specification of the ζ -direction in collinear treatments, might not apply when a second hadron, necessary for the measurement of non-collinear functions, fixes this direction and that of the transverse subspace.

Non-collinear evolution

7.1 Introduction

In this chapter we present an independent calculation of the first order in α_s Q^2 -evolution of non-collinear distribution functions. The calculations are performed in a light-cone gauge $A \cdot \zeta = 0$, where ζ^μ is the light-like direction, $\zeta^2 = 0$, that is determined by the hard direction q in which the hadron is probed. We consider only that part of the evolution system that is of relevance in the large N_c limit.

In the following section we will consider the three polarization states of a parent hadron separately. Only distribution functions are taken into account in this chapter, as at this order in α_s the results can easily be adapted for fragmentation functions.

In most results, the self-energy contributions will be left out. These contributions always involve only end-point contributions in the momentum fraction integration, and cannot change the structure of the evolution systems.

7.2 Unpolarized hadrons

For an unpolarized spin-1/2 hadron, the collinear set of functions that parametrize its T-even structure, consists of the leading order function $f_1(x)$, and the sub-leading order function $e(x)$. T-odd structure complements this collinear set the functions with the function $h(x)$. Note that there is no leading order T-odd structure. Considering quark transverse momentum generates a leading order T-odd structure denoted by the name $h_1^{\perp(1)}(x)$.

The evolution of $f_1(x)$ is very well known, and is shown at the same accuracy as the rest of the results in this thesis in equation (6.2). The evolution of the function $e(x)$ is also known, although to much lower accuracy. In the following section the evolution of $e(x)$ is used as a check on the calculation, and for illustrative purposes as it is the simplest sub-leading order evolution system. For a later discussion, it will also be of value to show the results for $e(x)$ together with the full results including all hadron polarizations.

7.2.1 Scale dependence of $e(x)$

The evolution of $e(x)$ is, compared to that of $f_1(x)$ more complicated. The large N_c evolution equation was first calculated in [Bali96], whereas the full result was first shown in [Beli97c].

Now there are several operators of the same dimension as the unit matrix. All these operators mix under renormalization and result in a more complicated form for the evolution equations.

Again using the following definition for $e(x)$ in order to extract the order α_s contributions to its Q^2 -dependence.

$$e(x) \equiv \int d^4k \delta(k \cdot \zeta - xP \cdot \zeta) \text{Tr} \left[\Phi(k) \left(\frac{P \cdot \zeta}{M} \frac{1}{2} \right) \right] \quad (7.1)$$

One finds after performing the calculation

$$\dot{e}(x) = \int_x^1 \frac{dy}{y} \left[B_{11} e(y) + \int_0^1 dy_1 B_{12} \text{Re} \{ E_A(y, y_1) \} \right] \quad (7.2)$$

where the kernel parts are given by

$$B_{11} = \frac{\alpha_s}{4\pi} N_c \quad (7.3)$$

$$B_{12} = \frac{\alpha_s}{4\pi} N_c \frac{4}{(x-y)}. \quad (7.4)$$

In order to be able to find a closed evolution set we might naively search for the evolution equations of the real part of E_A . A calculation gives

$$\text{Re} \{ \dot{E}_A(x, x_1) \} = \int_x^1 \frac{dy}{y} \left[B_{21} e(y) + \int_0^1 dy_1 B_{22} \text{Re} \{ E_A(y, y_1) \} \right] \quad (7.5)$$

completing the kernel with the expressions

$$B_{21} = \frac{\alpha_s}{4\pi} N_c \delta(x_1 - y) \frac{x}{2} \quad (7.6)$$

$$B_{22} = \frac{\alpha_s}{4\pi} N_c \left[\delta(x_1 - y) \frac{x^2 - y^2 - xy + 2yy_1 - y_1^2}{(y_1 - x)(y - y_1)} \right. \quad (7.7)$$

$$\left. + \delta(x_1 - y_1) \frac{x^3 + y^3 - 2x^2y_1 - 2y^2y_1 + xy_1^2 + yy_1^2}{(x-y)(x-y_1)(y-y_1)} \right]. \quad (7.8)$$

The obtained kernel satisfies the equations of motion involving $e(x)$, equation (3.75), which we regard as a check on our calculations. Use of this equation allows us to eliminate one of the two functions appearing in the evolution equations and reduce the evolution system to the autonomous evolution equation (6.14), in accordance with the literature.

7.2.2 Scale dependence of $h_1^{\perp(1)}(x)$

Inclusion of transverse momentum makes it possible to define a leading order T-odd, function $h_1^{\perp(1)}(x)$. This function is absent in the collinear case. The evolution of this function

has not been studied in the past except for a study based on the collinear evolution equations, equations of motion and equations naively based on Lorentz-invariance [Henn02]. In this section we show its evolution, resulting from a calculation in a redundant basis without using any of these relations.

In agreement with the parametrization (3.35), it is possible to define the function $h_1^{\perp(1)}$ in terms of a projection operation on a soft part,

$$h_1^{\perp(1)}(x) \equiv \int d^4k \delta(k \cdot \zeta - xP \cdot \zeta) \text{Tr} \left[\left(\frac{\epsilon_T^{kT\rho} \gamma_5 \not{k} \gamma_\rho}{4M} \right) \Phi(k) \right], \quad (7.9)$$

where $\Phi(k)$ is as in (3.1).

By performing this projection operation on all 2PI-diagrams of order α_s , which are shown in figure 5.4, one obtains

$$h_1^{\perp(1)}(x, Q^2) = \frac{\alpha_s}{4\pi} N_c \int_x^1 \frac{dy}{y} \left[A_{11} h_1^{\perp(1)}(y) + A_{12} h(x) + \int dy_1 A_{13} \text{Im}\{E_A(y, y_1)\} \right]. \quad (7.10)$$

The kernel functions A_{11} to A_{13} are given by

$$A_{11} = \frac{2x(2x - y)}{y(x - y)} \quad (7.11)$$

$$A_{12} = -x \quad (7.12)$$

$$A_{13} = \frac{2(xy(x - y) + xy_1(x - y_1) - y(y - y_1)^2)}{y(x - y_1)(y - y_1)} \quad (7.13)$$

It is important to note here that the evolution equation for $h_1^{\perp(1)}(x)$ (7.10), as found by direct calculation, differs from the equation found by a different method in chapter 6 and is expressed in terms of moments in equation (6.47). The evolution equation in chapter 6, conveniently, only involves the function $h_1^{\perp(1)}(x)$, whereas the result of direct calculation involves, besides the function itself, two additional sub-leading order functions, h and the imaginary part of the two-argument function E_A .

Equation (7.10) is formulated in an over-complete set of functions and one might naively hope that equivalence with the results of chapter 6 can be made manifest through the use of equation of motion and Lorentz-invariance relations, but this is not the case. Because we are not able to eliminate all y_1 -dependence from the kernel function A_{13} in equation (7.13), relation (3.80) cannot be used to eliminate all dependence on E_A from equation (7.10), as would be necessary to arrive at an autonomous evolution equation for $h_1^{\perp(1)}(x)$. In fact, all evolution equations for non-collinear leading order functions found by direct calculation, differ, because of this reason, from the results in chapter 6, shown in equations (6.42-6.47). We will see later, when considering polarized hadrons, that this residual momentum fraction dependence also occurs in the evolution equations for pure interaction parts and has as a consequence that the autonomous evolution of the pure interaction parts of the functions h_L and g_T , which is the starting point of the results presented in chapter 6, is not confirmed by our direct calculations.

Proceeding to find the closed set of functions that drive the evolution of $h_1^{\perp(1)}$, we have to calculate the perturbative contributions to the functions $h(x)$ and $E_A(x, x_1)$. Operational definitions of the functions $h(x)$ and $E_A(x, x_1)$, consistent with the parametrizations in equation (3.18) and equation (3.21), are given by

$$h(x) \equiv \int d^4k \delta(k \cdot \zeta - x P \cdot \zeta) \text{Tr} \left[\left(-P \cdot \zeta \frac{\epsilon_{T\rho\sigma} \gamma_5 [\gamma^\rho, \gamma^\sigma]}{8M} \right) \Phi(k) \right] \quad (7.14)$$

$$E_A(x, x_1) \equiv \int d^4k d^4k_1 \delta(k \cdot \zeta - x P \cdot \zeta) \delta(k_1 \cdot \zeta - x_1 P \cdot \zeta) \\ \times \text{Tr} \left[\left(\frac{P \cdot \zeta}{M} \frac{i\epsilon_{T\rho\sigma} \gamma_5 \not{\zeta} \gamma_\rho}{4} \right) \Phi_A^\alpha(k, k_1) \right]. \quad (7.15)$$

The evolution equations for these functions show similar mixing with other functions. The single-argument sub-leading order function h has the following evolution equation,

$$\dot{h}(x, Q^2) = \frac{\alpha_s}{4\pi} N_c \int \frac{dy}{y} \left[A_{21} h_1^{\perp(1)}(y) + A_{22} h(y) + \int_0^1 dy_1 A_{23} \text{Im}\{E_A(y, y_1)\} \right], \quad (7.16)$$

where the kernel functions have the following values,

$$A_{21} = \frac{2(3x - y)}{y(x - y)}, \quad (7.17)$$

$$A_{22} = 1, \quad (7.18)$$

$$A_{23} = \frac{4(y^2 - x y_1)}{y(x - y)(y - y_1)}. \quad (7.19)$$

For the two-argument function $E_A(x, x_1)$ one finds the following scale dependence,

$$\text{Im}\{E_A(x, x_1)\} = \frac{\alpha_s}{4\pi} N_c \int_x^1 \frac{dy}{y} \left[A_{31} h_1^{\perp(1)}(y) + A_{32} h(x) \right. \\ \left. + \int_0^1 dy_1 A_{33} \text{Im}\{E_A(y, y_1)\} \right]. \quad (7.20)$$

The kernel parts are now given by

$$A_{31} = -\delta(x_1 - y) \frac{x}{y} \quad (7.21)$$

$$A_{32} = -\delta(x_1 - y) \frac{x}{2} \quad (7.22)$$

$$A_{33} = \delta(x_1 - y) \frac{(x^2 - x y + y^2 + 2y y_1 - y_1^2)}{(x - y_1)(y - y_1)} \\ + \delta(x_1 - y_1) \frac{(x^3 + y^3 - 2x^2 y_1 - 2y^2 y_1 + x y_1^2 + y y_1^2)}{(x - y)(x - y_1)(y - y_1)}. \quad (7.23)$$

7.3 Longitudinally polarized hadrons

At leading order in $1/Q$ is the very well studied [Stra97] function $g_1(x)$ which considering flavor non-singlet in the large N_c limit evolves according to equation (6.3). The function

that parametrizes the soft structure at sub-leading order in the collinear case is $h_L(x)$. This function has a more complicated evolution structure than its unpolarized counterpart and was studied in [Koik95b] and its fragmentation function analogue in [Beli97c]. The evolution of $h_L(x)$ already introduces, through mixing, the function $h_{1L}^{\perp(1)}(x)$, and in the next section the evolution of these functions is considered.

The collinear parametrization of the soft parts includes a sub-leading order T-odd function $e_L(x)$ and has an identical evolution structure as the function $e(x)$. Inclusion of transverse momentum does not lead to new T-odd structures.

7.3.1 Scale dependence of $h_{1L}^{\perp(1)}(x)$

We define the function $h_{1L}^{\perp(1)}(x, Q^2)$ by the following projection operation,

$$h_{1L}^{\perp(1)}(x) \equiv \int d^4k \delta(k \cdot \zeta - x P \cdot \zeta) \text{Tr} \left[\Phi(k) \left(-\frac{\gamma_5 [\not{\zeta}, \not{k}_T]}{8MS_L} \right) \right]. \quad (7.24)$$

Performing this operation on all diagrams of order α_s leads to the following evolution equation

$$\begin{aligned} \dot{h}_{1L}^{\perp(1)}(x) = & \frac{\alpha_s}{4\pi} \int_x^1 \frac{dy}{y} \left[A_{11} h_{1L}^{\perp(1)}(y) + A_{12} h_L(y) \right. \\ & \left. + \int_0^1 dy_1 A_{13} \text{Re} \{ H_A(y, y_1) \} \right]. \end{aligned} \quad (7.25)$$

where the kernel functions $A_{11} \dots A_{13}$ are given in equations (7.11), (7.12) and (7.13), respectively. The functions that mix with $h_{1L}^{\perp(1)}(x)$ according to equation (7.25), are defined in the following way,

$$h_L(x) = \int d^4k \delta(k \cdot \zeta - xP \cdot \zeta) \text{Tr} \left[\Phi(k) \left(\frac{P \cdot \zeta \gamma_5 [\not{\eta}, \not{\zeta}]}{M 4S_L} \right) \right], \quad (7.26)$$

$$\begin{aligned} H_A(x, x_1) = & \int d^4k d^4k_1 \delta(k \cdot \zeta - xP \cdot \zeta) \delta(k_1 \cdot \zeta - x_1P \cdot \zeta) \\ & \times \text{Tr} \left[\Phi_A^\alpha(k, k_1) \left(\frac{P \cdot \zeta \gamma_5 \not{k} \gamma_{T\alpha}}{M 4S_L} \right) \right]. \end{aligned} \quad (7.27)$$

These two functions mix among each other as becomes clear from their evolution equations,

$$\dot{h}_L(x) = \int_x^1 \frac{dy}{y} \left[A_{21} h_{1L}^{\perp(1)}(y) + A_{22} h_L(y) \right] \quad (7.28)$$

$$+ \int_0^1 dy_1 A_{23} \text{Re} \{ H_A(y, y_1) \}, \quad (7.29)$$

$$\text{Re} \{ \dot{H}_A(x, x_1) \} = \frac{\alpha_s}{4\pi} N_c \int \frac{dy}{y} \left[A_{31} h_{1L}^{\perp(1)}(y) \right] \quad (7.30)$$

$$+ A_{32} h_L(x) + \int_0^1 dy_1 A_{33} \text{Re} \{ H_A(y, y_1) \}, \quad (7.31)$$

where the kernel functions A_{21} - A_{23} are given in equations (7.17)-(7.19), and the kernel functions A_{31} - A_{33} are given in equations (7.21)-(7.23).

7.3.2 Scale dependence of $e_L(x)$

In this section we will discuss the T-odd function $e_L(x)$. Defining this function consistently with the parametrization 3.35 in the following way.

$$e_L(x) \equiv \int d^4k \delta(k \cdot \zeta - x P \cdot \zeta) \text{Tr} \left[\left(i\gamma_5 \frac{P \cdot \zeta}{2M S_L} \right) \Phi(k) \right] \quad (7.32)$$

Using this definition and considering the contributions in the large- N_c limit shown in figure 5.4 one obtains the following Q^2 -dependence,

$$\dot{e}_L(x) = \int_x^1 \frac{dy}{y} \left[B_{11} e_L(y) + \int_0^1 dy_1 B_{12} \text{Im} \{E_A(y, y_1)\} \right]. \quad (7.33)$$

The kernel functions B_{11} and B_{12} already appeared in the evolution equation of the function $e(x)$, in equations (7.3) and (7.4).

If we now turn our attention to the mixing function, the imaginary part of $E_A(x, x_1)$, we find the following results. Defining this function as in equation (7.15) and considering the contributions shown in figure 5.5 one obtains the following results for the Q^2 -dependence of the imaginary part of $E_A(x, x_1)$.

$$\text{Re} \{ \dot{E}_A(x, x_1) \} = \int_x^1 \frac{dy}{y} \left[B_{21} e_L(y) + \int_0^1 dy_1 B_{22} \text{Im} \{E_A(y, y_1)\} \right] \quad (7.34)$$

where the kernel functions B_{21} and B_{22} are given by the expressions (7.6) and (7.8).

To our knowledge, the evolution of this functions has not been investigated in the past except for the results in reference [Henn02], which are presented in chapter 6. By identifying the function $e_L(x)$ as an imaginary part of $e(x)$ it was concluded that the two functions would evolve identically. Direct computation has confirmed that the evolution of the function $e_L(x)$ is identical to that of $e(x)$.

7.4 Transversally polarized hadrons

The leading order, T-even, collinear structure in a transversally polarized spin-1/2 hadron is parameterized by the function $h_1(x)$, also known by the name of the transversity function. Its evolution is known to next-to-leading (NLO) accuracy [Voge98, Haya97], just as its fragmentation analog [Stra02], but all we will need here is its LO approximation shown in equation (6.4). The T-even sub-leading order structure is parametrized by the function $g_T(x)$, which has also been studied extensively. We will start presenting our results for the g_T -evolution sector. The function g_T mixes with the function $g_{1T}^{(1)}(x)$ that parametrizes the non-collinear, T-even, leading order structure when transverse momentum is taken into account.

Consideration of the T-odd sector in a transversally polarized spin-1/2 hadron includes the collinear function $f_T(x)$. The evolution of this function cannot be considered without encountering the non-collinear function $f_{1T}^{\perp(1)}(x)$, the Sivers function, and a collinear, two-argument function parametrizing a pure interaction part.

7.4.1 Scale dependence $g_{1T}^{(1)}(x)$

Introducing again operational definitions for the functions consistent with the parametrizations in equations (3.33) and (3.21).

$$g_{1T}^{(1)}(x) \equiv \int d^4k \delta(k \cdot \zeta - x P \cdot \zeta) \text{Tr} \left[\left(\frac{k_T \cdot S_T \not{\zeta} \gamma_5}{M S_T^2} \right) \Phi(k) \right] \quad (7.35)$$

$$g_T(x) \equiv \int d^4k \delta(k \cdot \zeta - x P \cdot \zeta) \text{Tr} \left[\left(\frac{P \cdot \zeta \not{S}_T \gamma_5}{M 2 S_T^2} \right) \Phi(k) \right] \quad (7.36)$$

$$G_A(x, x_1) \equiv \int d^4k d^4k_1 \delta(k \cdot \zeta - x P \cdot \zeta) \delta(k_1 \cdot \zeta - x_1 P \cdot \zeta) \\ \times \text{Tr} \left[\left(-\frac{P \cdot \zeta i \epsilon_{T\rho}^{S_T} \not{\zeta}}{M 2 S_T^2} \right) \Phi_A^\rho(k, k_1) \right] \quad (7.37)$$

$$\tilde{G}_A(x, x_1) \equiv \int d^4k d^4k_1 \delta(k \cdot \zeta - x P \cdot \zeta) \delta(k_1 \cdot \zeta - x_1 P \cdot \zeta) \\ \times \text{Tr} \left[\left(\frac{P \cdot \zeta S_{T\rho} \not{\zeta} \gamma_5}{M 2 S_T^2} \right) \Phi_A^\rho(k, k_1) \right] \quad (7.38)$$

Using the above expressions on the first order in α_s kernels, one obtains.

$$g_{1T}^{(1)}(x, Q^2) = \int \frac{dy}{y} \left[E_{11} g_{1T}^{(1)}(y) + E_{12} g_T(y) \right. \\ \left. + \int dy_1 \left\{ E_{13} G_A(y, y_1) + E_{14} \tilde{G}_A(y, y_1) \right\} \right] \quad (7.39)$$

where the kernels have the following dependence on the fractions

$$E_{11} = \frac{\alpha_s}{4\pi} N_c \left[\frac{x(2x^2 - xy + y^2)}{y^2(y-x)} \right] \quad (7.40)$$

$$E_{12} = \frac{\alpha_s}{4\pi} N_c \left[\frac{x^2}{y} \right] \quad (7.41)$$

$$E_{13} = \frac{\alpha_s}{4\pi} N_c \left[\frac{x^2 - 2xy - y^2 - xy_1 - yy_1}{y(x-y_1)} \right] \quad (7.42)$$

$$E_{14} = \frac{\alpha_s}{4\pi} N_c \left[\frac{2x^3 - x^2y - y^3 - x^2y_1 + 3xyy_1 - xy_1^2 - yy_1^2}{y(y-y_1)(y_1-x)} \right] \quad (7.43)$$

The function g_T receives the following contributions.

$$g_T(x) = \int \frac{dy}{y} \left[E_{21} g_{1T}^{(1)}(y) + E_{22} g_T(y) + \right. \\ \left. \int dy_1 \left\{ E_{23} G_A(y, y_1) + E_{14} \tilde{G}_A(y, y_1) \right\} \right] \quad (7.44)$$

where

$$E_{21} = \frac{\alpha_s}{4\pi} N_c \left[\frac{2x^2 - xy + y^2}{y(y-x)} \right] \quad (7.45)$$

$$E_{22} = \frac{\alpha_s}{4\pi} N_c \left[\frac{x}{y} \right] \quad (7.46)$$

$$E_{23} = \frac{\alpha_s}{4\pi} N_c \left[\frac{x+y}{y(x-y)} \right] \quad (7.47)$$

$$E_{24} = \frac{\alpha_s}{4\pi} N_c \left[\frac{2x^2 - 3xy - y^2 + xy_1 + yy_1}{y(y-x)(y-y_1)} \right] \quad (7.48)$$

Then there are the two argument functions involved in the evolution that obtain the following contributions.

$$\begin{aligned} \dot{G}_A(x, x_1) &= \int \frac{dy}{y} \left[E_{31} g_{1T}^{(1)}(y) + E_{32} g_T(y) \right. \\ &\quad \left. + \int dy_1 \left\{ E_{33} G_A(y, y_1) + E_{34} \tilde{G}_A(y, y_1) \right\} \right] \end{aligned} \quad (7.49)$$

where the kernel parts are

$$E_{31} = \frac{\alpha_s}{4\pi} N_c \left[-\delta(x_1 - y) \frac{x}{2y} \right] \quad (7.50)$$

$$E_{32} = \frac{\alpha_s}{4\pi} N_c \left[\delta(x_1 - y) \frac{x}{2} \right] \quad (7.51)$$

$$\begin{aligned} E_{33} &= \frac{\alpha_s}{4\pi} N_c \left[-\delta(x_1 - y) \frac{x^2 - 2y^2 + 2yy_1 - y_1^2}{2(x-y)(x-y_1)(y-y_1)} \right. \\ &\quad \left. + \delta(x_1 - y_1) \frac{(x+y)(x^2 + y^2 - 2xy_1 - 2yy_1 + 2y_1^2)}{2(x-y)(x-y_1)(y-y_1)} \right] \end{aligned} \quad (7.52)$$

$$\begin{aligned} E_{34} &= \frac{\alpha_s}{4\pi} N_c \left[-\delta(x_1 - y) \frac{x - 2y + y_1}{2(y - y_1)} \right. \\ &\quad \left. - \delta(x_1 - y_1) \frac{(x-y)(x+y-2y_1)}{2(x-y_1)(y-y_1)} \right] \end{aligned} \quad (7.53)$$

The evolution of the function $\tilde{G}_A(x, x_1)$ is given in the limit of large- N_c by the following equation.

$$\begin{aligned} \dot{\tilde{G}}_A(x, x_1) &= \int \frac{dy}{y} \left[E_{41} g_{1T}^{(1)}(y) + E_{42} g_T(y) + \right. \\ &\quad \left. \int dy_1 \left\{ E_{43} G_A(y, y_1) + E_{44} \tilde{G}_A(y, y_1) \right\} \right] \end{aligned} \quad (7.54)$$

in which

$$E_{41} = \frac{\alpha_s}{4\pi} N_c \left[\delta(x_1 - y) \frac{x}{2y} \right] \quad (7.55)$$

$$E_{42} = \frac{\alpha_s}{4\pi} N_c \left[-\delta(x_1 - y) \frac{x}{2} \right] \quad (7.56)$$

$$E_{43} = \frac{\alpha_s}{4\pi} N_c \left[\delta(x_1 - y) \frac{(x - 2y + y_1)}{2(y - y_1)} \right]$$

$$-\delta(x_1 - y_1) \frac{(x - y)(x + y - 2y_1)}{2(x - y_1)(y - y_1)} \Big] \quad (7.57)$$

$$E_{44} = \frac{\alpha_s}{4\pi} N_c \left[\delta(x_1 - y) \frac{x^2 - 2y^2 + 2yy_1 - y_1^2}{2(x - y_1)(y - y_1)} \right. \\ \left. + \delta(x_1 - y_1) \frac{x^2 - 2y^2 - 2xy_1 - 2yy_1 + 2y_1^2}{2(x - y)(x - y_1)(y - y_1)} \right] \quad (7.58)$$

Quark self-energy

Until now no self-energy contributions have been taken into account. As mentioned before, these contributions are proportional to δ -functions that only let them contribute at end-points of the integration range of the momentum fraction. It is illustrative of the nature of different functions, to pay some attention to the contributions of the quark self-energy to the evolution system of the function $g_{1T}^{(1)}(x)$.

Starting with the following combination of diagrams

$$\frac{1}{2} \left\{ \begin{array}{c} \text{Diagram 1} \\ \text{Diagram 2} \end{array} \right\} \quad (7.59)$$

and inserting the appropriate projector for the function $g_{1T}^{(1)}(x)$ a short calculation reveals the quark self-energy contribution to $g_{1T}^{(1)}(x)$,

$$\dot{g}_{1T}^{(1)}(x) \Big|_{\text{QSE}} = \frac{\alpha_s}{2\pi} g_{1T}^{(1)}(x) \left(\frac{3}{2} - 2x \int \frac{dy}{y} \Theta_{11}^0(y, y - x) \right) \quad (7.60)$$

which is identical to the result for collinear leading order functions.

By now taking into account the diagram combination

$$\frac{1}{2} \left\{ \begin{array}{c} \text{Diagram 3} \\ \text{Diagram 4} \end{array} \right\} \quad (7.61)$$

and using the corresponding projectors for the sub-leading order functions $G_A(x, x_1)$ and $\tilde{G}_A(x, x_1)$, one obtains for the quark self-energy contribution to the evolution of these functions,

$$\dot{G}_A(x, x_1) \Big|_{\text{QSE}} = \frac{\alpha_s}{2\pi} G_A(x, x_1) \left(\frac{3}{2} - 2x \int \frac{dy}{y} \Theta_{11}^0(y, y - x) \right) \quad (7.62)$$

$$\dot{\tilde{G}}_A(x, x_1) \Big|_{\text{QSE}} = \frac{\alpha_s}{2\pi} \tilde{G}_A(x, x_1) \left(\frac{3}{2} - 2x \int \frac{dy}{y} \Theta_{11}^0(y, y - x) \right) \quad (7.63)$$

which again is identical to the case of leading order collinear functions. This is surprising as these results reflect the fact that these functions only involve *good* fields, which are renormalized in the same way for all the functions above.

A different situation is encountered when looking at a function that not only involves good fields, like the function $g_T(x)$. A calculation of the contribution of quark self-interaction to the function $g_T(x)$ reveals,

$$\begin{aligned} \dot{g}_T(x)\Big|_{\text{QSE}} &= \frac{\alpha_s}{2\pi} \left\{ g_{1T}^{(1)}(x) \left(1 - x \int \frac{dy}{y} \Theta_{11}^0(y, y-x) \right) \right. \\ &\quad \left. + \frac{1}{x} g_T(x) \left(2 - 4x \int \frac{dy}{y} \Theta_{11}^0(y, y-x) \right) \right\}, \end{aligned} \quad (7.64)$$

clearly differing from the contributions (7.60), (7.62) and (7.63), which only involve good fields.

7.4.2 Scale dependence of the Sivers function

Consideration of the T-odd sector results in an evolution structure that is identical to the evolution structure of the T-even sector. The leading order function $f_{1T}^{\perp(1)}(x)$, the Sivers function, mixes with the sub-leading order functions $f_T(x)$ and the *imaginary* parts of the two argument functions $G_A(x, y)$ and $\tilde{G}_A(x, y)$.

An operational definition of these functions is given by the following expressions

$$f_{1T}^{\perp(1)}(x) = \int d^4k \delta(k \cdot \zeta - xP \cdot \zeta) \text{Tr} \left[\Phi(k) \left(\frac{\epsilon_T^{S_T k_T} \not{\zeta}}{2M S_T^2} \right) \right] \quad (7.65)$$

$$f_T(x) = \int d^4k \delta(k \cdot \zeta - xP \cdot \zeta) \text{Tr} \left[\Phi(k) \left(-\frac{P \cdot \zeta}{M} \frac{\epsilon_T^{S_T \alpha} \gamma_{T\alpha}}{2M S_T^2} \right) \right] \quad (7.66)$$

and the two argument functions were already defined in equations (7.37) and (7.38).

The extraction of the evolution structure of order α_s diagrams leads to the structure,

$$\begin{pmatrix} f_{1T}^{\perp(1)}(x, Q^2) \\ f_T(x, Q^2) \\ \text{Im} \{G_A(x, x_1)\} \\ \text{Im} \{\tilde{G}_A(x, x_1)\} \end{pmatrix} = \begin{pmatrix} E_{11} & E_{12} & E_{13} & E_{14} \\ E_{21} & E_{22} & E_{23} & E_{24} \\ E_{31} & E_{32} & E_{33} & E_{34} \\ E_{41} & E_{42} & E_{43} & E_{44} \end{pmatrix} \begin{pmatrix} f_{1T}^{\perp(1)}(y, Q^2) \\ f_T(y, Q^2) \\ \text{Im} \{G_A(y, y_1)\} \\ \text{Im} \{\tilde{G}_A(y, y_1)\} \end{pmatrix} \quad (7.67)$$

in which all the functions E_{ij} are identical to the evolution kernel of the T-even sector functions.

7.4.3 Diagonal evolution of the pure interaction part

The pure interaction part in $g_T(x)$, indicated by $\tilde{g}_T(x)$, has been claimed to evolve diagonally in the large N_c limit [Ali91], with the kernel shown in equation (6.12). Our results can be put in diagonal form. Looking at the lower two rows in equation (7.67) and the identical evolution matrix for the functions $g_{1T}^{(1)}$, g_T , and the real parts of G_A and \tilde{G}_A , it is possible by use of the equations of motion, to eliminate the contributions from the kernel elements E_{31} , E_{32} , E_{41} and E_{42} . By defining a new two argument function,

$$Y(x, y) = \frac{(G_A(x, y) + \tilde{G}_A(x, y))}{2(x-y)}, \quad (7.68)$$

the evolution equation takes a diagonal form,

$$\dot{Y}(x, x_1) = \int dy dy_1 K(x, x_1; y, y_1) Y(y, y_1), \quad (7.69)$$

where the kernel function is given by

$$\begin{aligned} K(x, x_1; y, y_1) = & \delta(x_1 - y_1) \left(\Theta_{11}^0(x, x - y) \frac{x y (x + y - 4 y_1)}{(x - y)(y - y_1)^2} \right. \\ & \left. - \Theta_{11}^0(x, x - x_1) \frac{y_1 (x - y_1)^2}{(x - y)(y - y_1)^2} \right) \\ & + \delta(x - y) \left(\Theta_{11}^0(x_1, x_1 - y_1) \frac{(x^2 x_1 - 2x x_1^2 + x_1^3 + x^2 y_1 - 2x y_1^2 + y_1^3)}{(y - y_1)^2 (x_1 - y_1)} \right. \\ & \left. + \Theta_{11}^0(x_1, x_1 - y) \frac{(x_1 - y)(x_1 y + 2y^2 - x_1 y_1)}{2y (y - y_1)^2} \right). \end{aligned} \quad (7.70)$$

The relation of the object of which diagonal evolution is claimed and the function Y here above is given by the relation,

$$\tilde{g}_T(x) = \frac{1}{x} \int dy \operatorname{Re} \{Y(x, y)\} (x - y). \quad (7.71)$$

We did not succeed in rewriting the evolution equation (7.69) as an autonomous evolution equation of function depending on a single momentum fraction. An elimination of all dependence of the kernel (7.70) on one of the momentum fractions, which is necessary for rewriting in terms of single momentum fraction functions, does not seem possible. Note that although self-energy contributions are not included in the above evolution kernel, these contributions only matter at integration end-points and cannot bring the evolution equation into the desired form in the integration interval.

7.5 Reducing redundancy

As mentioned in chapter 3 and extensively used in chapter 6, two types of relations exist between the functions parametrizing collinear and non-collinear structure. At tree-level both types of relations can be used to reduce the number of independent functions. Study of the evolution equation sets found by direct computation indicates a difference in self-consistency under evolution between equation of motion and Lorentz-invariance relations.

The relations following from the equation of motion are invariant under evolution up to the accuracy of the calculation. For example, the relation involving the function $g_{1T}^{(1)}(x)$, shown in equation (3.77), neglecting the quark mass for brevity, is satisfied by the calculated order α_s perturbative corrections,

$$g_T(x) = \frac{1}{x} \dot{g}_{1T}^{(1)}(x) + \frac{1}{x} \int dy \operatorname{Re} \left\{ \dot{G}_A(x, y) + \dot{\tilde{G}}_A(x, y) \right\}. \quad (7.72)$$

More explicitly, the evolution kernels E_{ij} given by equations (7.40)-(7.43), (7.45)-(7.48), (7.50)-(7.53) and (7.55)-(7.58), satisfy the following equation,

$$E_{1i} - \frac{1}{x} E_{2i} - \frac{1}{x} \int dx \{E_{3i} + E_{4i}\} = 0, \quad (7.73)$$

for $i = 1, 2, 3, 4$. This means that the calculated kernels are such that the equation of motion relation remains valid under evolution *irrespective* of the momentum fraction dependence of all involved soft functions.

On the other hand, the Lorentz-invariance relation containing the function $g_{1T}^{(1)}(x)$ (3.66), is *not* invariant under evolution. The equation,

$$g_T(x) = g_1(x) + \frac{d}{dx} g_{1T}^{(1)}(x), \quad (7.74)$$

does *not* hold. This remains not being the case even given that the functions g_T , g_1 and $g_{1T}^{(1)}$ fulfill the Lorentz-invariance relation (3.66). Fulfillment of the Lorentz-invariance relation at all scales (7.74), implies the following additional condition, for *all* values of x , on the remaining independent functions (after elimination of the function g_1),

$$0 = \int_x^1 dy \left\{ \left[E_{21} - \frac{d}{dx} E_{11} + P \frac{d}{dy} \right] g_{1T}^{(1)}(y) + \left[E_{22} - \frac{d}{dx} E_{12} - P \right] g_T(y) \right. \\ \left. + \int dy_1 \left\{ \left[E_{23} - \frac{d}{dx} E_{13} \right] G_A(y, y_1) + \left[E_{24} - \frac{d}{dx} E_{14} \right] \tilde{G}_A(y, y_1) \right\} \right\} \quad (7.75)$$

where

$$P = \frac{x^2 + y^2}{y^2(y - x)}, \quad (7.76)$$

is the kernel in the evolution of the function g_1 . As condition (7.75) has to be valid for all x , and the kernel functions are ratios of polynomials in x , the only possible dependence on longitudinal momentum fractions for the soft functions is the trivial solution,

$$g_T(y) = g_{1T}^{(1)}(y) = G_A(y, y_1) = \tilde{G}_A(y, y_1) = 0. \quad (7.77)$$

In general, the consequences of the Lorentz-invariance relations beyond tree-level seem too restrictive and lead us to question their validity in a non-collinear treatment.

7.6 Discussion

We find a disagreement between the literature [Brau00] and our results for the evolution of the pure-interaction parts of functions $h_L(x)$ and $g_T(x)$. The evolution equation found for the function $e(x)$ agrees with what is found in the literature. The gluon self-energy contributions that are missing in our calculation, cannot be responsible for this mismatch as these only involve end-point contributions. The results are presented in a redundant basis of functions without application of equations of motion or equations resulting from Lorentz-invariance. All results presented in this chapter satisfy the equations of motion, giving us confidence in the validity of our results. The relations following from Lorentz-invariance seem not to be satisfied by the first order corrections, indicating that care must be taken in the application of these relations.

The results reveal a similar structure to the first order in α_s evolution of the flavor non-singlet leading order functions

$$\dot{f}_1 = \mathcal{P} \otimes f_1 \quad (7.78)$$

$$\dot{g}_1 = \mathcal{P} \otimes g_1 \quad (7.79)$$

$$\dot{h}_1 = \mathcal{D} \otimes h_1. \quad (7.80)$$

The evolution kernels of the functions f_1 and g_1 , given in equations (6.2) and (6.3) are both denoted by the symbol \mathcal{P} as they are identical. The evolution kernel for the function h_1 , given in equation (6.4) and denoted here by the symbol \mathcal{D} differs from \mathcal{P} . Considering the real and complex evolution sectors of the non-collinear functions one finds similar results. The evolution structure and kernels of longitudinally polarized and unpolarized functions is identical, only involving different functions,

Unpolarized

$$\begin{pmatrix} \dot{h}_1^{(1)} \\ h \\ \text{Im}E_A \end{pmatrix} = \left[\begin{array}{cc|c} A_{11} & A_{12} & A_{13} \\ A_{21} & A_{22} & A_{23} \\ \hline A_{31} & A_{32} & A_{33} \end{array} \right] \otimes \begin{pmatrix} h_1^{(1)} \\ h \\ \text{Im}E_A \end{pmatrix} \quad (7.81)$$

$$\begin{pmatrix} \dot{e} \\ \text{Re}E_A \end{pmatrix} = \left[\begin{array}{c|c} B_{11} & B_{12} \\ \hline B_{21} & B_{22} \end{array} \right] \otimes \begin{pmatrix} e \\ \text{Re}E_A \end{pmatrix} \quad (7.82)$$

Longitudinally polarized

$$\begin{pmatrix} \dot{h}_{1L}^{(1)} \\ h_L \\ \text{Re}H_A \end{pmatrix} = \left[\begin{array}{cc|c} A_{11} & A_{12} & A_{13} \\ A_{21} & A_{22} & A_{23} \\ \hline A_{31} & A_{32} & A_{33} \end{array} \right] \otimes \begin{pmatrix} h_{1L}^{(1)} \\ h_L \\ \text{Re}H_A \end{pmatrix} \quad (7.83)$$

$$\begin{pmatrix} \dot{e}_L \\ \text{Im}H_A \end{pmatrix} = \left[\begin{array}{c|c} B_{11} & B_{12} \\ \hline B_{21} & B_{22} \end{array} \right] \otimes \begin{pmatrix} e_L \\ \text{Im}H_A \end{pmatrix}, \quad (7.84)$$

$$(7.85)$$

whereas the evolution structure of the transversally polarized sector differs clearly from the former two cases,

Transversally polarized

$$\begin{pmatrix} \dot{g}_{1T}^\perp \\ g_T \\ \text{Re}G_A \\ \text{Re}\tilde{G}_A \end{pmatrix} = \left[\begin{array}{cc|cc} E_{11} & E_{12} & E_{13} & E_{14} \\ E_{21} & E_{22} & E_{23} & E_{24} \\ \hline E_{31} & E_{32} & E_{33} & E_{34} \\ E_{41} & E_{42} & E_{43} & E_{44} \end{array} \right] \otimes \begin{pmatrix} g_{1T}^\perp \\ g_T \\ \text{Re}G_A \\ \text{Re}\tilde{G}_A \end{pmatrix} \quad (7.86)$$

$$\begin{pmatrix} \dot{f}_{1T}^{(1)} \\ f_T \\ \text{Im}G_A \\ \text{Im}\tilde{G}_A \end{pmatrix} = \left[\begin{array}{cc|cc} E_{11} & E_{12} & E_{13} & E_{14} \\ E_{21} & E_{22} & E_{23} & E_{24} \\ \hline E_{31} & E_{32} & E_{33} & E_{34} \\ E_{41} & E_{42} & E_{43} & E_{44} \end{array} \right] \otimes \begin{pmatrix} f_{1T}^{(1)} \\ f_T \\ \text{Im}G_A \\ \text{Im}\tilde{G}_A \end{pmatrix}. \quad (7.87)$$

One also notices that the transversally polarized sector shows identical real and imaginary evolution sectors, whereas the longitudinal and unpolarized sectors show much asymmetry in these parts.

Summary and discussion

This thesis is about the set of distribution and fragmentation functions that parametrize the soft hadronic physics reflecting the quark and gluon content of spin-1/2 and spin-0 hadrons participating in hard electro-weak processes. The set of functions goes beyond a collinear treatment, by including transverse momentum, \mathbf{k}_T , of quarks with respect to their parent hadrons. In this non-collinear set the functions depend, besides the longitudinal momentum fraction, also on \mathbf{k}_T^2 , and their number is larger than in a collinear treatment, because \mathbf{k}_T is included in the structures that they parametrize. Of the additional non-collinear functions, some only parametrize the collinear structure in more detail and reduce into the collinear set after integration over \mathbf{k}_T . The rest of the additional functions parametrize structures that are *odd* in \mathbf{k}_T . In the collinear approximation, an approximation that suffices when only one hadron is relevant in the hard process, this \mathbf{k}_T -odd structure averaged out and does not appear in the cross-section. However, when more than one hadron participates in the hard process, it is possible to construct cross-sections which are determined by this non-collinear structure. Azimuthal asymmetries allow for the measurement of this \mathbf{k}_T -odd structure at leading order in $1/Q$.

This additional, non-collinear, leading order structure can enter the cross-section without any suppression because it involves only correlations between good components of the quark fields, which is the same reason why leading order collinear functions can contribute unsuppressed. In the rest frame of a parent spin-1/2 hadron and in a helicity basis for the good components of the quark field, the complementarity between collinear and non-collinear functions becomes clear. In this specific representation in quark spin space \times parent hadron spin space, one sees that the collinear set of functions spans a limited part of this product space. This product space is fully spanned after inclusion of the non-collinear structure.

Using this specific quark-spin \times hadron-spin representation, we were able to derive bounds between the leading order functions of the non-collinear set. Besides a \mathbf{k}_T -dependent version of the Soffer bound, a number of inequalities is found that bound the magnitude of non-collinear functions. Since these results are derived for the functions at tree level, the relations can be used as first estimates for experimental investigation. A more complete study is necessary to investigate the effect of interactions on the validity of these relations in practice.

The inclusion of interactions leads to logarithmic scale dependence of distribution and fragmentation functions which can be calculated perturbatively. In order to study this scale dependence of non-collinear functions, we employ *two* different methods. The first method relies on the large- N_c evolution equations presented in the literature for the so-called interaction dependent parts of sub-leading order functions. The connection with non-collinear functions is made through the use of relations following from the equations of motion and Lorentz invariance relations. The second method is based on direct calculation of the evolution equations in a light-cone gauge. The calculations are performed in an over-complete set of distribution functions without using equation of motion-, or Lorentz Invariance relations.

Direct calculation shows that the scale dependence of the non-collinear leading order functions is very different from that of collinear leading order functions, even when restricted to flavor non-singlet, first order in α_s accuracy. While collinear functions display autonomous evolution, the non-collinear functions are part of the evolution systems involving sub-leading order collinear functions. In general, one obtains an evolution matrix structure in which several functions mix among each other and even with two-momentum fraction functions from different types of correlators. In a special light-cone gauge the evolution equations take their simplest form and involve only a quark-quark correlator and a correlator including an additional transversally polarized gluon.

The evolution equations derived using collinear evolution as a starting point and supplemented with equations of motion and Lorentz-invariance relations are surprisingly simple and easier to apply than those resulting from direct calculation. The use of relations following from the equations of motion, seems legitimate. The results that follow from direct calculation reflect these equations, and we believe that the equation of motion relations can be used in a non-collinear treatment to reduce the over-complete set of functions. The evolution systems found by direct calculation do not seem to respect the Lorentz-invariance relations between functions, making us question the validity of these relations in a non-collinear treatment, without any consequence for Lorentz-invariance of the description itself. Their use might be a possible reason for the mismatch between the two sets of evolution equations. A second possible reason might be found in the validity of the autonomous evolution of the pure interaction parts. From the results of our calculations, only the autonomous evolution of the function $\tilde{e}(x)$ (and therefore $\tilde{e}_L(x)$) could be confirmed. The autonomous evolution forms of $\tilde{g}_T(x)$ and $\tilde{h}_L(x)$ as suggested in [Brau00], could not be confirmed, and requires further study.

An important issue is that of gauge invariance. The evolution systems calculated in chapter 7 involve soft parts that coincide in a light-cone gauge with gauge invariant quantities. Although we are confident of the self-consistency of our light-cone gauge evolution equations, the structure of the evolution equations might be modified in an arbitrary gauge. In particular the presence of the gauge-link operator might lead to modifications.

A correct treatment of gauge invariance in connection to \mathbf{k}_T -odd structure, leads to differences from a collinear treatment. The concept of hard factorization of \mathbf{k}_T -odd structure, when comparing e.g. DIS to Drell-Yan, is modified by additional minus signs originating from the special gauge-link structure. Furthermore, non-trivial gauge-link structure can lead to T-odd distribution functions. A study of the evolution of the non-collinear structure in an arbitrary physical gauge might help clarify some of these issues.

BIBLIOGRAPHY

- [Ali91] A. Ali, V. M. Braun and G. Hiller, *Phys. Lett.* **B** 266 (1991), p. 117.
- [Alta77] G. Altarelli and G. Parisi, *Nucl. Phys.* **B** 126 (1977), p. 298.
- [Alta84] G. Altarelli, R. K. Ellis, M. Greco and G. Martinelli, *Nucl. Phys.* **B** 246 (1984), p. 12.
- [Alta98] G. Altarelli, S. Forte and G. Ridolfi, *Nucl. Phys.* **B** 534 (1998), p. 277.
- [Amat78a] D. Amati, R. Petronzio and G. Veneziano, *Nucl. Phys.* **B** 140 (1978), p. 54.
- [Anse95] M. Anselmino, M. Boglione and F. Murgia, *Phys. Lett.* **B** 362 (1995) 164.
- [Anse01] M. Anselmino, D. Boer, U. D'Alesio and F. Murgia, *Phys. Rev.* **D** 63 (2001), p. 054029.
- [Artr90] X. Artru and M. Mekhfi, *Z. Phys.* **C** 45 (1990), p. 669.
- [Avak99] H. Avakian, *Nucl. Phys. Proc. Suppl.* **B** 79 (1999), p. 523.
- [Bacc00] A. Bacchetta, P.J. Mulders, *Phys. Rev.* **D** 62 (2000), p. 114004.
- [Bacc00b] A. Bacchetta, M. Boglione, A. A. Henneman and P. J. Mulders, *Phys. Rev. Lett.* 85 (2000), p. 712.
- [Bacc04] A. Bacchetta, P.J. Mulders and F. Pijlman, *Phys. Lett.* **B** 595 (2004), p. 309.
- [Bald81] F. Baldracchini *et al.*, *Fortsch. Phys.* 29/30 (1981) p. 505.
- [Bali88] I. I. Balitsky and V. M. Braun, *Nucl. Phys.* **B** 311 (1988/89), p. 541.
- [Bali96] I. I. Balitsky, V. M. Braun, Y. Koike and K. Tanaka, *Phys. Rev. Lett.* 77 (1996), p. 3078.
- [Barm03] V.V. Barmin et al., DIANA Collaboration, *Phys. Atom. Nucl.* **66** (2003), 1715.
- [Baro97] V. Barone, *Phys. Lett.* **B** 409 (1997), p. 499.
- [Bash79] C.L. Basham, L.S. Brown, S.D. Ellis and S.T. Love, *Phys. Rev.* **D** 19 (1979), p. 2018.

- [Basu84] R. Basu, A. Ramalho and G. Sterman, Nucl. Phys. **B** 244 (1984), p. 221.
- [Beli97] A. V. Belitsky, Lectures given at the XXXI PNPI Winter School on Nuclear and Particle Physics, St. Petersburg, Repino, February, 1997, hep-ph/9703432.
- [Beli97b] A.V. Belitsky, Phys. Lett. **B** 405 (1997), p. 312.
- [Beli97c] A.V. Belitsky and D. Müller, Nucl. Phys. **B** 503 (1997), p. 279.
- [Beli03] A.V. Belitsky, X. Ji and F. Yuan, Nucl. Phys. **B** 656 (2003), p. 165.
- [Bjor69] J. D. Bjorken, E.A. Paschos, Phys. Rev. **185** (1969), p. 1975.
- [Bloo69] E. D. Bloom *et al.*, Phys. Rev. Lett. **23** (1969), p. 930.
- [Bodw85] G.T. Bodwin, Phys. Rev. **D** 31 (1985), p. 2616; Erratum: Phys. Rev. **D** 34 (1986), p. 3932.
- [Boer97a] D. Boer, R. Jakob and P.J. Mulders, Nucl. Phys. **B** 504 (1997), p. 345.
- [Boer97b] D. Boer, R. Jakob and P.J. Mulders, Phys. Lett. **B** 424 (1998), p. 143.
- [Boer98] D.Boer and P.J. Mulders, Phys. Rev. **D** 57 (1998), p. 5780
- [Boer98c] D. Boer, P. J. Mulders and O. V. Teryaev, Phys. Rev. **D** 57 (1998), p. 3057
- [Boer99] D. Boer, R. Jakob and P.J. Mulders, Nucl. Phys. **B** 564 (2000), p. 471.
- [Boer00] D.Boer and P.J. Mulders, Nucl. Phys. **B** 569 (2000), p. 505-526
- [Boer00b] D. Boer, Phys. Rev. **D** 62 (2000), p. 094029
- [Boer01] D. Boer, Nucl. Phys. **B** 603 (2001), p. 195.
- [Boer03] D. Boer, P.J. Mulders and F. Pijlman, Nucl. Phys. **B** 667 (2003), p. 201.
- [Bogl99] M. Boglione and P.J. Mulders, Phys. Rev. **D** 60 (1999), p. 054007.
- [Bomh04] C.J. Bomhof, P.J. Mulders and F. Pijlman, Phys. Lett. **B** 596 (2004), p. 277.
- [Bour98] C. Bourrely, J. Soffer and O.V. Teryaev, Phys. Lett. **B** 420 (1998), p. 375.
- [Bran89] F.T. Brandt, J. Frenkel and J.C. Taylor, Nucl. Phys. **B** 312 (1989), p. 589.
- [Brau00] V. M. Braun, G. P. Korchemsky and A. N. Manashov, Phys. Lett. **B** 476 (2000), p. 455.
- [Brav99] A. Bravar (for the Brav99 Collaboration), Nucl. Phys. Proc. Suppl. **B** 79 (1999), p. 521.
- [Brod02a] S.J. Brodsky, D.S. Huang and I. Schmidt, Phys. Lett. **B** 530 (2002), p. 99.
- [Brod02b] S.J. Brodsky, D.S. Huang and I. Schmidt, Nucl. Phys. **B** 642 (2002), p. 344.

- [Bukh83a] A.P. Bukhvostov, E.A. Kuraev and L.N. Lipatov, *Sov. J. Nucl. Phys.* **38** (1983), p. 263.
- [Bukh83b] A.P. Bukhvostov, E.A. Kuraev and L.N. Lipatov, *JETP Lett.* **37** (1983), p. 482.
- [Bukh84a] A.P. Bukhvostov, E.A. Kuraev and L.N. Lipatov, *Sov. J. Nucl. Phys.* **39** (1984), p. 121.
- [Bukh84b] A.P. Bukhvostov, E.A. Kuraev and L.N. Lipatov, *Sov. Phys. JETP* **60** (1984), p. 22.
- [Call69] C.G. Callan and D.J. Gross, *Phys. Rev. Lett.* **22** (1969), p. 156.
- [Cole65] S. Coleman and R. E. Norton, *Nuovo Cim.* **38** (1965), p. 438.
- [Coll81b] J.C. Collins and D.E. Soper, *Nucl. Phys.* **B 193** (1981), p. 381; Erratum: *Nucl. Phys.* **B 213** (1983), p. 545.
- [Coll82a] J.C. Collins and D.E. Soper, *Nucl. Phys.* **B 194** (1982), p. 445.
- [Coll82b] J.C. Collins, D.E. Soper and G. Sterman, *Phys. Lett.* **B 109** (1982), p. 388.
- [Coll83] J.C. Collins, D.E. Soper and G. Sterman, *Nucl. Phys.* **B 223** (1983), p. 381.
- [Coll83b] J.C. Collins, D.E. Soper and G. Sterman, *Phys. Lett.* **B 126** (1983), p. 275.
- [Coll84] J.C. Collins, D.E. Soper and G. Sterman, *Phys. Lett.* **B 134** (1984), p. 263.
- [Coll85a] J.C. Collins, D.E. Soper and G. Sterman, *Nucl. Phys.* **B 261** (1985), p. 104.
- [Coll85b] J.C. Collins, D.E. Soper and G. Sterman, *Nucl. Phys.* **B 250** (1985), p. 199.
- [Coll85c] J.C. Collins and D.E. Soper, *Acta Phys. Pol.* **B 16** (1985), p. 1047.
- [Coll88] J.C. Collins, D.E. Soper and G. Sterman, *Nucl. Phys.* **B 308** (1988), p. 833.
- [Coll93] J. Collins, *Nucl. Phys.* **B 396** (1993), p. 161.
- [Coll02] J.C. Collins, *Phys. Lett.* **B 536** (2002), p. 43.
- [Coll04] J.C. Collins and A. Metz, [hep-ph/0408249](#).
- [Cort92] J.L. Cortes, B. Pire and J.P. Ralston, *Z. Phys.* **C 55** (1992), p. 409.
- [Curc80b] G. Curci, W. Furmanski and R. Petronzio, *Nucl. Phys.* **B 175** (1980), p. 27.
- [Cutk60] R. E. Cutkovsky, *J. Math. Phys.* **1** (1960), p. 429.
- [Davi84] C.H.T. Davies and W.J. Stirling, *Nucl. Phys.* **B 244** (1984), p. 337.
- [Doks80] Dokshitzer, Dyakonov and Trojan, *Phys. Rep.* **B 58** (1980), p. 269.
- [Dori80] R. Doria, J. Frenkel and J. C. Taylor, *Nucl. Phys.* **B 168** (1980), p. 93.

- [Efre81a] A. V. Efremov and A. V. Radyushkin, *Theor. Math. Phys.* **44** (1981), p. 664.
- [Efre99a] A.V. Efremov, O.G. Smirnova and L.G. Tkachev, *Nucl. Phys. Proc. Suppl.* **B 79** (1999), p. 554.
- [Elli79a] R.K. Ellis, H. Georgi, M. Machacek, H.D. Politzer and G.G. Ross, *Nucl. Phys.* **B 152** (1979), p. 285.
- [Elli82] R.K. Ellis, W. Furmansky and R. Petronzio, *Nucl. Phys.* **B 207** (1982), p. 1.
- [Elli83] R.K. Ellis, W. Furmansky and R. Petronzio, *Nucl. Phys.* **B 212** (1983), p. 29.
- [Feyn72] R.P. Feynman, *Photon-hadron interactions*, (Benjamin, Reading MA, 1972).
- [Fren84] J. Frenkel, J.G.M. Gatheral and J.C. Taylor, *Nucl. Phys.* **B 233** (1984), p. 307.
- [Furm81] W. Furmansky, Jagelonian University Habilitation thesis,
- [Furm81b] W. Furmansky, Trieste preprint ICTP 81-152 (1981).
- [Goek03] K. Goeke, A. Metz, P.V. Pobylitsa and M.V. Polyakov, *Phys. Lett.* **B 567** (2003), p. 27.
- [Gold95] G. Goldstein, R.L. Jaffe and X. Ji, *Phys. Rev.* **D 52** (1995), p. 5006.
- [Hagi83] K. Hagiwara, K. Hikasa and N. Kai, *Phys. Rev.* **D 27** (1983), p. 84.
- [Hamm97] N. Hammon, O. V. Teryaev and A. Schäfer, *Phys. Lett.* **B 390** (1997), p. 409.
- [Haya97] A. Hayashigaki, Y. Kanazawa and Y. Koike, *Phys. Rev.* **D 56** (1997), p. 7350.
- [Henn02] A.A. Henenman, Daniel Boer and P.J. Mulders, *Nucl. Phys.* **B 620** (2002), p. 331.
- [Jaff82] R.L. Jaffe and M. Soldate, *Phys. Rev. D* **26** (1982) 49.
- [Jaff83] R.L. Jaffe, *Nucl. Phys.* **B 229** (1983), p. 205.
- [Jaff91] R.L. Jaffe and X. Ji, *Phys. Rev. Lett.* **67** (1991), p. 552.
- [Jaff92] R.L. Jaffe and X. Ji, *Nucl. Phys.* **B 375** (1992), p. 527.
- [Jaff93] R.L. Jaffe and X. Ji, *Phys. Rev. Lett.* **71** (1993), p. 2547.
- [Jaff95] R.L. Jaffe, Notes for lectures presented at the international school of nucleon structure, *The Spin Structure of the Nucleon*, Erice 3-10 Aug. 1995, [hep-ph/9602233](#).
- [Jaff96] R.L. Jaffe, *Phys. Rev.* **D 54** (1996), p. 6581.
- [Jako97] R. Jakob, P.J. Mulders and J. Rodrigues, *Nucl. Phys.* **A 626** (1997), p. 937.
- [Ji90] X. Ji and C. Chou, *Phys. Rev.* **D 42** (1990), p. 3637.
- [Ji99] X. Ji and J. Osborne, *Eur. Phys. Jour.* **C 9** (1999) p. 487.

- [Koda82] J. Kodaira and L. Trentadue, Phys. Lett. **B** 112 (1982), p. 66.
- [Kogu70] J. B. Kogut and D. E. Soper, Phys. Rev. **D** 1 (1970), p. 2901.
- [Koik95a] Y. Koike and K. Tanaka, Phys. Rev. **D** 51 (1995), p. 6195.
- [Koik95b] Y. Koike and K. Tanaka, Prog. Theor. Phys. Suppl. **120** (1995) p. 247.
- [Kuma97] S. Kumano and M. Miyama, Phys. Rev. **D** 56 (1997), p. 2504.
- [Leve94] J. Levelt and P. J. Mulders, Phys. Lett. **B** 338 (1994), p. 357.
- [Liet81] L. Di'Lieto, S. Gendrom, I.G. Halliday and C.T. Sachrajda, Nucl. Phys. **B** 183 (1981), p. 223.
- [Mano90] A.V. Manohar, Phys. Rev. Lett. 65 (1990), p. 2511.
- [Mert96] R.Mertig and W.L. van Neerven, Z. Phys. **C** 70 (1996), p. 637.
- [Metz02] A. Metz, hep-ph/0209054.
- [Muel74] A.H. Mueller, Phys. Rev. **D** 9 (1974), p. 963.
- [Muel78] A.H. Mueller, Phys. Rev. **D** 18 (1978), p. 3705.
- [Muel81] A.H. Mueller, Phys. Rep. **B** 73 (1981), p. 237.
- [Muel97] D. Müller, Phys. Lett. **B** 407 (1997), p. 314.
- [Mul96] P.J. Mulders and R.D. Tangerman, Nucl. Phys. **B** 461 (1996), p. 197; Erratum: Nucl. Phys. **B** 484 (1997), p. 538.
- [Naka03] T. Nakano et al., LEPS Collaboration, Phys. Rev. Lett. 91 (2003), p. 012002.
- [Nach73] O. Nachtmann, Nucl. Phys. **B** 63 (1973), p. 237.
- [Pari73] G. Parisi, Phys. Lett. **B** 43 (1973), p. 207.
- [Pari79] G. Parisi and R. Petronzio, Nucl. Phys. **B** 154 (1979), p. 427.
- [Qiu90] J. Qiu and G. Sterman, *Proceedings of the Polarized Collider Workshop*, Eds. J.C. Collins, S.F. Heppelman and R.W. Robinett, University Park, PA (1990), AIP Conf. Proc No. 223, (AI, New York, 1990), p. 249.
- [Qiu91a] J. Qiu and G. Sterman, Nucl. Phys. **B** 353 (1991), p. 105.
- [Qiu91b] J. Qiu and G. Sterman, Nucl. Phys. **B** 353 (1991), p. 137.
- [Rals79] J. P. Ralston and D. E. Soper, Nucl. Phys. **B** 152 (1979), p. 109.
- [Ratc86] P. G. Ratcliffe, Nucl. Phys. **B** 264 (1986), p. 493.
- [Ruju71] A. De Rújula, J.M. Kaplan and E. de Rafael, Nucl. Phys. **B** 35 (1971), p. 365.

- [Scha00] A. Schäfer and O.V. Teryaev, Phys. Rev. D 61 (2000) 077903
- [Shur82] E.V. Shuryak and A.I. Vainstein, Nucl. Phys. B 201 (1982), p. 141.
- [Sive90] D. Sivers, Phys. Rev. D 41 (1990), p. 83.
- [Sive91] D. Sivers, Phys. Rev. D 43 (1991), p. 261.
- [Soff95] J. Soffer, Phys. Rev. Lett. 74 (1995), p. 1292.
- [Sope77] D. E. Soper, Phys. Rev. D 15 (1977), p. 1141.
- [Sope79] D. E. Soper, Phys. Rev. Lett. 43 (1979), p. 1847.
- [Stra02] M. Stratmann and W. Vogelsang, Phys. Rev. D 65 (2002), p. 057502.
- [Stra97] M. Stratmann and W. Vogelsang, Nucl. Phys. B 496 (1997), p. 41.
- [Tang95] R. D. Tangerman and P. J. Mulders, Phys. Rev. D 51 (1995), p. 3357.
- [Tery00] O.V. Teryaev, RIKEN rev. 28 (2000) 101.
- [Voge96a] W. Vogelsang, Phys. Rev. D 54 (1996), p. 2023.
- [Voge98] W. Vogelsang, Phys. Rev. D 57 (1998), p. 1886.
- [Vogt04] A. Vogt, S. Moch and J.A.M. Vermaseren, hep-ph/0407321.

Samenvatting

Schaalafhankelijkheid van correlaties op het lichtfront

Protonen en neutronen, of meer algemeen hadronen, bestaan uit quarks en gluonen die volgens de wetten van de quantum chromodynamica (QCD) de meest hecht gebonden toestanden vormen die in de natuur gevonden worden. Tot op heden zijn alle pogingen om hadronen in afzonderlijke quarks en gluonen te doen uiteenvallen, mislukt en hebben slechts geleid tot de schepping van meer hadronen. De overtuiging is dat de krachten die quarks en gluonen tot hadronen binden niet overwonnen *kunnen* worden en dat het bestaan van quarks en gluonen alleen binnen hadronen mogelijk is. Dit verschijnsel, dat de naam *confinement* draagt, is nog altijd niet begrepen en vormt een onoverkomelijk obstakel om, uitgaande van quarks en gluonen, uit eerste principes de eigenschappen van hadronen te berekenen.

Terwijl QCD verantwoordelijk is voor de sterkste kracht die we kennen, de sterke wisselwerking, weten we dat op afstanden die veel kleiner zijn dan de karakteristieke grootte van een hadron, quarks en gluonen juist geen krachten op elkaar uitoefenen, een limietgedrag van de theorie dat bekend is onder de naam van *asymptotische vrijheid*. Hoewel deze twee extremen voor een theorie op het eerste gezicht merkwaardig lijken, pleiten ze juist voor QCD, gezien de succesvolle beschrijving van bepaalde verstrooiingsexperimenten in het z.g. *Parton Model*, dat als uitgangspunt heeft dat quarks niet wisselwerken met de rest van het hadron waartoe ze behoren. Deze klasse van experimenten, die van de *harde elektrozwakke* verstrooiingsexperimenten, is zeer geschikt om het gedrag van quarks en gluonen in hadronen te kunnen zien.

Met een elektrozwak proces wordt een verstrooiingsproces bedoeld waarin, naast hadronen, ook leptonen betrokken zijn. Leptonen zijn fundamentele deeltjes die, in tegenstelling tot hadronen, ongevoelig zijn voor de sterke wisselwerking. De wisselwerking tussen de leptonen en de hadronen verloopt via de elektrozwakke wisselwerking, een interactie die zeer nauwkeurig beschreven kan worden d.m.v. de uitwisseling van één enkel elektrozwak krachtdeeltje, een elektrozwak boson. Omdat de betrokken leptonen gedetecteerd worden, weten we precies hoeveel energie en impuls aan de hadronen overgedragen wordt en kunnen we alleen naar die verstrooiingen kijken waarin de massa Q van het overgedragen boson veel groter is dan de massa's van de betrokken hadronen. Zulke processen worden *hard* genoemd.

In het hadron zijn quarks en gluonen verantwoordelijk voor de absorptie van het harde boson. Gluonen hebben geen elektrozwakke lading en zullen het elektrozwakke

boson niet voelen. Quarks, daarentegen, zijn wél elektrozwak geladen en zijn daarom als enige verantwoordelijk voor de directe koppeling aan het boson. Dit deelproces waarin de quark een hard boson absorbeert speelt in de beschrijving een centrale rol. De beschrijving berust op *factorisatie*, wat inhoudt dat de werkzame doorsnede, de kans dat een bepaalde verstrooiing plaatsvindt, geschreven kan worden als het product van een zacht en een hard stuk. Het harde stuk correspondeert met de interactie van de quark en het harde boson, onafhankelijk van de rest van het hadron, terwijl het zachte stuk de quark in het hadron beschrijft. Factorisatie verwijst naar het scheiden van de twee genoemde, totaal verschillende, aspecten van QCD; de fysica die confinement beschrijft, is te vinden in het zachte stuk en de asymptotisch vrije fysica in het harde stuk.

Het harde quarkverstrooiingsproces wordt gekarakteriseerd door de grote schaal Q , en kan beschreven worden in de asymptotisch vrije limiet. Hierdoor kan het nauwkeurig berekend worden, gebruikmakend van storingsrekening in de koppelingsconstante van QCD, α_s . Dit betekent dat de verstrooide quark in eerste benadering, tijdens de korte duur van de harde interactie, als een vrij deeltje beschouwd wordt en dat de wisselwerking van de quark met gluonen slechts kleine correcties hierop zijn. Het zachte stuk beschrijft de connectie tussen hadronen en quarks en wordt uitgedrukt in een aantal quark distributie- en fragmentatiefuncties. Distributiefuncties beschrijven de quarkinhoud van een hadron dat deelneemt aan een hard proces, terwijl fragmentatiefuncties de vervalmogelijkheid van een quark in een bepaald hadron beschrijven.

In QCD, een quantumveldentheorie, corresponderen distributie en fragmentatiefuncties met de verwachtingswaarden van quark- en gluonvelden geëvalueerd tussen hadron-toestanden. Een veldentheoretische analyse bevestigt de splitsing in een hard en een zacht stuk voor processen waarvoor de impulsoverdracht Q groot genoeg is. Dit maakt het mogelijk om de werkzame doorsnede als een expansie in machten van $1/Q$ op te schrijven. De harde stukken kunnen nauwkeurig berekend worden en zijn in feite instrumenten om de zachte stukken in hadronen te meten. De zachte stukken blijken te corresponderen met matrixelementen van quarkvelden geëvalueerd langs een heel specifieke richting. Deze speciale richting is een *licht-achtige* richting die bepaald wordt door de impulsen van het hadron en het uitgewisselde boson. Correlaties van het quarkveld langs een specifieke licht-achtige richting, corresponderen met wat distributie en fragmentatie functies genoemd worden. Er bestaat een aantal z.g. *collineaire* functies, dat alle mogelijke structuur die van belang is als één hadron aan het harde proces deelneemt, parametrizeert. In dat geval is alleen de impuls van de quarks langs de licht-achtige richting van belang en de functies hangen slechts van één enkele variabele af, de impulsfractie $x = P_{\text{quark}}/P_{\text{hadron}}$. Collineaire functies parametrizeert structuur die alleen de speciale licht-achtige richting bevat en ook een andere licht-achtige richting als ze subleidend in $1/Q$ kunnen bijdragen aan de werkzame doorsnede. Deze twee richtingen spannen samen een *lichtkegel* op, waardoor de collineaire correlaties ook wel lichtkegel-correlaties worden genoemd.

Dit proefschrift bestudeert een extensie van de collineaire distributie- en fragmentatiefuncties die van belang is als er meer dan een enkel hadron aan het hard proces deelneemt. Het stelsel van functies dat beschouwd wordt in dit proefschrift, houdt rekening met de transversale impuls, \mathbf{k}_T , van quarks ten opzichte van het collineaire richting waarlangs het harde proces zich afspeelt, en parametrizeert daarom structuur die afwezig is in de gangbare collineaire benadering. In deze parametrisatie van de niet-collineaire structuur, hangen de functies niet alleen van een longitudinale impulsfractie x af, maar

ook van \mathbf{k}_T^2 . Met deze transversale richting spreekt men niet langer van een lichtkegel maar van het lichtfront, waardoor deze niet-collineaire correlaties ook lichtfront correlaties genoemd worden. Het aantal functies is groter dan in het collineaire geval omdat het aantal mogelijke structuren groter is. Een aantal van de functies heeft alleen \mathbf{k}_T^2 als extra argument en deze functies reduceren tot de collineaire parametrisatie na integratie over \mathbf{k}_T . Daarnaast is er niet-collineaire structuur dat *oneven* is in \mathbf{k}_T . Als er slechts één enkel hadron meedoet wordt, middelt deze extra structuur uit en alleen de collineaire functies komen voor in de uitdrukking voor de werkzame doorsnede. Echter, als er meer dan één hadron een rol speelt, is het mogelijk om werkzame doorsneden te meten die juist de additionele niet-collineaire structuur bevatten. In azimutale asymmetrieën is het mogelijk om deze niet-collineaire structuur in leidende orde in $1/Q$ te meten.

De in leidende orde in $1/Q$ bijdragende correlaties hebben voor zowel het collineaire als het niet-collineaire geval betrekking op de *goede* componenten van het quarkveld. De goede componenten zijn, in een bepaalde ijk, de werkelijk onafhankelijke vrijheidsgraden van het quarkveld, terwijl de overige componenten niet onafhankelijk zijn, maar door de goede componenten van het quarkveld en het gluonveld bepaald worden. In het rust-stelsel van het moeder-hadron en in een heliceitsbasis van de goede componenten van het quarkveld, kan een dichtheidsmatrix geconstrueerd worden die de informatie voor alle mogelijke hadron- en partonpolarisaties bevat. In deze matrix is goed zichtbaar hoe de collineaire structuur aangevuld wordt door de niet-collineaire. De collineaire structuur vult slechts een deel van deze matrix in de product-ruimte van hadronspin \times quarkheliceit. Deze matrix wordt gecomplementeerd als de niet-collineaire structuur in beschouwing wordt genomen. Omdat deze dichtheidsmatrix positief-definiete eigenwaarden moet hebben, is het mogelijk om een aantal ongelijkheden te verkrijgen. Afgezien van een \mathbf{k}_T -afhankelijke versie van de Soffer-ongelijkheid, wordt een aantal ongelijkheden gevonden die de grootte van collineaire en niet-collineaire functies beperkt. Hoewel deze resultaten luscorrecties buiten beschouwing laten, zijn ze nuttig voor orde van grootte schattingen van de nieuwe functies. Het is echter wel nodig om de invloed van luscorrecties op de geldigheid van deze ongelijkheden nader te bestuderen.

Interacties tussen quarks en gluonen leiden tot een logaritmische schaalafhankelijkheid van distributie- en fragmentatiefuncties, die m.b.v. storingsrekening berekend kan worden. We berekenen de schaalafhankelijkheid, die ook bekend is onder de naam evolutie, van de leidende niet-collineaire functies tot eerste orde in α_s in de limiet van een oneindig aantal kleuren, volgens twee verschillende methodes. De eerste methode gaat uit van de autonome evolutievergelijkingen van het pure interactiedeel van in subleidend orde ($1/Q$) verschijnende functies in de limiet van oneindig veel kleuren, zoals die uit de literatuur [Brau00] bekend zijn. Door gebruik te maken van relaties volgend uit de bewegingsvergelijkingen van quarks (Dirac-relaties) en relaties volgend uit Lorentz-invariantie (Lorentz-relaties), is het mogelijk om uitdrukkingen te krijgen voor de evolutie van de niet-collineaire leidende orde functies. De tweede methode die gehanteerd wordt is een *ab initio* berekening van de schaalafhankelijkheid, uitgevoerd in een lichtkegel-ijk, zonder gebruik te maken van Dirac- of Lorentz-relaties.

De resultaten verkregen d.m.v. de twee methodes zijn, afgezien van de evolutie van de functie $\tilde{e}(x)$, verschillend en niet met elkaar in overeenstemming te brengen door gebruik te maken van de Dirac- of Lorentz-relaties. De evolutievergelijkingen van de leidende niet-collineaire functies die volgens de eerste methode autonoom zouden zijn, zijn dat niet

volgens de tweede methode. In het algemeen zijn de evolutievergelijkingen die door directe berekening gevonden zijn, ingewikkelder en vereisen kennis van subleidende functies. Van de drie autonome evolutievergelijkingen voor de subleidende functies $\tilde{h}_L(x)$, $\tilde{g}_T(x)$ en $\tilde{e}(x)$, zoals gepresenteerd in [Brau00], bevestigt onze directe berekening slechts de autonome evolutie van de functie $\tilde{e}(x)$. Voor de interactiestukken $\tilde{h}_L(x)$ en $\tilde{g}_T(x)$, kan in de tweede methode slechts een autonome evolutie verkregen worden voor de corresponderende twee-argument functies, maar niet voor de functies $\tilde{h}_L(x)$ en $\tilde{g}_T(x)$ zelf.

Uit de tweede methode volgt ook een belangrijk verschil tussen de Dirac-relaties en de Lorentz-relaties. De gevonden evolutiekernels zijn zodanig dat de perturbatieve correcties altijd aan de Dirac-relaties voldoen. Dit gebeurt volledig onafhankelijk van de x -afhankelijkheid van de daarbij betrokken functies. Wij concluderen hieruit dat de Dirac-relaties, tot eerste orde in α_s en in de limiet van oneindig veel kleuren, bij alle schalen geldig blijven. Voor de Lorentz-relaties is de situatie geheel anders. Ook al zouden de relaties bij een bepaalde schaal gelden, dan zijn de gevonden perturbatieve correcties zodanig dat, bij een andere schaal, deze relaties geschonden worden. Geldigheid bij alle (althans hogere) schalen volgt alleen als alle niet-collineaire en subleidend structuur nul gesteld worden. Onze conclusie op grond van de directe berekening, is dat de Lorentz-relaties onhoudbaar zijn onder evolutie.

Dankwoord

Dit proefschrift zou nooit geschreven zonder de hulp van anderen. Deze laatste bladzijde wil ik daarom aan hen wijden en enkelen met name noemen.

Piet, als eerste wil ik jou bedanken voor de mogelijkheid om dit onderzoek te doen en voor de tijd die je in mij gestoken hebt. Telkens als ik op onoverkomelijke problemen dacht te stuiten, gaf jouw pragmatische kijk mij, weliswaar niet altijd het antwoord dat ik zocht, maar wel altijd een oplossing waardoor ik verder kon. Je gaf mij niet alleen de vrijheid om zelf mijn weg te zoeken, wat ik altijd erg prettig heb gevonden, maar je gaf ook actieve steun daarbij, zoals bij mijn werkbezoek aan SLAC. Dit tezamen met je enthousiasme maken je een heel bijzondere begeleider.

Erg dankbaar ben ik de leden van de leescommissie, Elena, Elliot, Justus, Jo en Daniël voor de tijd en aandacht die ze aan mijn proefschrift besteed hebben. Hun opmerkingen hebben dit proefschrift op vele punten verbeterd.

De co-auteurs van mijn eerste echte publicatie, Elena en Alessandro, wil ik bedanken voor de efficiënte, vruchtbare en plezierige samenwerking. Daniël, mijn samenwerking met jou is de meest intensieve geweest. De lange en vaak late uren van gezamenlijk staren naar onwillige kernels en zoeken naar oplossingen, bevatten de spanning, het delen van kennis *en* onwetendheid, die het doen van onderzoek juist zo leuk maken. Ik zou je willen bedanken voor je tijd en inzet, ook bij het schrijven van de netelige passages in dit proefschrift, en voor aangename momenten buiten het werk.

Nico, dat ik naast een gehoorbeschadiging ook een mooie vriendschap zou overhouden aan onze collocatie, had ik bij mijn aanstelling niet kunnen weten; bedankt voor je steun op zo vele fronten. Alessandro, bedankt voor de heerlijke pasta's en warmte. De vele kamergenoten die daarna volgden en overige leden van de theoriegroep dank ik gezamenlijk voor hun hulpvaardigheid en vriendelijkheid.

Connie, zonder je steun en motivatie zou dit nooit gelukt zijn en daar wil ik je voor bedanken. Pablo en Jaime, jullie worden bedankt voor de alles-relativerende *chancherie*.